2013

Study of Glycation and Advanced Glycation on a Humanized Monoclonal Antibody

Hong Liu
University of Rhode Island, hliu2005@gmail.com

STUDY OF GLYCATION AND ADVANCED GLYCATION ON A HUMANIZED MONOCLONAL ANTIBODY

BY

HONG LIU

A DISSERTATION SUBMITTED IN PARTIAL FULFILLMENT OF

THE

REQUIREMENTS FOR THE DEGREE OF

DOCTOR OF PHILOSOPHY

IN

CHEMISTRY

UNIVERSITY OF RHODE ISLAND

2013

DOCTOR OF PHILOSOPHY DISSERTATION

OF

HONG LIU

APPROVED:

Thesis Committee

Major Professor: Joel A. Dain

David Freeman

Gongqin Sun

Nasser H. Zawia

DEAN OF THE GRADUTE SCHOOL

UNIVERSITY OF RHODE ISLAND

2013

ABSTRACT

In the presented work, we reviewed the protein glycation effect on recombinant monoclonal antibodies (MAbs), and demonstrated an *in vitro* glycation model on rhuMAb A was a successful tool to evaluate site-specific glycation. We also implemented this model to study MAb glycation in three aspects: the formation of glycation, the change of glycation adducts under thermal stress, and the control of glycation adducts stability by formulation compositions.

A protein characterization study demonstrated that the *in vitro* forced glycation model generated seven glycated amino acid sites on rhuMAb A. The lysine residue K49 was the preferably site, while others sites were at various low levels of glycation. Molecular dynamics (MD) analysis suggested that the high abundance of lysine 49 glycation observed on rhMAb A may be assisted by a strong electron-donating environment created by three aspartates, with D30, D31, and D105 near K49.

In the thermal stress stability study, the glycation adduct hydrolysis reaction was more pronounced than the AGE formation. It was found that glycation adducts hydrolysis continued for four weeks, but AGEs formation plateaued after one week. The overall combination of both reactions caused a loss of glycation with a first order reaction rate. The structure analysis of final degradation products agreed with kinetic observation that reverse of glycation adducts was the main degradation pathway of glycated rhuMAb A at 40°C in pH 6.5 phosphate formulation buffer. Reverse of glycation adducts on K49 could be catalyst by its adjacent aspartic acids.

Influencing parameters of glycation adduct degradation were also evaluated. Three formulation composition factors: pH, buffer, and oxidation control were compared. The study demonstrated the pH value was the key parameter that controls degradation pathways. pH also determined the rate constant of hydrolysis of glycated rhuMAb A. Buffer species and oxidation levels did not affect on the glycation adduct stability under the studied conditions. In addition, the effect of rhuMAb A's initial glycation level was also evaluated. The study demonstrated that higher protein glycation levels slow down the overall hydrolysis rate of glycation adduct, presumably by providing a complex electron transferring system on protein.

ACKNOWLEDGMENT

First and foremost, I would like to thank Dr. Joel A. Dain for many wonderful years that I during my graduate study. The most important thing that I have learned from him is to be a curious and humble scientist with an open mind.

I also would like to thank all the professors who spent their precious time on my graduate study. Thanks to Dr. Ying Sun who kindly served as my defense committee chair and organized my oral exam. Thanks to Dr. Gongqin Sun, who gave me advice and support on the fluorescence analysis. Many thanks to Dr. David Freeman and Dr. Sze Yang for being my committee members and my mentors to encourage me to know myself better through last 12 years.

There is now an enormous list of people that I am very grateful to. Their kindness was crucial, especially towards final finish of my study. Thanks for Dr. Thomas Patapoff, Dr. Trevor Swartz, Dr. Boyan Zhang and Mr. Yi Yang from Genentech, for engaging countless inspirational discussions, providing technical supports during my research studies. Dr. Jamie Moore and Dr. Mary Cromwell from Genentech for supporting my continuous education in past four years. Many thanks to my fellow graduate students, Weixi Liu and Sreekanth Suravajjala for their time and their help whenever I needed. Many thanks to Dr. Danielle Leiske who spent her precious time reviewing my thesis and provided great suggestions on editing and formatting all chapters.

Last and the most of all, I would like to thank my husband, Xinfeng Zhang, and my whole family. There are not enough words to express my gratitude for their tremendous support, patience and love.

PREFACE

This thesis was composed in manuscript format for intended publications. It contained four chapters: review of glycation on MAbs, characterization of an *in vitro* force glycated model rhuMAb A, degradation of glycated rhuMAb A, and the influceing parameter to control degradation of glycated rhuMAb A. Except the chapter on review of glycation on MAbs, three other chapters are intended for publication in journals.Therefore this thesis contained other introductory remaks. Currently, these three chapters (manuscripts) are in preparation stage prior to submission to journals.

TABLE OF CONTENTS

LIST OF FIGURES

Chapter 1

Chapter 2

Chapter 3

LIST OF TABLES

Chapter 1

Review of Formation and Characterization of Glycation on Therapeutic Monoclonal Antibodies (MAbs)

Abstract

Recent studies have shown that protein glycation reactions can occur to recombinant MAbs during cell culture in manufacturing, storage upon shelf life, clinical administration and circulation in the human body. Difference in these process conditions can generate structural heterogeneity in MAb glycation. Characterization and control of glycation modification has become increasingly important to ensure product quality as well as manufacturing process consistency for recombinant MAbs in the biopharmaceutical industry. A series of analytical technologies has been developed and applied to characterize the structure of glycated MAbs. These technologies include: mass spectrometry, affinity chromatography, ion exchange chromatography, biological binding activity, and others. Studies of certain MAbs have shown that glycation may impair a MAb's ability to bind antigens (Kennedy, D.M. *et al.*1994), while, in contrast, studies of others MAbs demonstrated that glycation has no effect in binding affinity (Quan, C. *et al.* 2008). Site specific glycation has also been reported recently (Zhang,B. *et al.* 2008, Gadgil, H.S. *et al.* 2010, Miller, A.K. *et al.* 2011), which has enhanced research interest in the formation, degradation and control of glycated MAbs. In the quality-by-design (QbD) paradigm for manufacturing MAbs, the decision to monitor and control glycation for a given MAb would require a thorough evaluation process, which is based on the impact of manufacturing

parameters on MAb glycation modification and the effect of glycation on MAb's biological function with regards to both safety and efficacy (Quan, C. *et al.* 2008).

Introduction

Glycation is a known reaction which occurs between reducing sugars and amine groups on proteins, amino acids, and nucleotides. Intensive *in vivo* studies in humans have shown that protein glycation is implicated in the pathogenesis of multiple chronic diseases. The most common reducing sugar found *in vivo* is glucose, which reacts with N-terminal amino acids or with free amino groups on lysine and arginine residues. This initial reaction between glucose and amine group is often referred as a glycation adduct. Further modification of glycation adducts result in a variety of different products known as advanced glycation endproducts (AGEs) (Maillard, L.C. 1912). This leads to irreversible modifications on the proteins (Sell, D. R. and Monnier, V. M. 1989), which can subsequently cause tissue damage (Valcourt, U. *et al.* 2007). Protein glycation level has been known as a biomarker for diseases. For example, individuals with diabetes have higher serum glucose concentration, are thought to be more prone to glycation than those in healthy persons. Therefore, the extent of glycation of hemoglobin *in vivo* is a distinctive marker for diabetes (Beisswenger, P.J. *et al.* 2001).

Glycation occurs *in vitro* as well. In the past several decades, an increasing number of recombinant humanized monoclonal antibodies (MAbs) have been developed as therapeutic agents (Figure1-1), due to their high specificity and affinity to therapeutic antigen targets (Figure 1-2). As a manufactured therapeutic protein, a MAb is subjected to many chemical modifications, including glycation throughout the manufacturing process. Chemical modifications may result in structural changes,

ultimately leading to potential biological function changes such as efficacy, safety and clearance rate. Thus, understanding glycation formation, degradation and how to control these processes on MAbs is important. The following sections summarize reported studies about glycation modification on MAbs throughout their life cycle including during cell culture, storage, administration in clinics and final circulation in the body.

Mechanism of Protein Glycation and Advanced Glycation Reactions

Glycation, originally described by Maillard (Maillard, L.C. 1912), refers to the nonenzymatic reaction between reducing sugars and proteins. This process involves a series of steps starting with the reaction between the reducing carbonyl group of a carbohydrate and an amino group present on proteins, usually at the epsilon amine on lysine residues or at the N-terminus, with initial formation of an aldimine (which is known as a Schiff base) (Figure 1-3). This unstable aldimine linkage can then rearrange to form a more stable ketoamine (which is known as an Amadori product) (Bucola, R. and Cerami, A. 1992).

Although the ketoamine linkage is considerably more stable than the aldimine linkage, it has been shown to be slowly broken under relatively mild conditions (Acharya, A.S. and Sussman, L.G., 1984; Miller, A.K. *et al.* 2011). There are also deglycating enzymes that limit glycation of intracellular proteins (Van Schaftingen, E. *et al*. 2007). The nonenzymatic reverse hydrolysis reaction is straightforward, releasing glucose and its C-2 epimer mannose, without much consequence (Zhang, Q. *et al.* 2009). The enzymatic reverse reaction involves phosphorylation of the Amadori product, followed by release of 3-deoxyglucosone.

Even though reverse of glycation reaction is relatively straightforward, the forward reactions are more complex, generating a wide range of reactive carbonyl and dicarbonyl compounds. These reactive intermediate carbonyl compounds may react with proteins to form stable, irreversible adducts and cross-links, known as AGEs (Figure 1-3). Oxidation and further rearrangement of the ketoamine and aldimine products can also generate AGEs.

Studies have shown that the extent of glycation of a protein depends on the rate of formation of the Amadori product and the rate of reversal or conversion to other products (Bucola, R. and Cerami, A. 1992; Cho, S.J. *et al.* 2007).

The study of AGEs is one of the most promising areas of research in chronic inflammation diseases today. Although the Maillard reaction, AGEs formation, has been known since 1912, it is only in the last 20 years that important works have done to elaborate the mechanism of AGEs formation. In 1988, Namiki reported the reactivity of different reducing sugars leading to AGEs formation. It was shown that compared with glucoses, aldehydes with short carbon chains (2-3 carbons) react with a model peptide, beta-alanine, faster and form AGEs more rapidly. Thus degradation of glucose to smaller reducing sugar may accelerate AGEs formation (Table 1-1, Namiki, M. 1988). In 2004, Jakus, *et al*. summarized three major pathways for AGEs formation: the Wolf pathway for reducing sugar initiated AGEs; the Namiki pathway for reverse aldose reaction of Schiff base to form AGEs; the Hodge pathway for Amadori product dehydration, and oxidation formed AGEs. All three pathways are thought to be trigged by oxidation (Jakus, V. *et al*. 2004).

Inhibitors, that prevent AGEs formation, have also been investigated by researchers. An AGEs-inhibitor is a molecule that can interrupt the covalent crosslinking of proteins and peptides by sugars or sugar derived oxidation products. For example, it may contain a nucleophilic amino group that reacts carbonyl group on reducing sugars to compete with epsilon amine groups on lysine residues and other primary amines. Carnosine, a dipeptide, β-alanyl-L-histidine, found in long-lived tissues, such as brain, at concentrations up to 20 mM in humans, has been regarded as

an anti-oxidant and a free radical scavenger. More recently, an anti-glycating potential has been discovered whereby carnosine can react with low-molecular-weight compounds that bear carbonyl groups (aldehydes and ketones). Another example can be found in the Wolf pathway. Since the crucial step of AGEs crosslinking depends on the presence of transition metals for the formation of glycoxidation products and radicals, a family of metal chelators and radical scavengers (especially superoxide dismutase mimetics) could be regarded as AGEs-inhibitors. In addition, several natural and synthetic compounds (Figure 1-4) have been shown to be inhibitors of AGEs-formation *in vitro* and *in vivo* (Cameron, N.E. and Cotter, M.A. 1993).

In short, the chemical processes and pathways that ultimately lead to AGEs formation step by step have yet to be fully clarified. As our knowledge of AGEs expands, it is becoming apparent there are many unknown AGEs, while those that have been characterized are both complex and heterogeneous, making it an important area of research.

Glycation and AGEs in Aging and Diseases

There is an increasing amount of evidence that AGEs may play a role in Alzheimer's disease (AD), diabetes and aging, as well as other chronic disease complications. The presence of AGEs are closely related to hyperglycaemia and the patho-biochemistry of AGEs could explain many of the observed changes in diabetes related complications.

From biochemical, cell based, and animal studies, it has been demonstrated that AGEs accumulate as a function of the level of chronic hyperglycemia. It is thought that AGEs accumulation *in vivo* causes dysfunctional changes in extracellular matrix, abnormal receptor-mediated production of cytokines, and altered function of intracellular proteins.

In the early 80's, Monnier and Cerami (Monnier, V. and Cerami, A. 1981), the pioneers of the nonenzymatic glycation theory of aging, proposed that the AGEs-mediated crosslinking of long-lived proteins contributes to the AGEs-related decline in the function of cells and tissues in normal aging (Table 1-2) (Brownlee, M. *et al.* 1992). Recent progress in the study of chronic diseases has confirmed that AGEs play a significant role in the evolution of vascular complications in aging, diabetes and renal failure. Pathological results showed that chronic inflammation may be triggered by endogenous trans-membrane receptor of AGEs (RAGEs) (Basta, G. *et al.* 2002).

Among the many factors proposed to be involved in the etiology or progression of AD, AGEs are a relatively new and interesting approach to unravel the mysteries of the etio-pathogenesis of this multi-factorial disease. Recent studies

suggest that AGEs are active promoters of the progression of AD, not only simply a secondary epiphenomenon (Shaw, S.M. and Crabbe, M.J. 1994). However, one has to be careful not to overestimate AGEs' role in the disease process as long as only circumstantial evidence is presented. Therefore, the specific role of AGEs and which particular AGEs are involved in the disease complications needs to be established. The possibility of effective therapeutic intervention enhances the importance of detecting AGEs. Advancements in measuring extent and type of AGEs using reliable methods will help to determine the role that AGEs have in the pathogenesis of many diseases.

Overview of Chemistry, Manufacture and Controls of Therapeutic Monoclonal Antibodies (MAbs)

Therapeutic MAbs, like other therapeutic proteins, are enormously complex drugs. They are typically produced in mammalian tissue culture cells through recombinant DNA technology (Goetze, A.M. *et al.* 2010). MAbs are a fast growing therapeutic modality in the pharmaceutical industry due to their higher specificity, lower toxicity, and greater *in vivo* predictability than small molecule pharmaceuticals (Banks, D.D. *et al*. 2009). However, unlike small molecule drugs, protein drugs are generally more susceptible to various conformational instabilities which can potentially influence immunogenicity and biological activity (Banks, D.D. *et al*. 2009).

As of May 2008, there were 15 recombinant MAbs and fusion proteins approved in the US for human therapeutic use (Table 1-3), with the majority approval for oncology and immunological indications (Zider, A. and Drakeman, D.L. 2010). To date, There are over 450 MAb products that are under development across the biopharmaceutical industry.

The manufacturing processes for recombinant MAb drug substance (DS) and drug product (DP) are complex. A stable chinese hamster ovarian (CHO) cell line contains recombinant DNA capable of expressing a desired MAb product. Cells are cultured and aliquots of cell are frozen in small vials. When production occurs, thawed cell line vials are cultured through a series of reactors at different scales (milliliter to kiloliter). Eventually, cells are grown in a production bioreactor using serum-free modified medium supplemented with glucose and, as appropriate, galactose. Cells are separated from the cell culture fluid using centrifugation followed

by filtration. The harvested cell culture fluid is purified across multiple column chromatography steps, typically in series which may include for example: a protein A affinity column, an ion exchange column, and a hydrophobic interaction column and/ or one more additional ion exchange column or other chromatography column(s). Virus inactivation and filtration operations are also designed and executed during the downstream processing. The purified MAb product is eventually formulated and filled into either drug product vials or pre-filled syringes. Subsequently, the DP is stored under recommended storage conditions before being shipped for clinical use.

Health authority approval for these protein drugs requires chemical and biological analyses designed to determine product identity, purity, and potency—which is not a trivial task for an approximately 1,300-amino-acid, 150-kDa hetero-dimer structure. The resulting analytical description encompasses the protein sequence, size, and charge as well as the degree of heterogeneity associated with each parameter. To complete the physiochemical and biological characterization, forms of variants need to be identified and their impact on potency needs to be determined. Typical recombinant protein modifications include asparagine deamidation, aspartate isomerization, methionine oxidation, protein aggregation and fragmentation, and protein glycation.

Control of micro-heterogeneity within defined analytical specifications has been used in quality control laboratories to guarantee consistent product quality during current good manufacturing process (cGMP) (Goetze, A.M. *et al.* 2010). Defining and adhering to the appropriate range of specifications ensures drug safety and efficacy to patients.

Formation of Glycation Products During Cell Culture Step in Manufacturing of Therapeutic Monoclonal Antibodies

Recombinantly produced MAbs are exposed to reducing sugars during mammalian cell culture after they are secreted into the cell culture medium that contains sugars. Sugars are present in medium as energy and carbon sources for the cells, and as a way to modulate glycosylation. For example, galactose may be added to the cell culture medium to control the level of galactosylation (Clark, K.J. *et al*. 2005). In addition, standard process parameters of cell culture such as temperature (~37°C physiological condition), pH (~ pH 7.4 physiological conditions), time (10-14 days), and reactant (amine and sugar) concentrations, affect both the glycation reaction kinetics and extent.

Under typical batch-feed manufacturing conditions for MAbs, the cell culture medium is maintained at approximately 10,000-fold molar excess reducing sugar per mole protein product for the cell culture duration, indicating that the bimolecular glycation reaction kinetics would be pseudo first-order for the protein (Quan, C . *et al.* 2008). However, each MAb molecule has more than 100 primary amines, and the cell culture medium also contains significant levels of free amino acids and other compounds containing potentially reactive amines, thereby reducing the sugar molar excess for the glycation reaction. The protein glycation reaction extent is thought be governed mostly by the reactivity of accessible amino groups, although different sugars have different reactivity. For example, galactose is 5-fold more reactive than glucose (Bunn, H.F. and Higgins, P.J. 1981). In the artificial environment with complex chemical components present in cell culture medium and feeding conditions,

protein glycation occurrence can be expected, but the reaction kinetics and extent can be difficult to predict and control.

As the protein sequence differs between MAb molecules, the degree of glycation would also be expected to differ, even under similar cell culture conditions. Differences in cell culture process length, expressed MAb concentration, glucose feed strategy and the glucose concentration in the medium feeds would also be expected to impact glycation levels, making this a difficult problem to understand and control (Zhang, B. *et al.* 2008, Miller, A.K. *et al.* 2011, Yuk., I.H. *et al.* 2011).

Specificity and Structural Analysis of Glycation Sites on MAbs

In the past several decades, the primary sites of glycation have been analyzed for a number of proteins under a variety of conditions. On some proteins, glycation is evenly distributed, while on other proteins, the N-terminus (Holmquist, W.R. and Schroeder, W.A. 1964) and specific lysine residues (Zhang, B. *et al*. 2008, Gadgil, H.S. *et al.* 2010, Miller, A.K. *et al*. 2011) can have a greater degree of modification. Glycation distribution difference between studied protein molecules indicates that sequence or structure may determine the specificity of glycation reactions. In the past, it was thought that the apparent pKa and exposure of the amine attachment site determines the degree of Schiff base formation. In addition, the proximity of amino acids capable of proton abstraction helps catalyze the formation of the ketoamine, or Amadori product (Venkatraman, J. *et al*. 2001, Zhang, B. *et al*. 2008). Buffer components that can bind near the reaction site and abstract protons from sugars, such as phosphate, can also serve as a catalyst to increase the rate of formation of stable products (Watkins, N.G. *et al*. 1987). Thus, the protein amino acid sequence and reaction conditions can all affect the site specificity of glycation reactions.

A MAb contains many primary amine groups. In addition to four N-terminal amino acids, most MAbs have approximately 80 Lys residues, giving MAbs many potential sites for glycation (Lapolla, A. *et al*. 2000).

Historical data has shown that a typical MAb can be modified by glucose that results in very low abundances of glycation, with sites distributed over different amino acid residues. Often, the abundance of glycation product can be below the

detection limit of many analytical methods. For example, a study by Quan and coworkers showed that MAbs produced in a 10 day glucose containing cell culture were approximately 18% glycated overall including both light chains, and both heavy chains. The quantification of this MAb's overall glycation is based on percentage of glycated MAb separated from total MAb by boronate affinity chromatography (Quan, C. *et al*. 2008). Within this 18 % population of glycated MAbs, the glycation modification appeared as mono-glycation on 8 lysine residues on half of the molecule with low frequency (1–12%) at each of the eight lysine residues. (Quan, C. *et al*. 2008). These glycated species were separated from nonglycated material based on an approximately 0.05-pI charge unit difference and appeared as an acidic variant form in charge-based assays (Quan, C. *et al*. 2008). Because of the disperse locations and low abundance of glycation, chromatography methods did not produce good charge- or hydrophobicity-based separation to detect glycation modifications, therefore different glycation modification could not be detected. However, mass spectrometry and boronate affinity chromatography can be used to detect glycation. Both methods coalesce multiple glycation adducts into a single-unit modification, allowing separation between glycated and unglycated protein species, and specific detection on large and complex molecules such as MAbs (Zhang, B. *et al*. 2008, Quan, C. *et al.* 2008).

In recent years, researchers have reported site specific glycation on MAbs (Miller, A.K. *et al.* 2011, Gadgil, H.S. *et al.* 2010, Zhang, B. *et al.* 2008). For example, Zhang's group published a significant amount of work of a site specific glycation on lysine K49 of a particular MAb molecule. The glycation level on this

particular lysine K49 residue can be as high as 50% under typical cell culture conditions. Intensive studies have been carried out to study the effect of glucose to protein ratio and glucose feed strategies on MAb glycation in the hope of optimizing the cell culture condition to control the total glycation level of the MAb (Yuk, I.H. *et al.* 2011). This finding contrasts with historical data that have suggested that glycation sites are typically located randomly at all accessible lysine residues distributed over the entire molecule (Zhang, B. *et al*. 2008).

To date, only a few publications had proposed a mechanism of site specific glycation on MAbs. One theory is that site specific glyaiton is due to proton transfer with assistance from nearby amino acids. Sometimes,a histidine residue is hypothetically involved (Quan, C. *et al.* 2008). In other cases, a aspartic acid residue is thought to be involved (Zhang, B. *et al.* 2008). However, the exact mechanism of site specific glycation on MAbs is till yet to be determined. This uncertainty enhances the interest of study in the formation and control of glycation in MAbs.

Glycation in MAbs Drug Product Stability and Administration

Protein glycations may occur during formulation, packaging, long term storage, or clinical administration steps, where sugars are commonly used as excipients in liquid or lyophilized formulations of therapeutic proteins (Chang, B.S. and Hershenson, S. 2002). This modification of glycation is one of the primary reasons that formulation scientists tend to avoid using reducing sugars (glucose, lactose, fructose, maltose) in formulations.

Even for non-reducing disaccharides, such as sucrose, there is still a potential to generate reducing sugars by *in situ* hydrolysis, resulted in subsequent glycation modification. For example, sucrose can undergo hydrolysis – e.g. at low pH – to glucose and fructose. Smales, *et al.* demonstrated this hydrolysis for sucrose-based formulations undergoing viral inactivation at elevated temperatures (Smales, C.M. *et al*. 2000 and 2001). Similarly, glycation in sucrose-based formulations has been observed during storage studies (Fischer, S. *et al*. 2008, Gadgil, H.S. *et al*. 2007), although, at elevated temperatures and acidic pH. These extreme conditions are not within typical pharmaceutical formulation conditions, therefore the risk of protein glycation induced by sucrose hydrolysis in protein therapeutic is very low during the storage shelf life.

Finally, for delivering a drug to patients, sugars are often used in IV (intravenous) solutions to prevent precipitation of proteins, attain isotonicity of drug and provide an energy source for patients. Since some of the sugars commonly used for these purposes are reducing sugars (5% dextrose), the spontaneous glycation of

MAbs during IV administration cannot be prevented. In a recent study, two MAbs were 70% glycated after a 14 day incubation with 5% dextrose at ambient temperature. (Fischer, S. *et al.* 2008). However, under typical clinical conditions, MAbs are only in contact with IV solutions for a maximum of 8 hours. To the best of our knowledge, the glycation of MAbs under administration conditions in a clinical setting has not yet been reported yet (Vrdoljak, A. *et al*. 2004). Nevertheless, it is important to understand the glycation effect on MAbs during IV delivery, as drug compatibility with administration route is the final controllable step for ensuring the MAb's safety and efficacy to patient.

Impact of MAb Glycation on Its Biological Activities

Glycation of MAbs is of special interest due to the possible influence on the functionality of antigen binding, Fc effector function, and neonatal Fc receptor (FcRN) binding.

Antigen Binding

Quan, *et al.* 2008, studied the effect of glycation on *in vitro* potency of a MAb, where the second most susceptible site to glycation was located within the second complementarity-determining region (CDR) on the heavy chain (HC CDR2 K65). The glycated and unglycated MAb were separated by and fraction collected from boronate affinity chromatography. *In vitro* biological activity were assayed for each fraction. Even though there was glycation at an active binding site, there was little observable effect on bioactivity for the glycated boronate fraction, compared to unglycated. The glycated MAb showed similar binding activity to a biologically functional ligand. Although glycation at the 10% level at this one residue (K65) within one CDR was insufficient to affect potency, additional increase in glycation levels may ultimately be expected to interfere with the ligand-binding ability of the MAb. Also, the effect of glycation modification impact depends on the location of modified lysine, e.g. whether it is directly involved in antigen binding (Quan, C. *et al.* 2008).

Researchers are also interested in glycation impact on the stability of antibody-antigen complex. For example, Kennedy and coworkers reported antibody-antigen complex study based on surface plasmon resonance, in 1994. Although glycated MAbs had similar association constant (k_{ass}) with their antigen, compared with unglycated MAbs, the glycated MAbs have significantly higher dissociation constant

(k_{dis}) with their antigen, indicating that the glycated MAbs dissociate with their antigen faster. Therefore, glycation lowered the affinity ($Kd= k_{dis}/k_{ass}$) of MAbs to their antigens (Kennedy, D.M. *et al.* 1994). Because of the different approaches and detection techniques used, the results from different studies were not coherent, especially regarding the influence of glycation on the ability of MAbs to bind antigens and induce the complement cascade.

Fc effector Function, and FcRN Binding

Forced glycation studies using high pH conditions have shown that Fc functions of human antibodies, such as protein A binding and complement activation, can be impaired by glycation (Dolhofer-Bliesener, R. and Gerbitz, K.D. 1990). However, under physiologic conditions, binding activity of the Fc is less sensitive, presumably due to lower levels of glycation.

Goetze, *et al.* 2012 reported glycation of MAbs can result from incubation with a reducing sugar during circulation *in vivo*. The contributions to total glycation from the labile aldimine and more stable ketoamine forms were separately monitored via the use of selective sodium borohydride reduction. Since the Fab protein sequences are versatile, the Fab susceptibility to glycation, differs between antibodies. A number of studies have focused primarily on the conserved Fc regions (Goetze, A.M. *et al.* 2012). An attempt was made to model physiological glycation rates observed using a simple *in vitro* system. The impact of Fc glycation on function was also explored using surrogate binding assays that probed the interaction between MAbs and FcγRIIIa, neonatal Fc receptor (FcRn) and immobilized protein A (Goetze, A.M. *et al.* 2012).

Upon injection of a recombinantly produced human therapeutic IgG into humans, changes in the glycation levels could be observed as a function of circulation time (Goetze, A.M. *et al.* 2012). Mass changes on the individual MAb polypeptide chains as the results of glycation were determined using reversed-phase liquid chromatography/mass spectrometry. Changes to the light and heavy chains were low but easily detectable at 0.00092 and 0.0021 glucose additions per chain per day, respectively. Levels of glycation found on the Fc portion of MAb were, on average, 0.045 glucose molecules per fragment, after being isolated from healthy subjects. *In vivo* glycation rates can be approximated *in vitro* by modeling the physiological glycation reaction with a simplified incubation containing physiological glucose concentrations, pH and temperature, but with a high concentration of a single purified MAb. To test the impact of glycation on MAb function, highly glycated IgG1 and IgG2 were prepared containing on average 42–49 glucose molecules per MAb. In this study, binding to FcγIIIa receptors, neonatal Fc receptor, or protein A was similar or identical to the non-glycated MAb controls. Although the modifications were well distributed throughout the protein sequence, and at high enough levels to affect the elution position by size-exclusion chromatography, no changes in the tested Fc functions were observed (Goetze, A.M. *et al.* 2012).

Conclusions

Protein glycation reactions can occur to recombinant MAbs during many manufacturing process steps such as cell culture and storage, as well as during clinical administration to a patient and circulation in human body. Cell culture process is the initial place generating glycated recombinant MAbs. Clinical administration is the final step for controlling MAb glycation before introduction into patients.

Glycation modification results in structural heterogeneity in the MAbs. It changes MAbs charge, target binding capacities, and degradation rates (Zhang, Q. *et al*. 2009). However, the site specific glycation mechanism and effect of glycation impact on efficacy, safety and stability of MAbs are not well understood.

Development of sensitive and specific methods to monitor advanced glycation products is important to fully understand and monitor glycation during the manufacturing process and clinical administration of MAbs. Improved and more specific assays are also needed to assess the impact of novel protection strategies aimed at designing glycation inhibitors for therapeutic applications (Zhang, Q. *et al*. 2009).

In the quality-by-design (QbD) paradigm for manufacturing MAbs, the decision to monitor and control glycation for a given MAb would be a thorough evaluation process based on the impact of manufacturing parameters on MAb

glycation modification and the effect of glycation on MAb's biological function for safety and efficacy (Quan, C. *et al.* 2008).

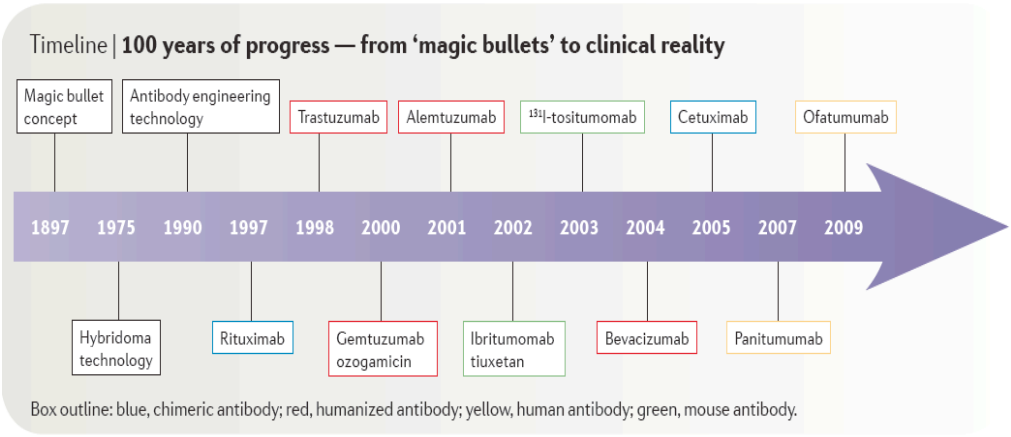

Figure 1-1: History of therapeutic monoclonal antibody from concept to FDA approval.

Reference: Weiner, L.M., Surana, R. and Wang, S. 2010.

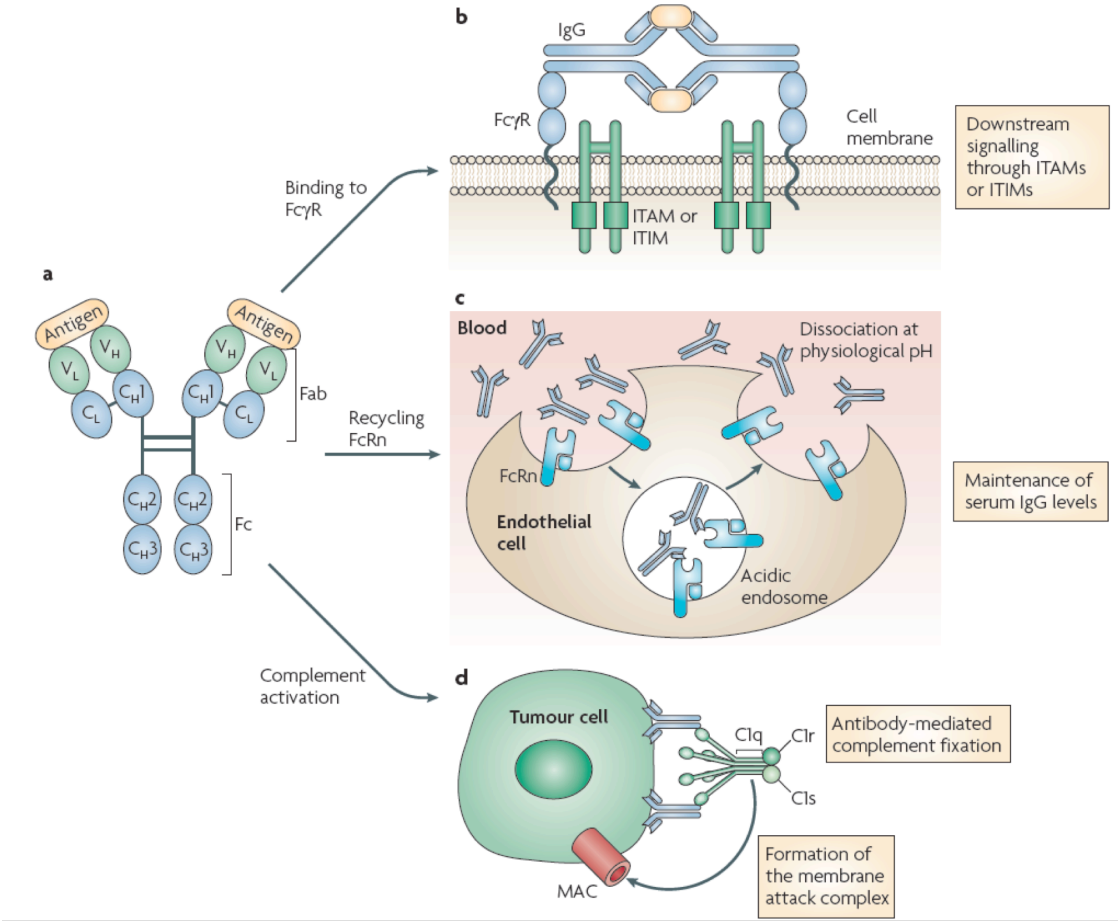

Figure 1-2: Diagram of structure of an antibody and its bioactivity.

Reference: Weiner, L.M., Surana, R. and Wang, S. 2010.

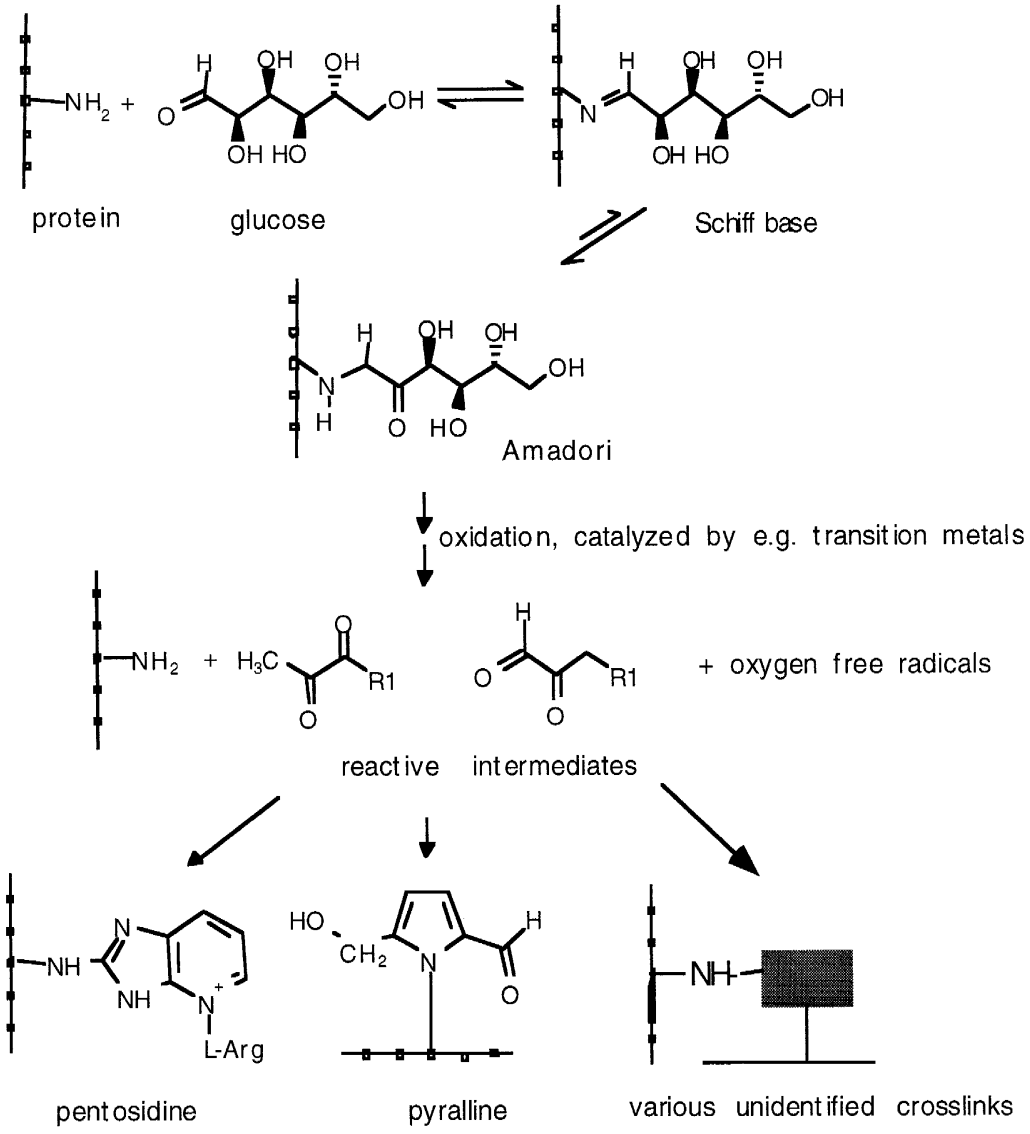

Figure 1-3: Chemistry of glycation reaction and advanced glycation reaction. Reference: Munch, G., Thome, J., Foley, P., Schinezel, R., Riederer, P. 1997.

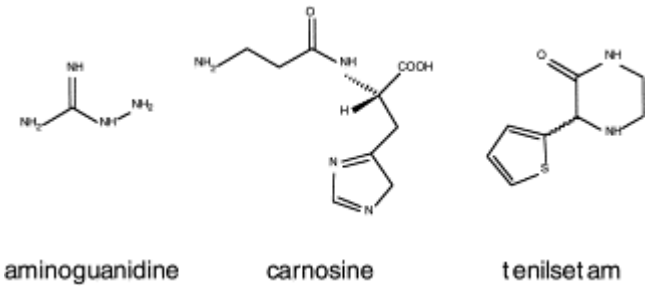

Figure 1-4**:** Chemical structures of the AGE-inhibitors: aminoguanidine, carnosine and tenilsetam.
Reference: Cameron, N.E. and Cotter, M.A. 1993.

Sugar	Formation of Chromophores (Browning)	Radical Formation (Intensity of ESR Spectra)
Glucose (C-6)	1	++
Fructose (C-6)	0.74	+
Xylose (C-5)	8.74	++
Methylglyoxal (C-3)	654	Not Determined
Glyceraldehyde (C-3)	1976	+++
Glycolaldehyde (C-2)	2109	++++

Table 1-1: Reactivity of different sugars (with beta-alanine as amino component) in the Maillard reaction.
Reference: Namiki, M. 1988.

Failure of Maintenance in Cells or Tissues	**Major Pathologies**
Neurones	Dementias
Retina, Lens	Blindness
Insulin Metabolism, Signaling	Complications of diabetes
Blood Vessels	Cardiovascular Diseases
Glomeruli	Renal Failure

Table 1-2: Human degenerative diseases with a proposed involvement of AGEs. Reference: Brownlee, M., 1992.

Trade and non-proprietary names	Type	Indication
Amevive (alefacept)	Fusion	Immunology
Avastin (bevacizumab)	Naked	Oncology
Bexxar (tositumomab)	Conjugate	Oncology
Campath (alemtuzumab)	Naked	Oncology
Cimzia (certolizumab pegol)	Fragment	Immunology
Enbrel (etanercept)	Fusion	Immunology
Erbitux (cetuximab)	Naked	Oncology
Herceptin (trastuzumab)	Naked	Oncology
Humira (adalimumab)	Naked	Immunology
Lucentis (ranibizumab)	Fragment	Ophthalmology
Mylotarg (gemtuzumab-ozogamicin)	Conjugate	Oncology
Orencia (abatacept)	Fusion	Immunology
Orthoclone OKT-3	Naked	Immunology
Raptiva (efalizumab)	Naked	Immunology
Remicade (infliximab)	Naked	Immunology
ReoPro (abciximab)	Fragment	Cardiovascular
Rituxan (rituximab)	Naked	Oncology
Simulect (basiliximab)	Naked	Immunology
Soliris (eculizumab)	Naked	Immunology
Synagis (palivizumab)	Naked	Infectious Disease
Tysabri (natalizumab)	Naked	Immunology
Vectibix (panitumumab)	Naked	Oncology
Xolair (omalizumab)	Naked	Immunology
Zenapax (daclizumab)	Naked	Immunology
Zevalin (ibritumomab tiuxetan)	Conjugate	Oncology

Table 1-3: Monoclonal antibodies and fusion proteins approved in the US as of May 2008.
Reference: Zider, A. and Drakeman, D.L. 2010.

Chapter 2

Characterization of an *In Vitro* Forced Glycated rhuMAb A and the Site Specificity

by

Hong Liu[1,3], Yi Yang[2]. Heather Flores[1], Trevor Swartz[1],

Thomas Patapoff[1], Paul Brandt[1] and Joel A. Dain[3]

is in preparation for submission to Analytical Biochemistry

1 Early stage pharmaceutical development, Genentech, 1 DNA way, South San Francisco, CA 94404.

2 Protein analytical chemistry, Genentech, 1 DNA way, South San Francisco, CA 94404.

3 Department of Chemistry, University of Rhode Island, 51 Lower College Road, Kingston, RI 02881.

Abstract

Recently, a site specific glycation on lysine K49 of rhuMAb A was reported (Zhang, B. *et al.* 2008), with a proposed mechanism of spatial proximity effect between lysine residue (K49) and nearby aspartate (D31) residue. To elucidate the mechanism of site specific glycation on K49 of rhuMAb A, an *in vitro* forced glycation model was employed to generate fully glycated rhuMAb A, a detailed analytical characterization on the glycated rhuMAb A was performed. Finally, molecular dynamics simulations were used to model the local electrostatic environment under solution conditions.

The *in vitro* forced glycation model showed that seven glycation sites were identified on this rhuMAb A, by using a series of analytical technologies such as boronate affinity chromatography, ESI-Mass spectrometry and peptide map. Among these seven sites, K49 was the primary glycation amino acid residue with 90% glycated. The six other sites were at various low levels of glycation. Molecular dynamics (MD) analysis results provided an insight that the high abundance of K49 glycation observed on rhMAb A may be caused by a strong electron-donating environment with three surrounding aspartates: D30, D31, and D105.

I. Introduction

In the past decades, there has been an increasing number of recombinant humanized monoclonal antibodies (MAbs) developed as therapeutics due to their high specificity and affinity to therapeutic antigen targets. As manufactured proteins, MAbs have the potential to be chemically modified during manufacturing process. MAbs are typically manufactured via a 10-14 day cell culture process. In this process a MAb is produced in Chinese Hamster Ovarian cells (CHO) then secreted outside the cell, into the culture medium, which contains glucoses as the cell's nutritional carbon source. This protein-glucose contact results in MAbs glycation (Quan, C. *et al.* 2008, Zhang, B. *et al.* 2008).

In most MAbs, the glycation level is <15% and widely distributed over the entire MAb molecule. In recent years, researchers have also reported site specific glycation on MAbs (Miller, A.K. *et al.* 2011, Gadgil, H.S. *et al.* 2010, Zhang, B. *et al.* 2008). Zhang's group, in particular, has published a significant amount of work describing a site specific glycation on lysine K49 of a rhuMAb A molecule. The glycation level on this particular lysine K49 residue can be as high as 50% under typical cell culture conditions. Intensive studies have been carried out to study how glucose to protein ratio, and glucose feed strategies can be altered to optimize the cell culture condition. The ultimate goal is control the total glycation level of rhuMAb A (Yuk, I.H. *et al.* 2011).

In the artificial environment with complex chemical components present in cell culture media and feeding conditions, the glycation kinetics and extent on MAbs can vary with cell culture conditions (Zhang, B. *et al.* 2008; Yuk, I.H. *et al.* 2011).

As the protein sequence differs between MAb molecules, the degree of glycation would also be different, even under similar conditions. The uncertainty of controlling MAbs glycation enhances the interest of study in the mechanism site-specific of glycation in MAbs.

To date, only a few publications have proposed a mechanism of site-specific glycation on MAbs. The proposed glycation mechanism suggests that nearby amino acids may facilitate proton transfer. Sometimes, a histidine residue is thought to be involved (Quan, C. *et al.* 2008), in other cases an aspartate residue may be involved (Zhang, B. *et al.* 2008).

With a great amount of mutation work on rhuMAb A, Zhang proposed that an adjacent aspartate residue D31 is the local catalyst for site specific glycation in rhuMAb A. D31 is spatially located 11 Å to lysine residue K49 based on the crystal structure of rhuMAb A. The mutation of this D31 to other amino acids may reduced the glycation level of K49. However, in Zhang's study, there were several cases where K49 lysine was still glycated up to 20% after replacing D31 with different amino acids.

In order to further examine the mechanism of site specific glycaiton on K49 of this rhuMAb A, we employed an *in vitro* forced glycation model to generate close to 100% glycated rhuMAb A. We also performed comprehensive analytical characterization on the glycated rhuMAb A produced using this model system. Then, we applied molecular dynamics simulations to determine the local environment of the primary modified lysine K49 by mimicking the rhuMAb A in aqueous solution.

II. Experimental

II. 1. Materials and Reagents

A regular lot of rhuMAb A (27 mg/mL, PBS buffer, pH 7.4) bulk material was obtained from Genentech. Sequencing grade trypsin (TPCK treated) was purchased from Promega (Madison, WI), and Peptide: N-glycosidase F (PNGase F) from New England BioLabs Inc (Ipswich, MA). *N*-(2-Hydroxyethyl)piperazine-*N*¢-(3-propanesulfonic acid) (EPPS; 99.0%) and dithiothreitol (DTT; ultrapure) were obtained from USB Corp. (Cleveland, OH). D-Sorbitol (minimum 98%), R-D-glucose (ACS reagent), iodoacetic acid (IAA; _99%), and R-cyano-4-hydroxycinnamic acid (CHCA) were procured from Sigma-Aldrich (St. Louis MO). HPLC grade acetonitrile (ACN) and methanol were purchased from Fisher Scientific (Fair Lawn, NJ). Water used in all experiments was obtained from a Milli-Q Plus purification system (Millipore, Bedford, MA).

II.2. *In Vitro* Glycation of rhuMAb A

The rhuMAb A in PBS buffer, pH 7.4, was further glycated *in vitro*. rhuMAb A was buffer exchanged into glycation buffer with dialysis prepared in 15 ml cassette with 10kD membrane. The final *in vitro* glycation solution contains 50mg/ml rhuMAb A with 1200 mM D-glucose, in 20 mM sodium phosphate buffer, pH 7.4. The *in vitro* glycation solution was kept in an incubator at 37 °C for 24 hours. The *in vitro* glycation solution was immediately buffer exchanged using a 15 ml dialysis cassette with 10kD membrane into phosphate buffer, pH 6.5. The samples were then stored at -70°C until analysis.

II.3. Boronate Affinity HPLC

Early stage glycation adducts often can be identified by a boronate affinity HPLC method to determine the overall glycation level on a whole protein, using a TSK gel boronate 5PW column 7.5x75mm. The mobile phase A was 50mM EPPS, 10mM Tris, 200mM NaCl, at pH 8.7, and mobile phase B, 500mM sorbitol added mobile phase A. The mobile phase flow rate 1 mL/min and the column temperature was maintained at 40°C with a UV and fluorescence detector. The gradient for HPLC elution required optimization for rhuMAb A. (Zhang, B. *et al.* 2008)

II. 4 Enzymatic Digestion of rhuMAb A

Several enzymatic treatments were performed on rhuMAb A samples before they were analyzed for reverse phase-HPLC, or mass spectrometric analyses, to determine the amino acid sequence and structural integrity of rhuMAb A.

PNGase F Treatment. PNGase F was used to remove the oligosaccharides in the Fc portion of a MAb. The rhuMAb A samples were buffer exchanged into 50 mM Tris buffer, pH 7.5, using a NAP-5 column. The protein concentration was adjusted to 2.5 mg/mL. PNGase F was added in an enzyme-to-substrate ratio of 1:600 (w/w). The digestion was performed at 37°C overnight (15 h).

Tryptic Digestion. Prior to tryptic digestion, rhuMAb was reduced with DTT and then alkylated with IAA. Typically, 250 μL of antibody sample (2 mg/mL) was mixed with 20 μL of 1 M DTT in 730 μL of 6 M guanidine, 50 mM Tris, pH 8.0. The mixture was incubated at 37 °C for 1 h. It was then cooled to room temperature, and 50 uL of 1 M (IAA) in 1 M NaOH was added for carboxymethylation. The

alkylation reaction was incubated at room temperature in the dark for 15-20 min. The residual IAA was quenched by the addition of 10 μL of 1 M DTT. The reduced and carboxymethylated rhuMAb A was then buffer exchanged into the digestion buffer, which contained 25 mM Tris, 1 mM $CaCl_2$, pH 8.3, using a PD-10 column (Sephadex G-25 medium, GE Healthcare). Trypsin was added at an enzyme-to-substrate ratio of 1:50 (w/w). The solution was mixed briefly and incubated in a 37°C water bath for 5 h. The digestion was terminated by adding 0.3% (v/v) trifluoroacetic acid (TFA) to the solution. The digest was then stored at -70°C until analysis.

II.5. Reverse Phase-HPLC with Electron Spray Ionization/ Mass Spectroscopy (RP-HPLC-ESI/MS)

The molecular masses of the intact, PNGase F-treated, and reduced rhuMAb A samples were determined by using a LC/ESI-MS setup coupled with an Agilent 1090 HPLC system with a PE Sciex API 3000 electrospray ionization triple-quadrupole mass spectrometer (Applied Biosystems, Foster City, CA). The samples were desalted by reverse phase –HPLC (RP-HPLC) using a capillary column (Poros R1, 0.33 _ 200 mm) equilibrated at a flow rate of 200 *u*L/min with 0.2% formic acid (solvent A) at a column temperature of 40 °C. Samples were eluted using a linear gradient from 25% solvent B (0.2% formic acid in acetonitrile) to 70% solvent B over 16 min. The elutant from the RP-HPLC column was directed into the mass spectrometer operating in the positive ion mode. For post-reduction analysis, samples were incubated in 25 mM DTT for 15 min at 37 °C prior to LC/MS analysis.

II.6. Tryptic Peptide Mapping

The flow through factions (intact unglycated rhuMAb A) and retained factions (intact glycated rhuMAb A) on BAC were collected. Both glycated and unglycated rhuMAb A fractions were then digested by enzyme trypsin. Peptides profiles of tryptic-digested rhuMAb A were analyzed subsequently by an RP-HPLC using a Jupitor C18 2.0x250 mm column at 45°C and UV detection at 214nm. The flow rate was at 0.25ml/min, in mobile phase A: 0.1% TFA in water and B: 0.09% TFA in acetonitrile. The gradient was optimized for this rhuMAb A. By comparing the peptide maps of glycated and unglycated rhuMAb A, the distinctive peptide factions on glycated rhuMAb A were collected for further characterization by MALDI-TOF MS/MS sequencing.

II.7. Protein Chip Matrix Assisted Laser Desorption Ionization- Time-Of-Flight mass spectrometry (MALDI-TOF)

Isolated tryptic peptides were spotted individually on a SCOUT 384 multi-probe plate with a CHCA matrix and analyzed in the positive mode using a Bruker Ultraflex-I MALDI-TOF-TOF mass spectrometer (Bremen/Leipzig, Germany). Selected precursor ions were subjected to collision-induced dissociation with argon as the collision gas. LIFT mode was used to analyze all fragment ions in single sweep, and data were processed with Flex Analysis software.

II.8. Molecular Dynamics (MD) Simulations

To compare K49's property with all lysine residues on this rhuMAb A, molecular dynamics simulations were performed to analyze the movements of lysine residues by calculating their motions in aqueous solution. Based on the IgG1 protein framework, a generic model was built which includes common intra-molecule forces for a MAb. rhuMAb A's particular protein amino acid sequence was applied to this model to generate a molecule specific 3D structure in aqueous solution. Lysine's solvent accessible surface area (SASA) was determined by AREAIMOL (CCP4 supported Program), which is based on a "rolling ball" algorithm (Lee, B., and Richards, F.M., 1971). This algorithm uses a sphere of water as a particular radius to 'probe' the surface of the rhuMAb A molecule then calculate the exposure area of a particular lysine.

Furthermore, molecular dynamics was applied to determine the lysine's local environment via a computer simulation of physical movements of atoms and molecules. In a given time, the atoms on this rhuMAb A were allowed to interact with and move in the aqueous solution, resulting a view of the motion of the atoms. In these simulations we performed explicit water (with 11780 water molecules) molecular dynamics (MD) simulations of a set of FAb fragments and calculated different properties. Focus was placed on lysine residues to identify the properties of lysine residues which might correlate to experimentally observed glycation formation propensities in rhuMAb A. This approach is different from the empirical methods discussed above, because we calculated dynamic properties of the protein that could not be determined from the static structure.

Throughout these simulations, the temperature was kept constant by coupling the system to a temperature bath of 300 K using simulation algorithm (Bussi, G., Donalido, D., Parrinello, M., 2007) at pH7.4. Histidines on rhuMAb A were unprotonated. During equilibration, the volume was initially kept constant by coupling the system to a pressure bath at 1.0 atm (Bernedsen, H.J.C., Postma, J.P.M. *et al.* 1984). Following equilibration, the simulations were kept at constant pressure. Following equilibration, a set of trajectories with 75ns duration was performed. Trajectories from MD simulations were then analyzed with various tools available in AMBER program suite. (Case, D.A. *et al.* 2005)

III. Results

III.1. Boronate Affinity HPLC

We determined total glycation level of rhuMAb A by using boronate affinity chromatography (BAC). Boronate affinity chromatography is based on the formation of a five- member ring structure between a sugar's cis-hydroxl groups and boronate ion's negative charge on the column (Figure 2-1). The affinity to sugar ensures boronate capture the glycated protein under alkaline condition. After loading onto a boronate affinity column, protein samples were eluted with a gradient of a competing sugar, sorbitol. Unglycated proteins were eluted at ~2.4 min, while glycated proteins were detected at ~25 min. The elution conditions used here did not provide resolution of proteins with different sugar to protein ratios. Therefore, the overall glycation level was defined as percent peak area of the retained peak on boronate affinity chromatograms.

From this study result, glycated rhuMAb A from a regular glucose batch feed process (batch feed protein to glucose concentration, 1.5g/L titer: 8g/L glucose feed) was 42.0% based on the integration of the retained peak area, as shown in Figure 2-2a. This indicates 42% of rhuMAb A contained at least one glucose addition modification per protein. In comparison, under forced glycation condition (24 hours incubation with 1.2M of glucose in 20mM sodium phosphate, pH 7.4 at 37°C), this rhuMAb A was nearly fully glycated, such that 99.3% of the rhuMAb A contained at least one glycation modification (Figure 2-2 b).

III.2. RP-HPLC-ESI/MS

Because BAC cannot determine the glucose to protein ratio, Electron Spray Ionization/ Mass spectrometry (ESI/MS) was applied to determine the approximate numbers of glucose per rhuMAb A on the forced glycated rhuMAb A sample. In order to measure the mass, rhuMAb A was reduced, then separated into light chains and heavy chains on reverse phase chromatography. The eluted chromatography fractions went through an ESI/MS mass analyzer. Molecular mass of the light chains and the heavy chains species were determined individually. As shown in Figure 2-3, four species with different molecular weights were detected in the mass profile of the fully glycated rhuMAb A light chains. They ranged from no glucose to a maximum of three glucoses per light chain. The majority of glycated light chains contained only single glycated specie. For glycated heavy chains, as shown in Figure 2-4, three different heavy chain glycation species were observed. They ranged from no glucose to a maximum of two glucoses addition per heavy chain. The majority of heavy chains were native species containing no glucose modification. It is notable that the most abundant glycation was found on the light chain of rhuMAb A.

III.3. Tryptic Peptide Map

The next question to be answered was which amino acid sites on the primary sequence level were glycated. Identification of the glycated amino acid sites was attempted by tryptic peptide mapping. Tryptic peptides were generated by enzymatic digestion of rhuMAb A. The digested peptide fragments were separated on RP-HPLC, resulting in a unique peptide elution profile of each protein faction

(unglycated and glycated fractions) from BAC. By comparing peptide-map profile of the glycated and unglycated samples, glycated peptide fragments were detected. MS/MS analysis was performed on the putative glycated peptide fragments to assign the peptide sequence and identify the amino acid site of modification. Table 2-1 summarizes the glycation level of amino acid sites that were glycated under forced glycation condition. There were a total of seven amino acid sites on rhuMAb A that had various levels of susceptibility to glycation. It is notable that light chain lysine 49 (K49) was the primary amino acid site modified by glycation, where 90% of this particular residue on rhuMAb A was glycated. The next most glycated site was the heavy chain N-terminal, glutamic acid's alpha amino group, with 5% glycated only. All the other sites were glycated at very low levels, less than 5% modified. This site-specific result agrees with published work on non-forced glycation of rhuMAb A by Zhang, *et al* . (Zhang, B. *et al* . 2008).

III.4. Understanding The Cause of Site Specific Glycation by Molecular Dynamic (MD) Simulations

What special property does K49 have that allows such a high extent of modification by glycation? Does it happen to be more solvent accessible, which increases the probability of reaction with glucoses? Or is there a special local electrostatic environment?

The solvent accessible surface area (SASA) of each lysine residue was determined using AREAIMOL calculation. The summary of average SASA on each

lysine residue is shown in Table 2-2. It is notable that K49 was not the most solvent accessible lysine residue on rhuMAb A.

Also, the local environment of glycated lysine residues, especially the potential aspartate to lysine pairing effect, was evaluated. There were three major results: the average distance between D31 to K49 was 11.8Å, which agrees with Zhang's report. However, D31 to K49 is not the only spatial adjacent (D:K) pair in rhuMAb A. There were five other (D:K) pairs of a distance ~5.5 Å. Interestingly, only two of the five lysine residues were glycated. More importantly, lysine K49 was surrounded by three aspartates. They were light chain D30, D31 and another aspartate on heavy chain, D105. D30 and D31 had similar spatial distance to K49. However, the D105 was only 5.4 Å to K 49, a much closer spatial distance than D30 or D31 had (Figure 2-6). These three aspartate residues also had different solvent accessible surface areas. As shown in Table 2-3, D30 and D31 had the highest SASA value among all aspartate residues that were paired with lysine residues. On the other hand, D 105 had the lowest SASA value.

IV. Discussion

From the characterization study result, *in vitro* forced glycation can successfully produce a nearly 100% glycated rhuMAb A. The ESI/MS result indicated that the forced glycation of rhuMAb A forms a heterogeneous mixture, with different extents of glucose modification. To understand the complexity of the fully glycated rhuMAb A, we calculated the possible glucose to rhuMAb A ratio, based on different scenarios of glucose modification on light chains and heavy

chains. By combining possible glucose ratio on both heavy chains and both light chains, we estimated that the average intact rhuMAb A may contain from one to ten glucoses per molecule, with the majority containing at least one glucose on the light chain.

The forced glycation model of rhuMAb A was also proven to mimic the site specific glycation in typical cell culture conditions, meaning the most susceptible glycation site is still light chain lysine, K49. Since this forced glycation model provides high abundance of glycated rhuMAb A in a much rapid manner than a 10-14 day cell culture, it becomes a great tool to investigate site specific glyation reaction on MAbs and proteins.

In the past, researchers had shown that glycation specificity is not governed by the pKa of an amine group, rather by the internal micro-environment of a protein. Neighboring amino acids can often involve a catalyst effect. Watkins, *et al.* first reported specificity of glycation on RNase in 1985. They reported that certain lysine residues, especially the ones close to the RNase active site, were easy to be glycated. On the other hand, the surface lysine residues were relatively inactive. Watkins also proposed that both the Schiff base equilibrium concentration and the rate of Amadori rearrangement at lysine residues were important in determining the specificity of RNase glycation (Watkins, N.G. *et al.* 1985 and 1987). For site specific glycation in MAbs, Quan, *et al.* had observed histidine presence near a lysine residue, and proposed that a histidine residue may act as a proton transfer which could help to glycate nearby lysines (Quan, C. *et al.* 2008).

In the case of rhuMAb A glycation specificity, Zhang's group proposed an aspartate catalyst effect in 2008. The proposed mechanism was based on intensive mutation work, suggesting that light chain aspartate D31 is the essential catalyst for K49 site-specific glycation phenomenon. However, even with mutations of D31 to other amino acids, such as threonine, lysine K49 was still glycated to a relatively high level, ~ 25% compared to ~ 40% before mutation . Since Zhang's estimation of spatial distance of D31 and K49 was based on static crystal structure, it does not represent the lysine residue's activity and movement in a dynamic liquid environment.

In our study, molecular dynamics was used to evaluate K49's dynamic motions in aqueous solution. Two parameters were calculated 1) solvent accessible surface area, and 2) the distance between aspartate residues and lysine residues on this rhuMAb A's Fab region.

The presented work demonstrated: Lysine K49 does not exhibit the highest solvent accessible surface area (SASA) compared with other lysine residues. Rather K49 is on the lower rank of exposed lysine residues, indicating that site-specific glycation on rhuMAb A is not determined by solvent accessibility. Among five lysine residues, which have aspartate spatially close to them, only two lysines (K49 and K75) were significantly glycated. This indicates that the presence of aspartate near by lysines does not necessarily catalyze glycation either. Finally, a total of three aspartates are thought to be involved in K49 microenvironment. However, the distances and angles between these aspartate residues and K49 do not favor formation of hydrogen bond. D30 and D31 are located 11 Å from K49, which is too

far to form hydrogen bonds with K49. D105 is only 5.3 Å from K49, which is still too far to form a hydrogen bond. Therefore, it is unlikely that these aspartate residues react or bond to lysine K49 directly to promote glycation. Instead, the three aspartate residues together are thought to provide a strong electron-donating environment around K49 at physiological pH.

How would this catalysis work? Do the aspartate residues directly react with glucose rather than lysine? We are inspired by knowledge learned from nature, especially the enzymatic mechanism of two enzymes in sugar metabolism: Aldose B and Triose phosphate isomerase. Aldose B has an active site involving an aspartate residue D33, and a lysine residue K229. These two residues act as mediators to shuttle the electron on the carbonyl group and the hydroxyl group on sugar. (Cox, T.M. 1994 ; Garrett, R.H and Crisham, C.M., 2010). Triose phosphate isomerase also contains a basic glutamate residue E165 and an acidic proton-donating histidine residue H95 to convert the –CHO aldehyde to a –C=O ketone group of sugar (Harris, T.K. *et al.* 1998). These two enzymes both use an electron donating rich residue (aspartic acid, glutamic acid) that are negatively charged (aspartate, glutamate) at physiological pH, to help extract a proton from hydroxyl group on sugar. At the same time, an acidic proton-donating residue (lysine, histdine) donates a proton to sugar's carbonyl group, resulting in conversion of carbon one's carbonyl group to a hydroxyl group. These reactions are also essential steps for glycation Schiff base formation and Amadori rearrangement as well.

With the knowledge obtained from mechanisms of sugar metabolism enzymes, we hypothesize that D30, D31 and D105 work cooperatively around K49

to promote K49 glycation in two steps. First, by creating a negatively charged microenvironment, D30, D31 may act as a porter to attract glucose and keep glucose in the vicinity close to K49. D30 or D31, that has high solvent accessible surface area, withdraws the hydrogen from carbon two in glucose. The hydrogen withdraw causes carbon two to carry a negative charge and carbon one to carry positive charge. At physiological condition pH 7.4, K49 is unprotonated, allowing it to attack the carbon one, assisting in the formation of a Schiff base. Once a Schiff base is formed, the extra aspartate D105, which is close to K49, may be involved in further electron transfer, by shifting an electron of the C=N double bond on carbon one to the C=O double bond on carbon two, to form a ketone. This is assisting the Amadori rearrangement. Thus, the high abundance of K49 glycation observed on rhMAb A may be a consequence of two sequential steps, catalyzed by neighboring aspartate residues

V. Conclusions

The unique site-specific glycation of rhuMAb A makes this rhuMAb A a valuable model protein to study IgG structure modification by glycation. Several conclusions can be made from this study.

1) The forced glycation model is successful to analyze glycation modification from the whole protein level to the primary amino acid level.
2) The forced glycated rhuMAb A molecule is shown to be a mixture of species with various levels of glycation with complex structure modification.
3) Site-specific glycation on K49 is not due to spatial proximity of D31. Instead, a strong electron-donating environment created by three near by aspartates: D30, D31, and D105 may facilitate K49's specific glycation.

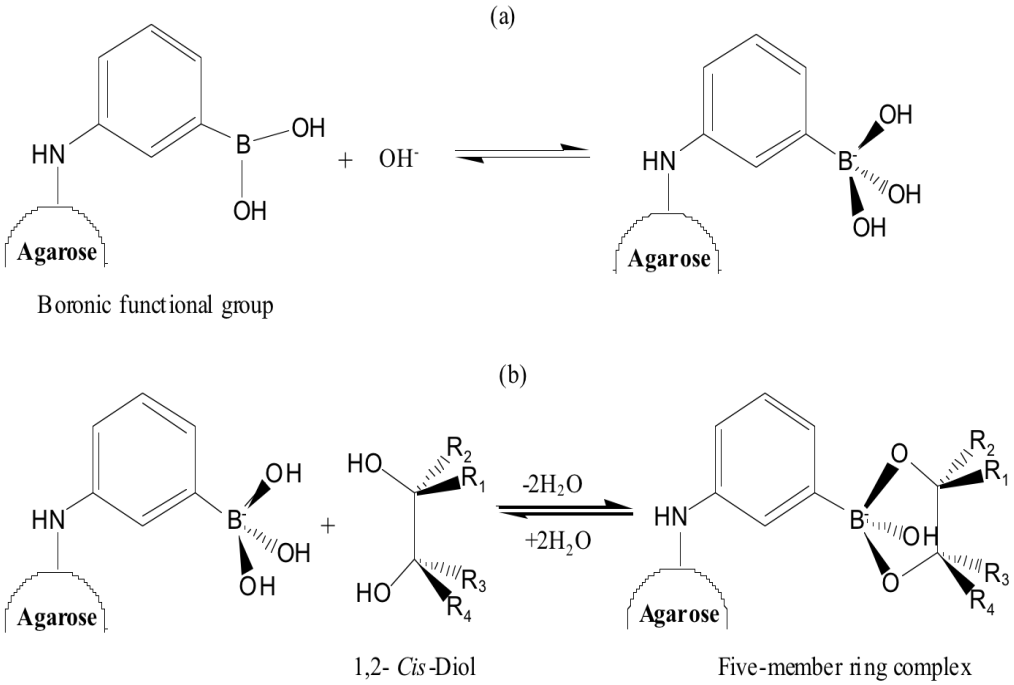

Figure 2-1: Schematic illustration on boronate affinity resin reacts with carbohydrate's cis-diol group.
a) boronate carries a negative charge under alkaline condition.
b) Cis-diol group forms a five-member ring with boronate by dehydration then retains on resin.

Reference from: Li, A., Pfuller, U., Larsson E.V., Jungvid, H., Galaev, I.Y., Mattiasson, B. (2001). Separation of mistletoe lectins based on the degree of glycosylation using boronate affinity chromatography. *Journal of Chromatography A*. **925** , 115-121.

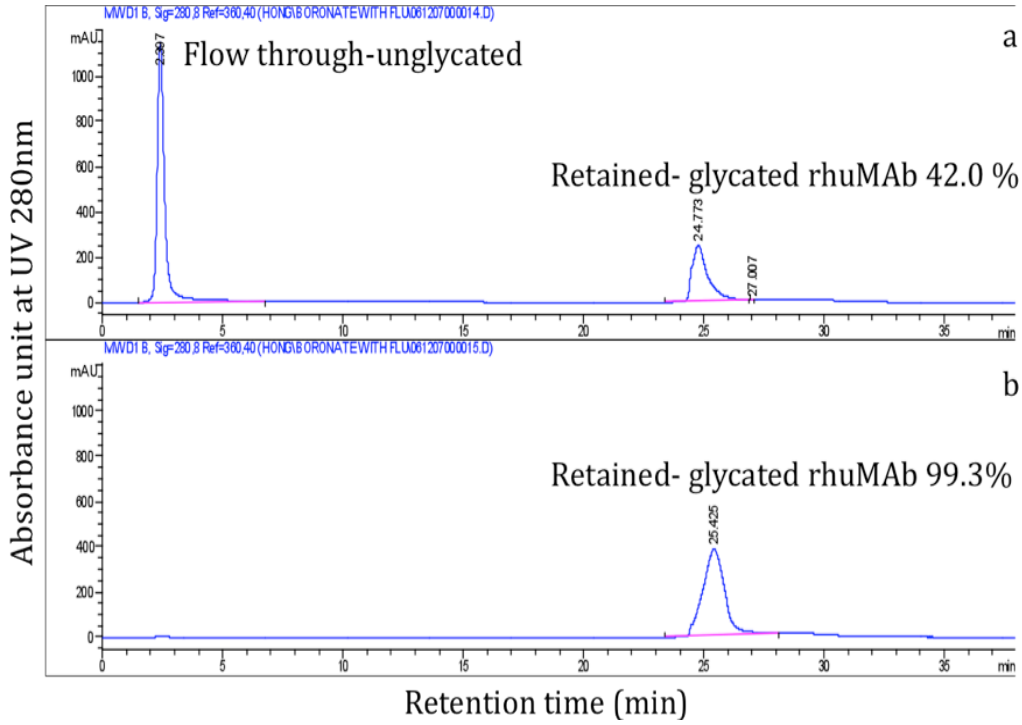

Figure 2-2: Boronate affinity chromatograms of rhuMAb A.
a) rhuMAb A from regular batch feed process.
b) Forced glycated with 1M glucose in phosphate buffer pH 7.4 for 24hours at 37°C *in vitro*.

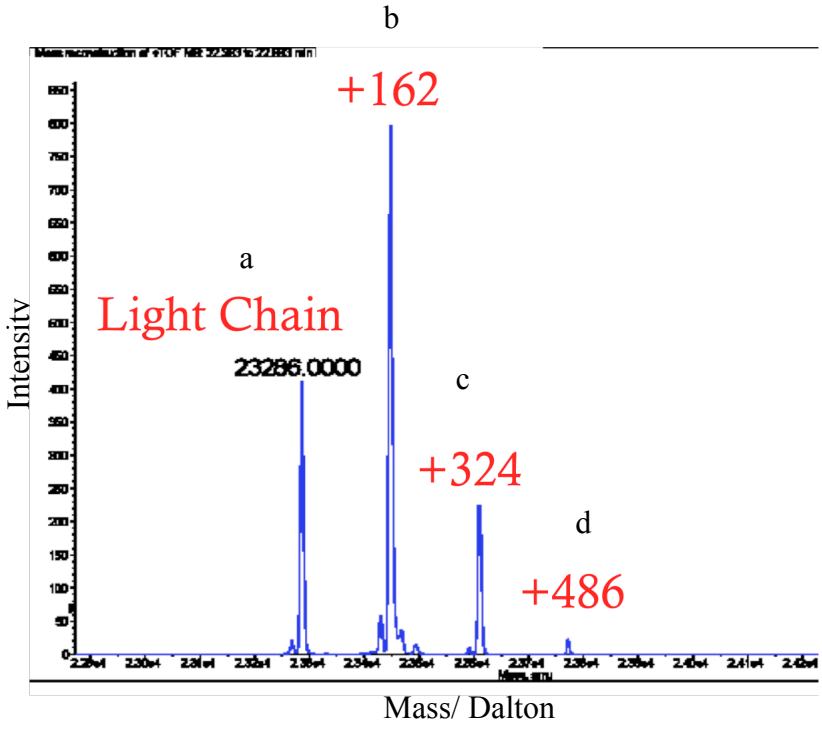

Figure 2-3 : ESI-MS measured the molecular mass of glycated rhuMAb light chain. Four molecular weight peaks were detected:

a) native light chain mass 23286 dalton/mol;
b) one glucose added light chain with mass 23448 dalton/mol;
c) two glucose added light chain with mass 23610 dalton/mol;
d) three glucoses added light chain with mass 23772 dalton/mol.

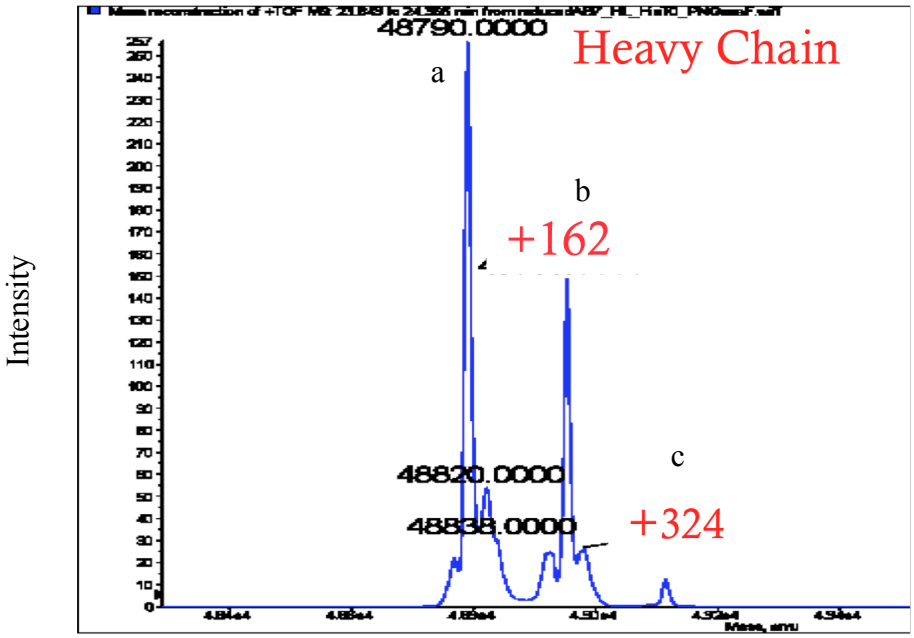

Figure 2-4: ESI-MS measured the molecular mass of glycated rhuMAb A heavy chain.
Three molecular weight peaks were detected:
a) native heavy chain mass 48790 dalton/mol;
b) one glucose added heavy chain with mass 48952 dalton/mol;
c) two glucoses added heavy chain with mass 49114 dalton/mol.

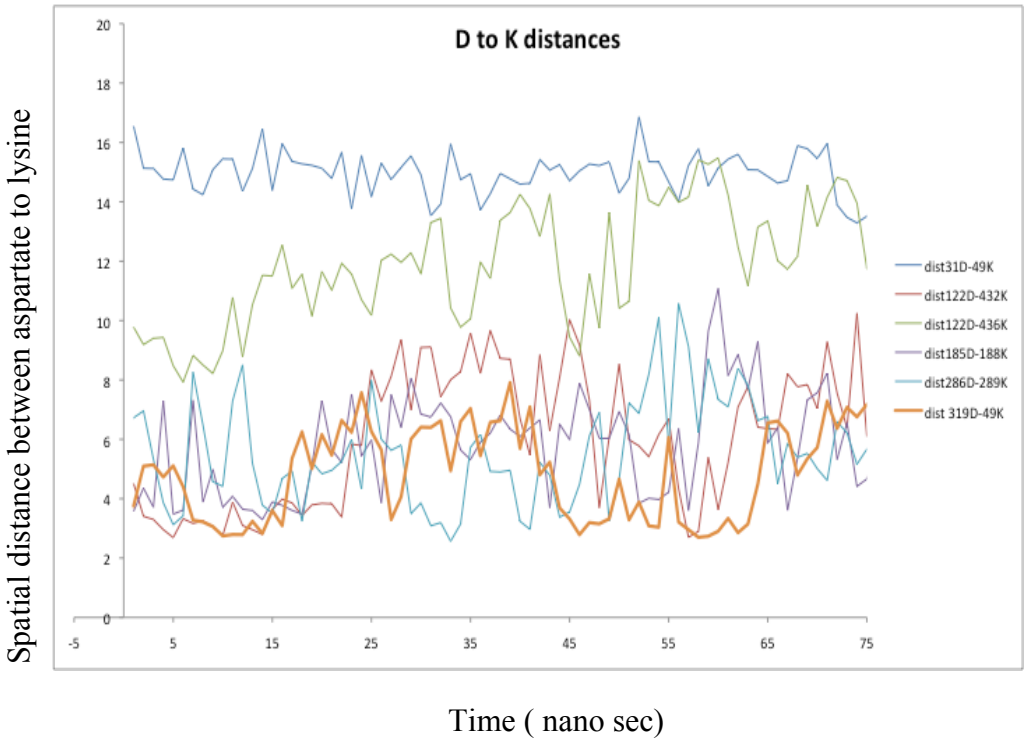

Figure 2-5: Graph of spatial distance (between aspartate residues to lysine residues) vs. time over 75 nanoseconds by molecular dynamics simulations.

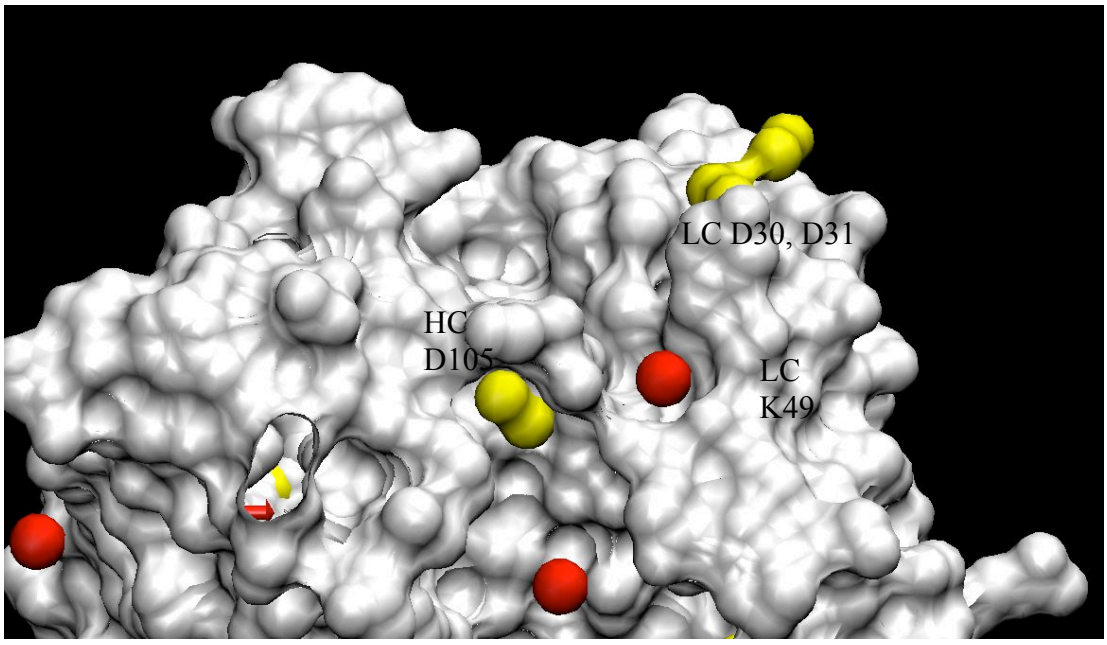

Figure 2-6: Illustration of MD simulated locations of K49, D30, D31 and D105 on rhuMAb A's Fab region.

Table 2-1: Summary of glycation level on primary amino acid sites of rhuMAb A's light chain and heavy chain.
Glycation modification extent was measured by tryptic peptide map.

Modified amino acid sites	Glycated (%)
LC-K49	90.5
LC-K149	0.9
HC-K64	0.5
HC-K75	2.2
HC-K133	0.5
HC-E1 (heavy chain N-terminal)	4.9
LC-D1 (light chain N-terminal)	0.3

Amino Acid	Heavy Chain or Light Chain	#	Solvent Accessible Surface Area (Å^2)	Detected Glycation
LYS	HC	222	148.572	
LYS	LC	169	144.434	
LYS	HC	205	127.637	
LYS	HC	210	124.482	
LYS	LC	145	124.274	
LYS	LC	126	121.164	
LYS	**HC**	**64**	**116.242**	**+/0.5%**
LYS	HC	43	114.802	
LYS	LC	42	113.749	
LYS	**HC**	**75**	**111.675**	**+/2.2%**
LYS	**HC**	**133**	**110.161**	**+/0.5%**
LYS	LC	188	109.156	
LYS	LC	190	107.675	
LYS	HC	214	93.7401	
LYS	LC	45	93.4605	
LYS	LC	107	92.3458	
LYS	LC	183	90.6972	
LYS	HC	121	90.5255	
LYS	LC	207	85.7253	
LYS	LC	103	68.0554	
LYS	LC	39	67.3747	
LYS	**LC**	**49**	**63.3898**	**+ /90.5%**
LYS	HC	218	57.2227	
LYS	HC	213	50.0781	
LYS	**LC**	**149**	**48.2433**	**+/0.9%**

Table 2-2: Solvent accessible surface area of all the lysine residues on rhuMAb A.

Lysine Position	Aspartate Position	Average Distance (Å)	Detected Lysine GLycation	Aspartate SASA
LC K49	LC D30	11.8	+	70
LC K49	LC D31	11.8	+	77
LC K49	HC D105	5.3	+	33
LC K188	LC D185	5.3		63
HC K75	HC D72	5.5	+	44
HC K218	LC D122	5.5		85
HC K222	LC D122	5.5		85

Table 2-3: Summary of lysine to aspartate pairs with average spatial distance between lysine and aspartate.

Citations:

Zhang, B., Yang, Y., Yuk, I., Pai, R., Mckay, P. and Eigenbrot, C. (2008). Unveiling a glycation hot spot in a recombinant humanized monoclonal antibody. *Analytical Chemistry,* **80**, 2379–2390.

Quan, C.P., Alcala, E., Petkovska, I., Matthews, D., Canova-Davis, E. and Taticek, R. (2008). A study in glycation of a therapeutic recombinant humanized monoclonal antibody: where it is, how it got there, and how it affects change-based behavior. *Analytical Biochemistry*, **373**, 179–191.

Miller, A.K., Hambly, D.M., Kerwin, B.A., Treuheit, M.J. and Gadgil, H.S. (2011). Characterization of site-specific glycation during process development of a human therapeutic monoclonal antibody. *Journal of Pharmaceutical Science,* **100**, 2543–2550.

Gadgil, H.S., Bondarenko, P.V., Pipes, G., Rehder, D., McAuley, A., Perico, N. (2007). The LC/MS analysis of glycation of IgG molecules in sucrose containing formulations. *Journal of Pharmaceutical Science* **96**, 2607–21.

Yuk, I.H., Zhang, B., Yang, Y., Dutina, G., Leach, K.D., Vijayasankaran, N., Shen, A.Y., Andersen, D.C., Snedecor, B.R., Joly, J.C., (2011) Controlling glycation of recombinant antibody in fed-batch cell cultures. *Biotechnology and Bioengineering,* **108**, 2600-2610.

Lee, B., and Richards, F.M., (1971). The interpretation of protein structures: estimation of static accessibility, *Journal of Molecular Biology*, **55**, 379-400.

Bussi, G., Donalio, D., Parrinello, M. (2007) Canonical sampling through velocity rescaling *Journal of Chemical Physics* 126.

Berendsen, H.J.C., Postma, J.P.M., Vangunsteren, W.F., Dinola, A., Haak, J.R. (1984). Molecular-Dynamics with couping to an external bath. *Journal of Chemical Physics*. **81**, 3684

Case, D.A., Cheatham, T.E., Darden, T., Gohlke, H., Luo, R., Merz, K.M., Onufrlev, A., Simmerling, C., Wang, B., Woods, R.J., (2005) The Amber biomolecular simulation programs. *Journal of Computation Chemistry*. **26** (16) 1668-1688.

Li, A., Pfuller, U., Larsson, E.V., Jungvid, H., Galaev, I.Y., and Mattiagsson, B., (2001) Separation of misletoe lectins based on the degree of glycosylation using boronate affinity chromatography. *Journal of Chromatography,* **925** 115-121.

Watkins, N.G., Thorpe, S.R., and Baynes, J.W. (1985) Glycation of amino group in protein. *Journal of Biological Chemistry*, **260**, 10629-10636.

Watkins, N.G., Neglia-Fisher, C.I., Dyer, D.G., Thorpe, S.R. and Baynes, J.W. (1987). Effect of phosphate on the kinetics and specificity of glycation of protein. *Journal of Biological Chemistry*, **262**, 7207–7212.

Cox, T.M. (1994). Aldolase B and fructose intolerance. *FASEB Journal*, **8** 62-71.

Garrett, R.H., Crisham, C.M., (2010) *Biochemistry 4th Edition.* Brooks/Cole.

Harris,T.K., Cole, R.N., Mildvan, A.S. (1998) Proton transfer in the mechanism of triosephosphate isomerase. *Biochemistry* **37,** 16828-16838.

Chapter 3

Degradation Pathway and Degradation Products of Glycated rhuMAb A

by

Hong Liu[1,3], Yi Yang[2]. Heather Flores[1], Trevor Swartz[1],

Thomas Patapoff[1], and Joel A. Dain[3]

is in preparation for submission to Journal of Pharmaceutical Sciences

1 Early stage pharmaceutical development, Genentech, 1 DNA way, South San Francisco, CA 94404.

2 Protein analytical chemistry, Genentech, 1 DNA way, South San Francisco, CA 94404.

3 Department of Chemistry, University of Rhode Island, 51 Lower College Road, Kingston, RI 02881.

Abstract

An *in vitro* forced glycation model was applied to evaluate glycation product stability, degradation pathway, and the degradation products of glycated rhuMAb A. During an accelerated stability study, upon thermal stress at 40°C for four weeks, glycated rhuMAb A went through two reactions: hydrolysis of glycation adducts (Schiff base and Amadori product) and formation of advanced glycation products. While hydrolysis reaction was more pronounced than the AGEs formation. Kinetically, it was found that hydrolysis of glycation adduct continued for four weeks, but AGEs formation plateaued after one week. The overall combination of both reactions caused glycated rhuMAb A to lose affinity to boronate resin, with a first order reaction rate. A set of analytical characterization on final degradation products structures was performed. The results demonstrated that the unglycated form of rhuMAb A, which was generated by hydrolysis of glycation site at K49 is the main final degradation products after thermal stress. This observation agreed with kinetic observation that reverse hydrolysis of both the Schiff base and Amadori product is the main degradation pathway of glycated rhuMAb A at 40°C in pH 6.5 phosphate formulation buffer. The reversibility of glycation adduct on K49 may be catalyzed by adjacent aspartic acids.

I. Introduction

The common manufacturing process of a MAb involves production in mammalian chinese hamster ovarian cells (CHO) by cell culture for 10-14 days. During this process a MAb is expressed in CHO and secreted into the cell culture medium, which contains glucoses, where the MAb can undergo glycation. Thus the purified MAb contains a certain level of glycation (Quan, C. *et al.* 2008, Zhang, B. *et al.* 2008). Several studies have been performed to understand the cell culture conditions that control the total glycation level (Yuk, I.H. *et al.* 2011). However, little knowledge is available regarding impact of glycation on most final purified MAbs. In particular, the stability and degradation pathway of glycation adducts under pharmaceutical drug product conditions are not well understood. This is due to wide distribution of glycation sites on a large protein, low level of glycation on each site, and lack of a robust analytical technology capable of quantify glycation level and changes.

As described in previous study (Chapter 2) , a forced glycation rhuMAb A model was developed and shown to be a successful tool to evaluate amino acid susceptibility to glycation. Fully glycated rhuMAb A was produced from this accelerated *in vitro* model. This highly glycated product provides an opportunity to understand the glycation adduct's degradation pathways and to perform further structural characterization.

The glycation reaction has multiple steps and produces multiple intermediate species. The end-product may differ based on pH and electrostatics of the local

environment (Figure 3-1). The initial linkage between a glucose molecule and a protein molecule forms a Schiff base. The Schiff base (aldimine) formation is a readily reversible reaction by hydrolysis. Schiff base also can rearrange to a more stable Amadori (ketoamine) product under high pH (Amadori, W. *et al.*1931). The ketone-containing Amadori product can further react with another free amino group in the surrounding environment to form advanced glycation end products, AGEs.

Researchers have extensively investigated the reactions involved in continuous exposure of glycated protein to reducing reagents to mimic the protein's modification in human body under *in vivo* chronic condition. Studies have demonstrated that the formation of AGEs is markedly accelerated with an increased availability of reducing sugars (Dutta, U. *et al.* 2005). One question that remains unanswered is, can AGEs formation be initiated on MAbs under the common pharmaceutical storage conditions in the absence of reducing sugars in the formulation?

The forced glycation model for rhuMAb A described in previous study was implemented to investigate the stability and degradation pathways of glycated rhuMAb A under pharmaceutical storage conditions. To understand the destiny of Schiff base (aldimine) and Amadori product (ketoamine), we focused on glycation adduct stability in formulation buffer in the absence of exogenous carbonyl reagents. An accelerated stability study of glycated rhuMAb A upon thermal stress was performed. The samples were incubated at 40°C for 4 weeks at pH 6.5 in 20 mM sodium phosphate. The total level of glycation adduct (% protein glycated) was monitored by boronate affinity HPLC (BAC) with UV detection at 280 nm as

previously described. In addition, the glycation adduct's glucose to protein ratio was monitored under reduction conditions by LC-ESI/MS. Fluorescence spectroscopy and BAC with fluorescence detection were used to monitor the formation of AGEs upon thermal stress. The total amount of AGEs was measured via quantification of overall polyclonal antibody binding to different AGEs species. Relative intensity of AGEs during a thermal stability study was reported.

II. Experimental

II. 1. Materials and Reagents

A regular lot of rhuMAb A (27 mg/mL, PBS buffer, pH 7.4) bulk material was obtained from Genentech. Trypsin, sequencing grade (TPCK treated), was purchased from Promega (Madison, WI), and Peptide:N-glycosidase F (PNGase F) from New England BioLabs Inc (Ipswich, MA). *N*-(2-Hydroxyethyl) piperazine-*N*¢-(3-propanesulfonic acid) (EPPS; 99.0%) and dithiothreitol (DTT; ultrapure) were obtained from USB Corp. (Cleveland, OH). D-Sorbitol (minimum 98%), R-D-glucose (ACS reagent), iodoacetic acid (IAA; _99%), and R-cyano-4-hydroxycinnamic acid (CHCA) were procured from Sigma-Aldrich (St. Louis MO). HPLC grade acetonitrile (ACN) and methanol were purchased from Fisher Scientific (Fair Lawn, NJ). Water used in all experiments was obtained from a Milli-Q Plus purification system (Millipore, Bedford, MA).

II.2. *In Vitro* Glycation of rhuMAb and Stability

The rhuMAb A in PBS buffer, pH 7.4, was further glycated *in vitro*. rhuMAb A was buffer exchanged into incubation buffer with dialysis prepared in a 15 ml cassette with 10kD membrane. Final *in vitro* glycation solution contains 50mg/ml rhuMAb A with 1200 mM, D-glucose, in 20 mM sodium phosphate buffer, pH 7.4. The *in vitro* glycation solution was kept in an incubator at 37 °C for 24 h. The reaction mixtures were submitted for immediate buffer exchange using a 15 ml dialysis cassette with 10kD membrane into phosphate buffer, pH 6.5. After

conditioning with trehalose and surfactant, glycated rhuMAb A was formulated as 20mg/ml in 20mM sodium phosphate with 8% trehalose and 0.04% polysorbate 20.

Glycated rhuMAb A was sterile filtered and filled into 2 cc glass vials, with 1 ml of solution in each vial. The stability study was set up at 40°C for 4 weeks with two vial replicates per week. At each time point, samples were pulled then stored at -70°C until analysis

II.3. Boronate Affinity HPLC (BAC)

Early stage glycation adducts can often be identified by a Boronate HPLC method using A TSK gel boronate 5PW column 7.5x75mm. The BAC mobile phase A was 50mM EPPS, 10mM Tris, 200mM NaCl, at pH 8.7, and BAC mobile phase B, was 500mM sorbitol in mobile phase A. The mobile phase flow rate 1 mL/min and the column temperature were maintained at 40°C with both UV and fluorescence detecto0sr. The gradient for HPLC elution was optimized for this rhuMAb A.

II. 4 Enzymatic Digestion of rhuMAb A

Several enzymatic treatments were performed on rhuMAb A samples before they were analyzed for reverse phase-HPLC, or mass spectrometric analyses, to determine the amino acid sequence and structural integrity of rhuMAb A.

PNGase F Treatment. PNGase F was used to remove the oligosaccharides in the Fc portion of a MAb. The rhuMAb A samples were buffer exchanged into 50 mM Tris buffer, pH 7.5, using a NAP-5 column. The protein concentration was

adjusted to 2.5 mg/mL. PNGase F was added in an enzyme-to-substrate ratio of 1:600 (w/w). The digestion was performed at 37°C overnight (15 h).

Tryptic Digestion. Prior to tryptic digestion, rhuMAb was reduced with DTT and then alkylated with IAA. Typically, 250 μL of antibody sample (2 mg/mL) was mixed with 20 μL of 1 M DTT in 730 μL of 6 M guanidine, 50 mM Tris, pH 8.0. The mixture was incubated at 37 °C for 1 h. It was then cooled to room temperature, and 50 uL of 1 M (IAA) in 1 M NaOH was added for carboxymethylation. The alkylation reaction was incubated at room temperature in the dark for 15-20 min. The residual IAA was quenched by the addition of 10 μL of 1 M DTT. The reduced and carboxymethylated rhuMAb A was then buffer exchanged into the digestion buffer, which contained 25 mM Tris, 1 mM $CaCl_2$, pH 8.3, using a PD-10 column (Sephadex G-25 medium, GE Healthcare). Trypsin was added at an enzyme-to-substrate ratio of 1:50 (w/w). The solution was mixed briefly and incubated in a 37°C water bath for 5 h. The digestion was terminated by adding 0.3% (v/v) trifluoroacetic acid (TFA) to the solution. The digest was then stored at -70°C until analysis.

II.5. Reverse Phase-HPLC with Electron Spray Ionization/ Mass Spectroscopy (RP-HPLC-ESI/MS)

The molecular masses of the intact, PNGase F-treated, and reduced rhuMAb A samples were determined by using a LC/ESI-MS setup. AnAgilent 1090 HPLC system was coupled with a PE Sciex API 3000 electrospray ionization triple-quadrupole mass spectrometer (Applied Biosystems, Foster City, CA). The samples

were desalted by reverse phase –HPLC (RP-HPLC) using a capillary column (Poros R1, 0.33 x 200 mm) equilibrated at a flow rate of 200 *u*L/min with 0.2% formic acid (solvent A) at a column temperature of 40°C. Samples were eluted using a linear gradient from 25% solvent B (0.2% formic acid in acetonitrile) to 70% solvent B over 16 min. The elutant from the RP-HPLC column was directed into the mass spectrometer operating in the positive ion mode. For post-reduction analysis, samples were incubated in 25 mM DTT for 15 min at 37°C prior to LC/MS analysis.

II.6. Tryptic Peptide Mapping

Peptides profiles of tryptic-digested rhuMAb A were analyzed by an RP-HPLC using a Jupitor C18 2.0x250 mm column at 45°C and UV detection at 214nm. The flow rate was 0.25ml/min, in mobile phase A: 0.1% TFA in water and B: 0.09% TFA in acetonitrile. The gradient was optimized for rhuMAb A. By comparing the peptide maps of time zero and stressed glycated rhuMAb A, the distinctive peptide fractions on degraded glycated rhuMAb A were collected for further characterization by MALDI-TOF MS/MS sequencing.

II.7. Protein Chip Matrix Assisted Laser Desorption Ionization- Time-Of-Flight mass spectrometry (MALDI-TOF)

Isolated tryptic peptides were spotted individually on a SCOUT 384 multi-probe plate with a CHCA matrix and analyzed in the positive mode using a Bruker Ultraflex-I MALDI-TOF-TOF mass spectrometer (Bremen/Leipzig, Germany). Sele8cted precursor ions were subjected to collision-induced dissociation with

argon as the collision gas. LIFT mode was used to analyze all fragment ions in single sweep, and data were processed with Flex Analysis software.

II. 8. Fluorescence Spectroscopy

Fluorescence emission spectra were measured using a Fluoromax-4 spectro-fluorometer by Horiba Jobin Yvon (Edison NJ, USA). The excitation wavelength was 350 nm, emission wavelength was 440nm. A circulating water bath set at 25 ± 1°C controlled the sample cell temperature during the measurements. Both spectrometric analyses were performed using cuvettes (12.5 × 12.5 × 36 mm) from Fisher Scientific (New Lawn, NJ, U.S.A.).

II.9. Total AGEs Enzyme-linked Immunosorbent (ELISA) assay

AGEs ELISA is an enzyme immunoassay for rapid detection and quantification of AGEs-protein adducts. The quantity of AGEs adducts in protein is determined by comparing absorbance of protein sample with that of a known AGE-BSA standard curve.

An AGEs-ELISA kit and BSA were purchased from Cell Biolabs. A layer of anti-AGE polyclonal antibody was plated in the 96 well. 100ul of protein samples were diluted in serial dilution then adsorbed on to 96-well plate for 1 hour at room temperature on an orbital shaker. The AGE protein adducts generated by rhuMAb A from thermal stress present in the sample were probed and bound with anti-AGE polyclonal antibody. After incubation, buffer three cycles of buffer wash were performed with 250 ul phosphate buffered saline (PBS) buffer on each well. Excess solution was removed after each wash. 100 ul of Anti-HRP conjugated secondary

antibody were added into wells and incubated for 1hour at room temperature on orbital shaker, allowing the secondary antibody binds to the rhuMAb A. The anti-AGEs complex plate was wash for five times with 250ul wash buffer. Substrate solution was warmed up to room temperature, then 100ul was added to each well and incubated for 10 min on an orbital shaker. The enzymatic reaction was stopped by stop solution. Absorbance of each well was measured on a micro-plate reader using 450nm as the primary wave length. The AGE protein adduct content in the unknown sample was determined by comparing with standard curve of by AGE-BSA standard (Cell Biolabs product manual).

III. Results

III.1. BAC

The thermally stressed samples exhibited a rapid loss of total glycation level over 4 weeks at 40°C, as shown in Figure 3-2. The glycation level dropped from 98.5% at initial time, to 69.6% after one week, 60.5% after two weeks, and 32.8% after four weeks. The decrease of glycation is a linear plot on natural log vs. time, indicating this is a first order reaction for glycation loss (Figure 3-3).

III.2. LC-ESI/MS

The decrease of glycation can occur because of the Schiff base reversibility, that resulting in a loss of glucose or formation of AGE products that alter the cis-hydroxal structure. Reduced ESI/MS analysis confirmed the glucose loss on both

light chains and heavy chains (Figure 3-4). No new mass species were detected on the mass spectrometry profile besides known glycated and un-glycated rhuMAb A peaks. Most importantly, there was an obvious change on light chain mass spectrometry profile. The glycated light chain intensity decreased after thermal stress, while the un-glycated light chain peak intensity increased. Unglycated rhuMAb A finally became the main light chain peak in mass spectrometry profile (Figure 3-4). This indicates most glycated light chains went to the unglycated form, demonstrating the reversibility of glycation modification under the thermally stressed condition at pH 6.5.

III.3. Fluorescence Spectroscopy and BAC

While thermal stress reduced the amount of glycation, can it also introduce more advanced glycation products? Formation of pentosidine-like AGEs can be measured by fluorescence spectroscopy at excitation 350nm/emission 440 nm (Dutta, U. *et al. 2005*). After thermal stress, fluorescence spectroscopy and boronate affinity chromatography with fluorescence detection, were utilized to monitor fluorescent AGEs. Fluorescent analysis was performed on bulk property for solution of glycated rhuMAb A at 1 mg/ml (Figure 3-5). The result showed a jump of emission intensity between initial time zero and one week after thermal stress. After one week the relative emission intensity plateaued out. This indicates the formation of pentosidine like fluorescent AGEs occurred rapidly and stabilized after one week.

Fluorescence traces on BAC showed two peaks with fluorescent signal at 350/440nm (Figure 3-6). Peak 1, at retention time 2.4 min, overlapped with

unglycated rhuMAb A. Peak 2, at retention time 2.7 min, is a new peak formed upon thermal stress (Figure 3-6). The intensity of both peaks increased during the thermal stress, peak 1 being the major peak. However, the total peak area based on fluorescence signal was very low, making it hard to quantify the exact amount of AGEs. Figure 3-7 shows the comparison of the UV and fluorescence signals in flow through portion on BAC, while the fluorescence signal increased linearly with time, the size of the peak at 280nm increased. This was due to the continuous increasing amount of rhuMAb A in the flow-through portion. After normalizing the fluorescence peak area by the protein amount, the normalized fluorescence signal/protein amount is consistent with spectroscopy measurements, the amount of AGEs detected on BAC increase in the first week of thermal stress, then plateaued (Figure 3-8). Therefore, BAC with tandem-UV 280nm - fluorescence 350/440nm detection is capable of monitoring both glycation level change and AGEs formation.

III.4. Peptide Mapping

What are the degradation end-products of the amino acid level after thermal stress? The possible degradation products from thermally stressed, glycated rhuMAb A were studied using tryptic peptide mapping. By comparing the time zero control to thermally stressed samples, several peptide fragments were found after thermal degradation, shown in Figures 3-9 and Figure 3-10. Due to the protein fragmentation in MS analyzer, pentosidine-like AGEs may have been destroyed; the amino acid modification by peptide map MS/MS analysis did not detect or quantify any pentosidine-like AGEs. Table 3-1 summarizes the degradation products on each

glycated amino acid site. The MS/MS analysis on these peptides identified two major degradation products. One is the non-fluorescent AGE: carboxyl-methyl lysine (CML) modified peptides which eluted around 40 min on peptide map (Figure 3-9). The other is the unglycated rhuMAb A, which eluted around 79 min (Figure 3-10). The presence of these two products confirms that glycated rhuMAb A underwent both pathways: reversal of glycation and formation of advanced glycation endproducts. The abundance of unglycated rhuMAb A was greater than that of the CML modified rhuMAb A. It is notable that majority of glycation reversal occurred on K49, other glycation site appeared to be more stable, maintaining consistent glycation levels after thermal stress.

III.5. Total AGE ELISA

AGE ELISA is based on binding of a family of polyclonal antibodies against AGEs. Total AGEs was measured by using polyclonal antibodies to capture variety of different AGEs structures, including fluorescent structures and non-fluorescent structures (Figure 3-11). The ELISA result showed an increase of relative intensity of AGEs upon thermal stress. This confirmed AGEs formation during the 40°C incubation. The increasing trend was similar to fluorescence and BAC results, where a rapid AGEs formation was detected in the first week then plateaued (Figure 3-12).

IV. Discussion

Degradation pathway of glycated rhuMAb A

The thermal stability study demonstrated that glycated rhuMAb A can undergo two possible parallel reactions (Figure 3-13). The glycated rhuMAb A either reverses back to the unglycated rhuMAb A, or moves forward to form AGEs. It is important to note that 1) the glycation adduct hydrolysis reaction is more pronounced than the AGE formation, and 2) glycation adducts hydrolysis continued for four weeks, but AGEs formation plateaued after one week. What could be the scientific rationale behind these observations?

Amadori rearrangement is favored at pH greater than pH 7.0, where the C=N double bond can shift to a C=O double bond. At pH 6.5, the rearrangement from Schiff base to Amadori product is not at the optimum condition, and the most of early glycation adducts should be in the Schiff base form. Since the Schiff base is thermodynamically unstable in liquids at neutral pH, the hydrolysis reaction is favored. Thus, the reversal to unglycated amino acid on protein is the predominant reaction and it proceeds towards completion. Second, the amount of carbonyl groups (C=O group) in Amadori products restrained further reaction to advanced glycation, because advanced glycation needs continuous attack of carbonyl group to amine group. Without additional free glucose in the formulation, the only carbonyl group available to initiate further advanced glycation reaction is the ketone in Amadori products or its degradation bi-carbonyl products. Since amount of precursor Amadori product is limited, the amount of ketone carbonyl available for advanced glycation reaction is also limited. In addition, the ketone group in the Amadori product is less

reactive than the regular aldehyde group in free glucose. Therefore, under the studied pharmaceutical storage condition, the total amount and reactivity of carbonyl groups were limited, and the AGEs formation reaction is not the dominant reaction. This is why AGEs formation reached plateau after one week.

AGEs Structures

The low level AGE products formed after thermal stress was confirmed to be a mixture. The fluorescent pentosidine-like ring structures and straight chain CML structures were both indentified (Figure 3-14). However, due to the limitations of analytical methods, it is not possible to quantify the exact amount of fluorescent pentosidine-like AGEs, or to further characterize their structures. The straight chain CML can be identified and quantified by peptide map with MS/MS analysis. CML was less than five percent of the final degraded rhuMAb A.

Degradation at Modified Sites

Although we did not study the glycation loss of each site during thermal stress kinetically, the glycation reversibility of each site can still be evaluated, based on the final glycation level at each site that were summarized in the Table 3-1. K49 and heavy chain N terminal had the highest glycation level initially, but these two sites also have the most rapid reversibility of glycation adduct. As we described in Chapter 2, three aspartic acids catalyze the glycation on K49. Based on catalyst nature of the K49 microenvironment, the nearby aspartic acids can also facilitate the reverse

reaction: hydrolysis of glycation adducts. The reason for glycation reversal on the heavy chain N –terminal is yet to be known.

V. Conclusions

The unique site specific glycation nature of rhuMAb A makes it a great candidate to study MAb structure modification by glycation and glycation adduct stability. The following conclusions can be drawn from the studied performed:

1) The forced glycation model is successful to analyze glycation chemical modification on whole protein levels and primary amino acid levels.

2) BAC with tandem-UV 280- fluorescence 350/440nm method is a great tool to monitor both glycation level change and AGEs formation.

3) Upon thermal stress, the forced glycated rhuMAb A showed a rapid and continuous hydrolysis reaction, and a slow and limited advanced glycation reaction. The overall combination of both reactions caused glycated rhuMAb A to lose affinity to boronate resin with a first order reaction rate.

4) The structure analysis of final degradation products agreed with kinetic observation that reversibility of Schiff base is the main degradation pathway of glycated rhuMAb A at 40°C in pH 6.5 phosphate formulation buffer.

5) Reversibility of glycation adduct on K49 is catalyzed by its adjacent aspartic acids.

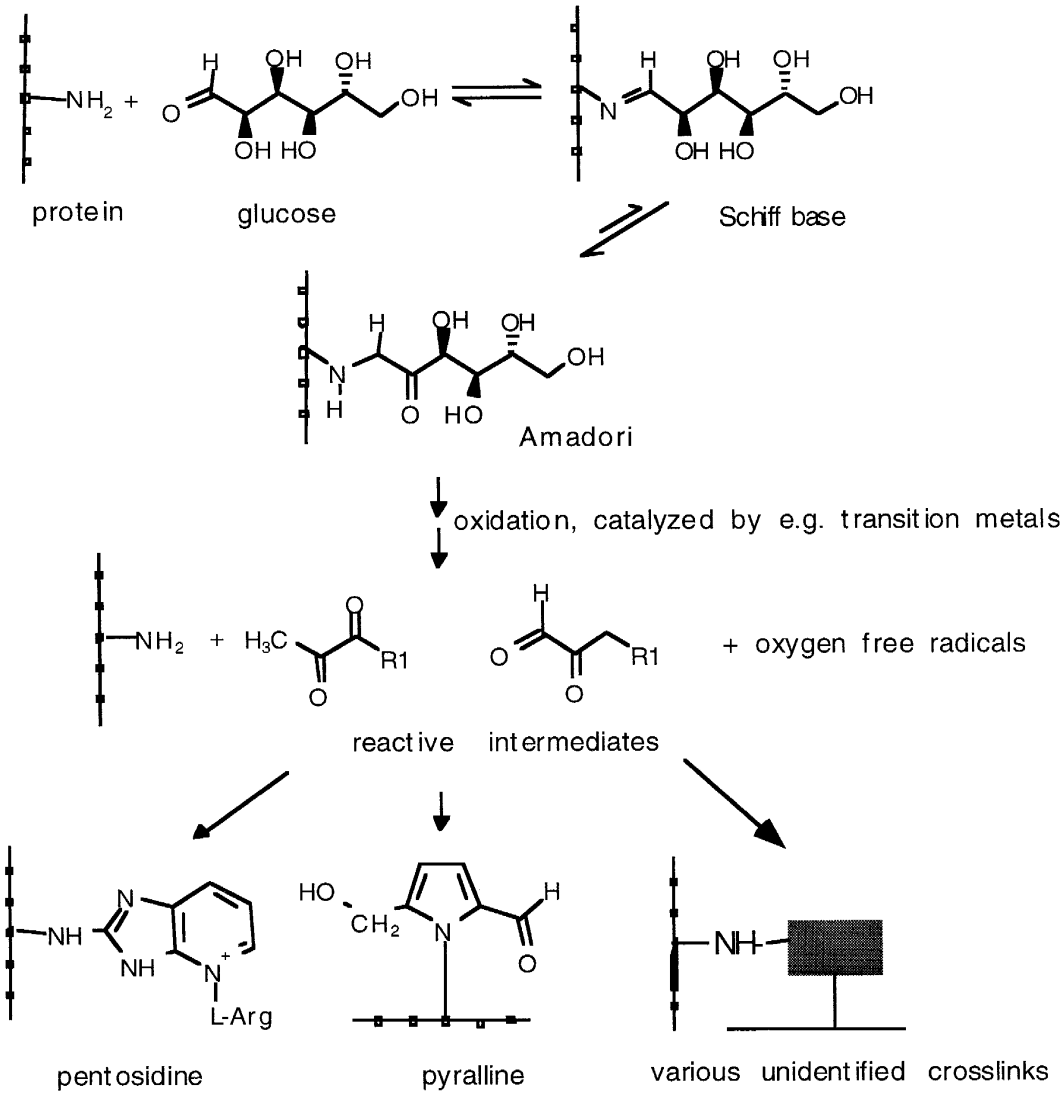

Advanced glycosylation endproducts (AGEs)

Figure 3-1: Chemistry of glycation reaction and advanced glycation reaction .
Reference:
Munch, G., Thome, J., Foley, P., Schinezel, R., Riederer, P. *Advanced glycation end products in aging and Alzheimer's disease* Brain Research Reviews 1997, **23,**134-143.

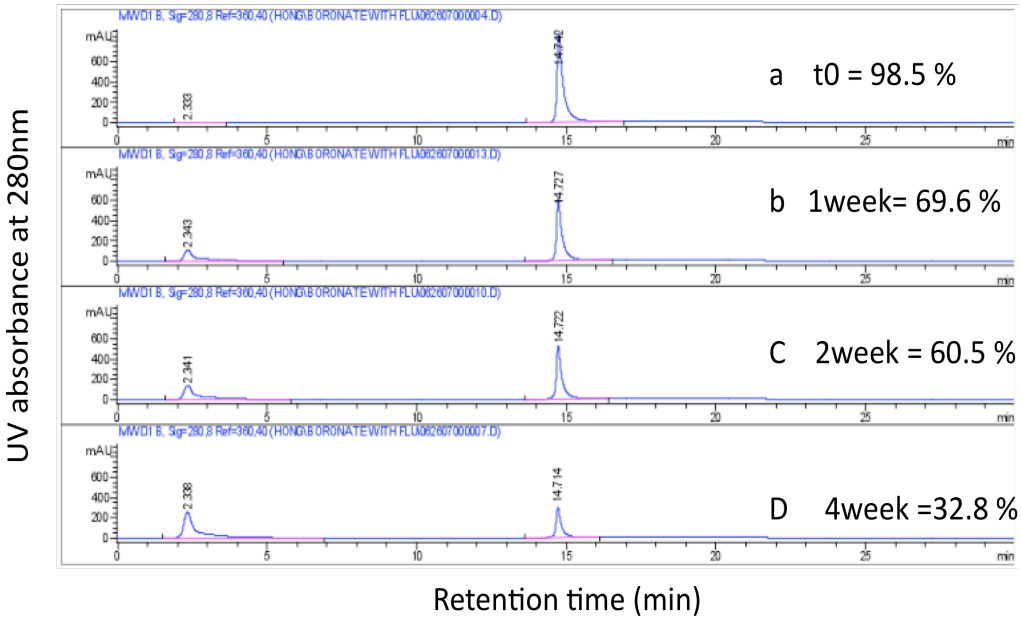

Figure 3-2: Boronate affinity chromatograms showed that glycation level dropped during thermal stress on fully glcyated rhuMAb A at 40°C over 4weeks.

a) at control t0 rhuMAb A is 98.5% glycated;
b) at 1week 40°C rhuMAb A is 69.6% glycated;
c) at 2weeks 40°C rhuMAb A is 60.5% glycated;
d) at 4weeks 40°C rhuMAb A is 32.8% glycated.

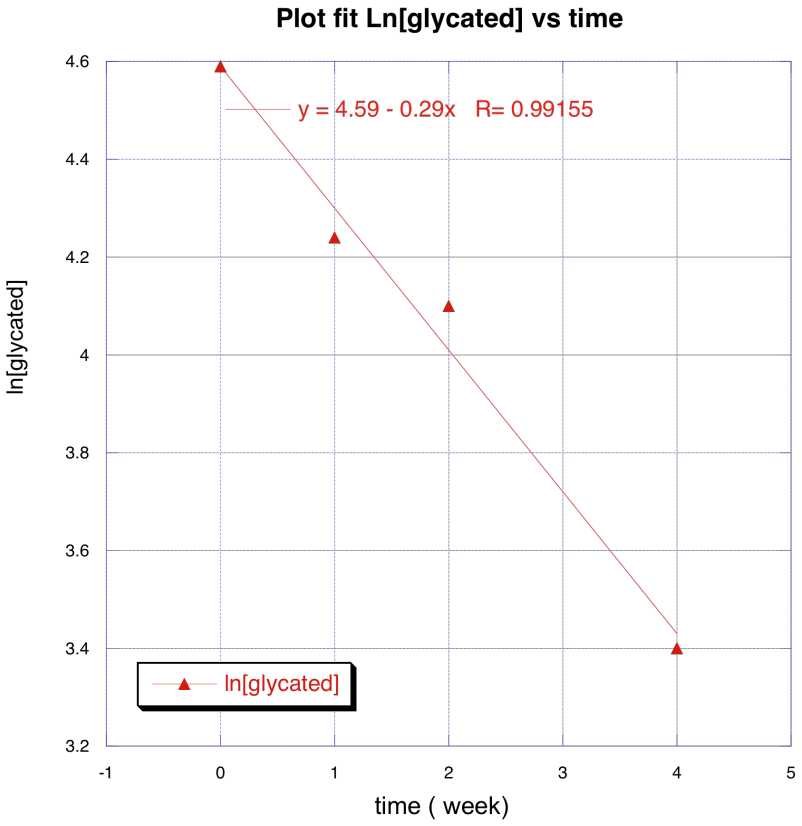

Figure 3-3: Plot fitting of ln[glycated rhuMAb A] vs. time is a linear plot, indicating the loss of glycation is a first order reaction.

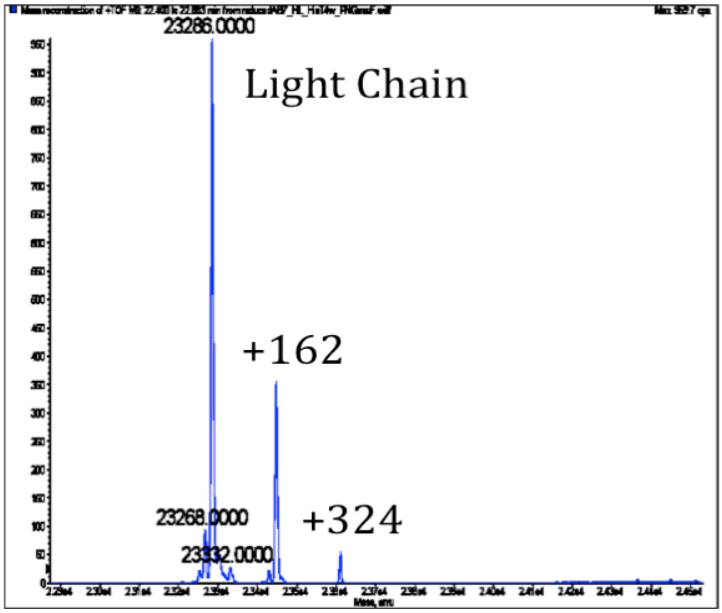

Dalton

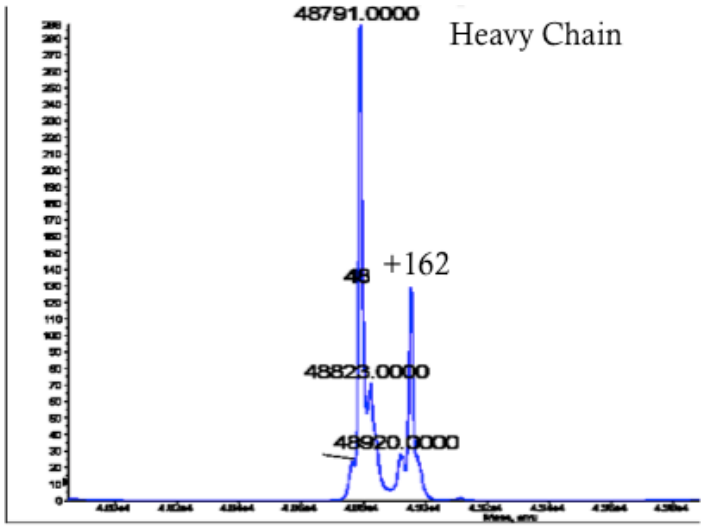

Dalton

Figure 3-4: ESI-MS mass profile of glycated rhuMAb A after 4weeks at 40°C.

A: In light chain three molecular mass were observed: native unglycated light chain is the main peak.

a) native light chain mass 23286 dalton/mol;
b) one glucose added light chain with mass 23448 dalton/mol;
c) two glucoses added light chain with mass 23610 dalton/mol.

B: In heavy chain, two molecular mass were observed: native unglycated heavy is the main peak.

a) native heavy chain mass 48791 dalton/mol;
b) one glucose added heavy chain with mass 48953 dalton/mol.

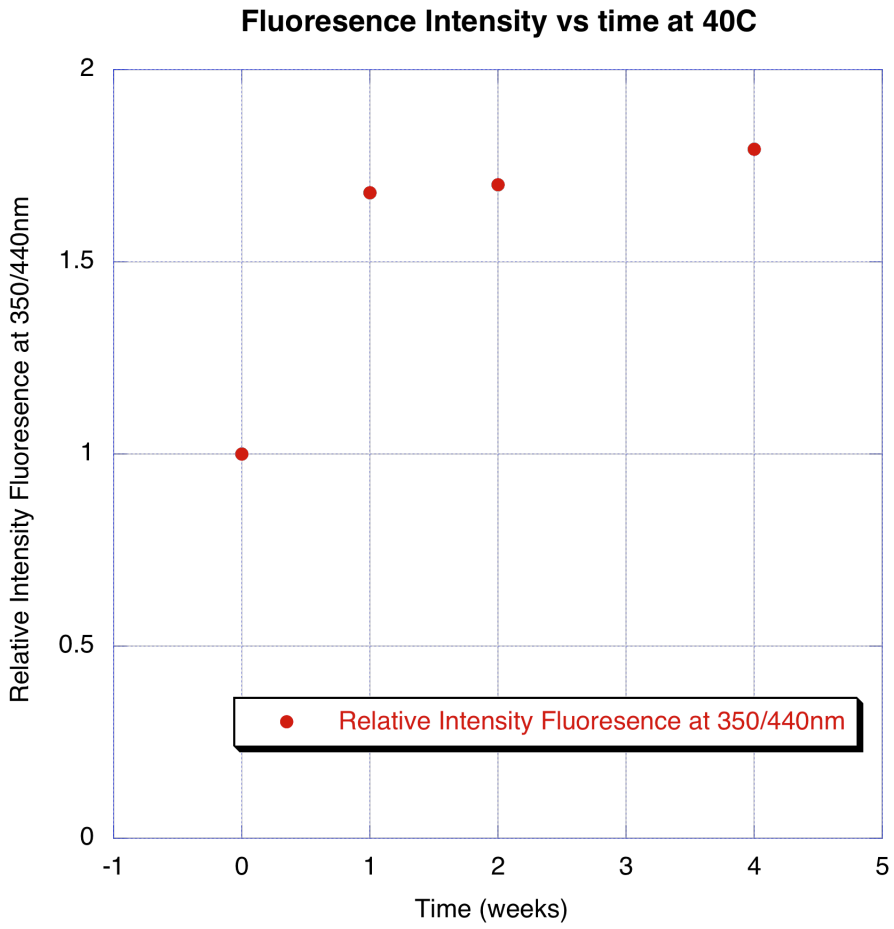

Figure 3-5: Fluorescence intensity vs. time at 40°C.
In fluorescence spectroscopy, relative intensity at 350/440nm increases over time at 40°C at 1 mg/ml rhMAb A concentration. AGEs formation increased the fastest in first week, then plateaued out.

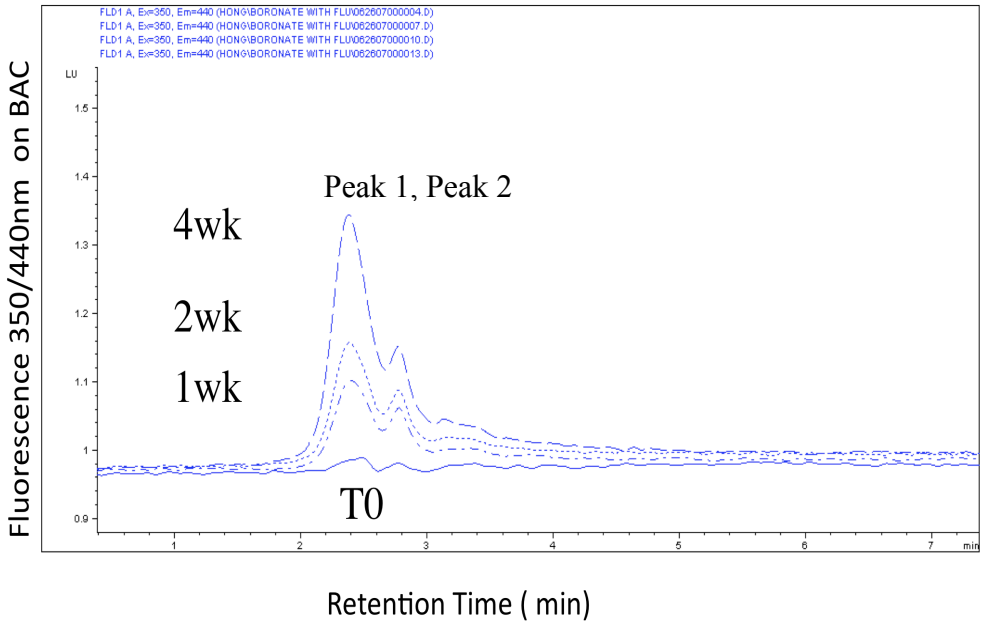

Figure 3-6: BAC fluorescence 350/440nm.

1) Fluorescence signal showed up in flow through portion of BAC.
2) There are two peaks, Peak 1 at 2.5 min overlapped with unglycated rhuMAb A, Peak 2 at 2.7 min formed upon incubation.
Intensity of both peaks increases over time upon thermal stress at 40°C.

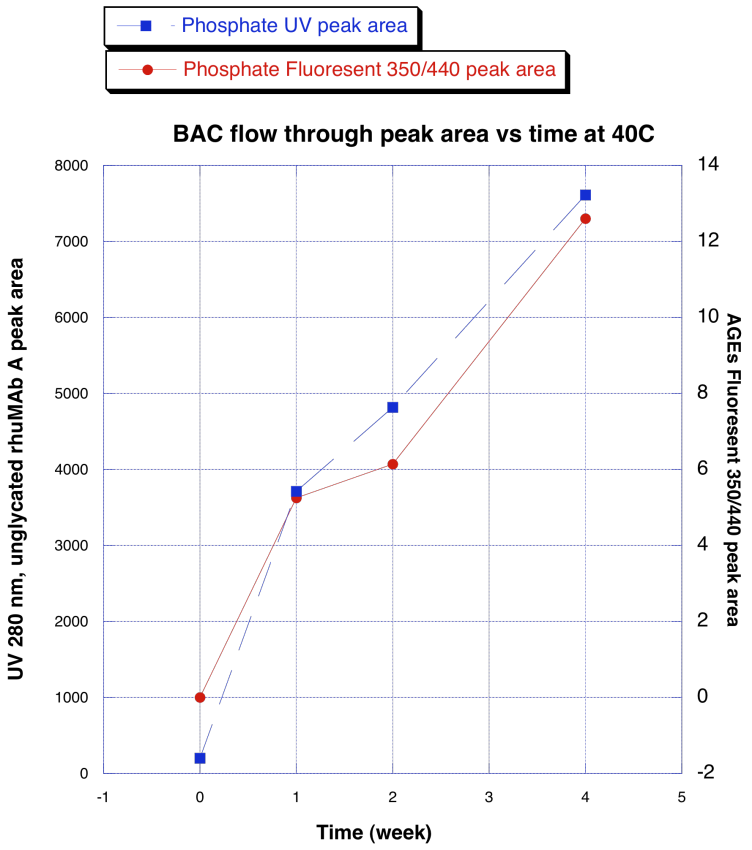

Figure 3-7: BAC flow-through peak area vs. time at 40°C.

BAC signal of flow-through portion UV 280 nm for total protein amount, fluorescence 350/440 nm for AGEs intensity.
Fluorescence signal showed an increase with time. Signal increased due to formation of AGEs and the increase of total unglycated protein amount

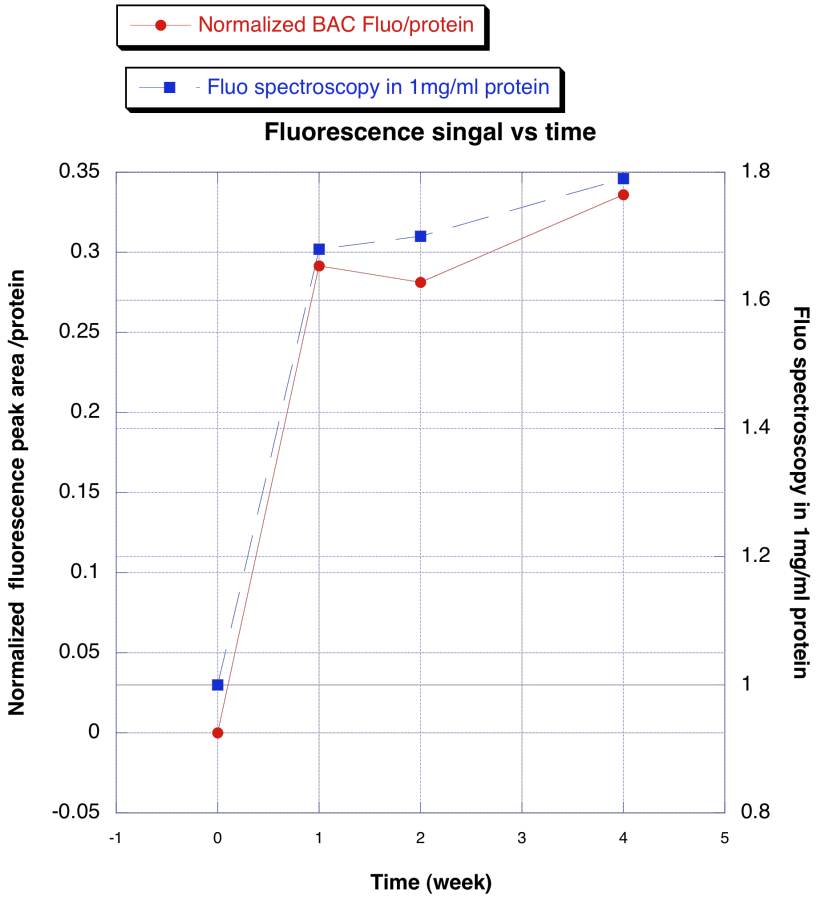

Figure 3-8: Comparison of BAC fluorescence signal and fluorescence spectroscopy signal.

Two signal responses agreed with each other.
BAC –UV-Flu is suitable to monitor both glycation and advanced glycation level on protein.

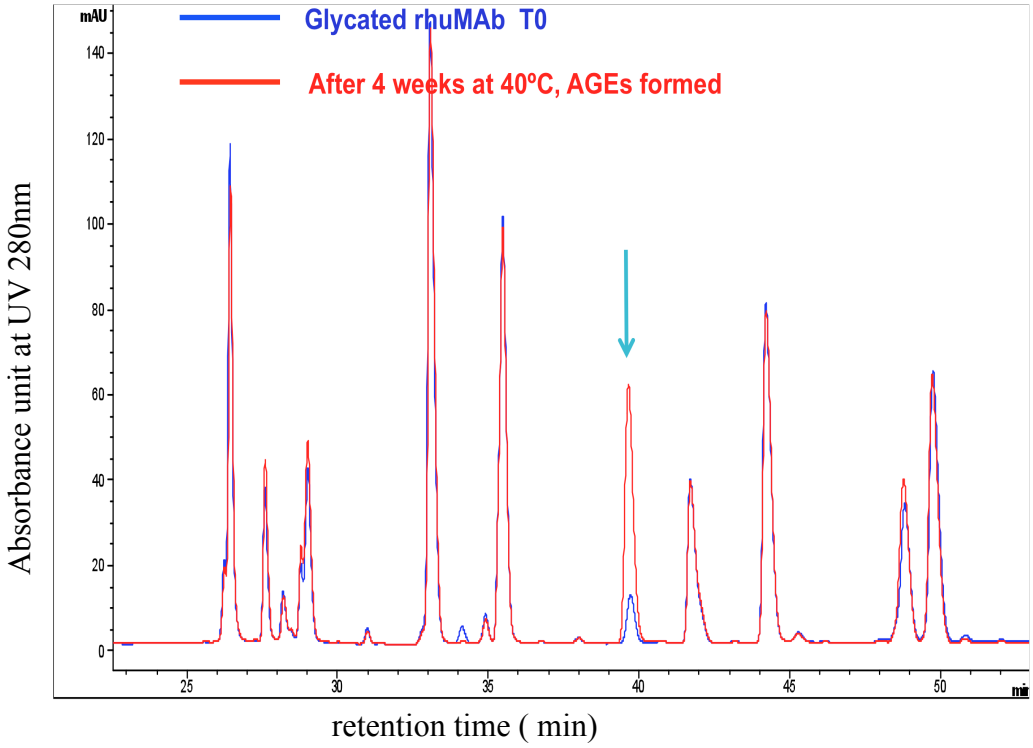

Figure 3-9: Overlaid chromatograms of tryptic peptide mapping of glycated rhuMAb A before (blue trace) and after (red trace) thermal stress at 40°C for 4weeks. (20min-50 min).

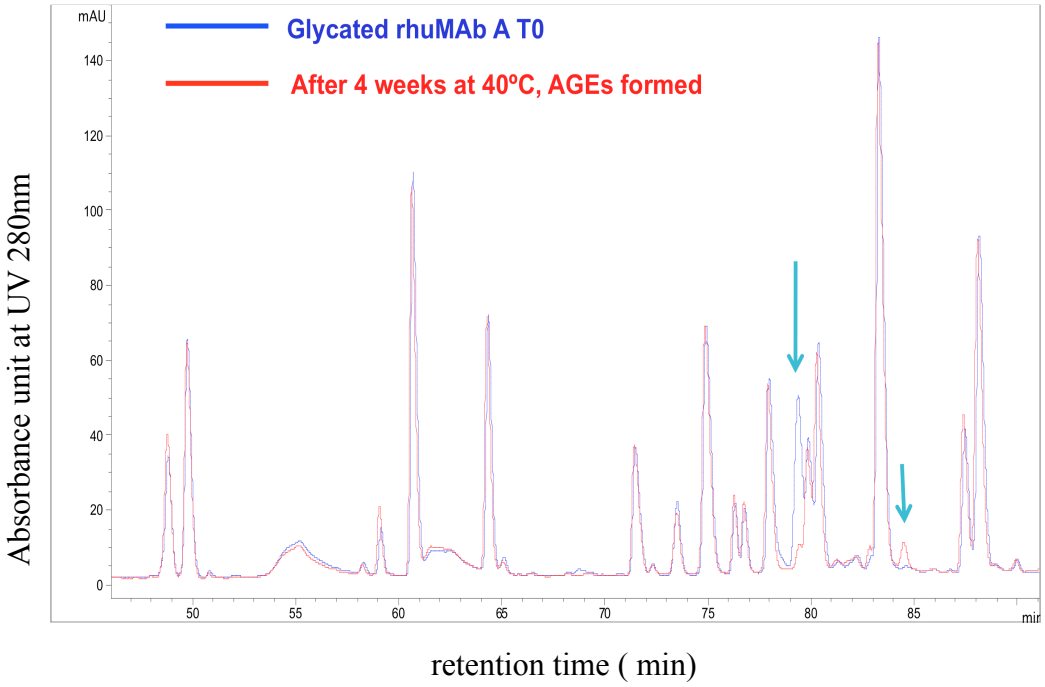

Figure 3-10: Overlaid chromatograms of tryptic peptide mapping of glycated rhuMAb A before (blue trace) and after (red trace) thermal stress at 40°C for 4weeks (50min-85min).

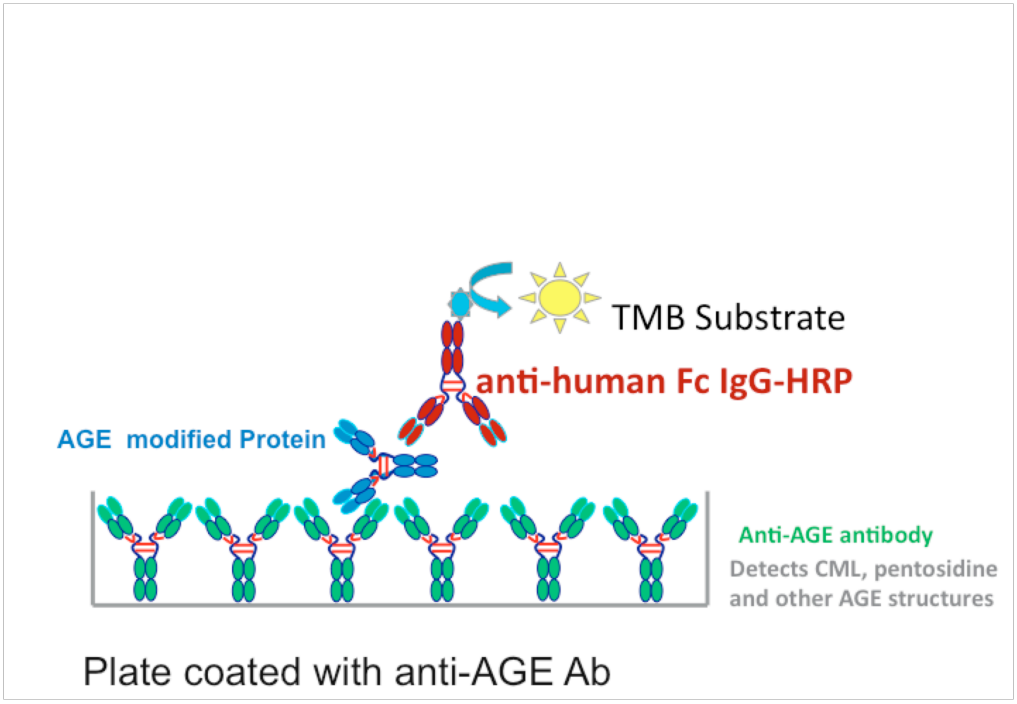

Figure 3-11: Illustration of the total AGEs ELISA assay.

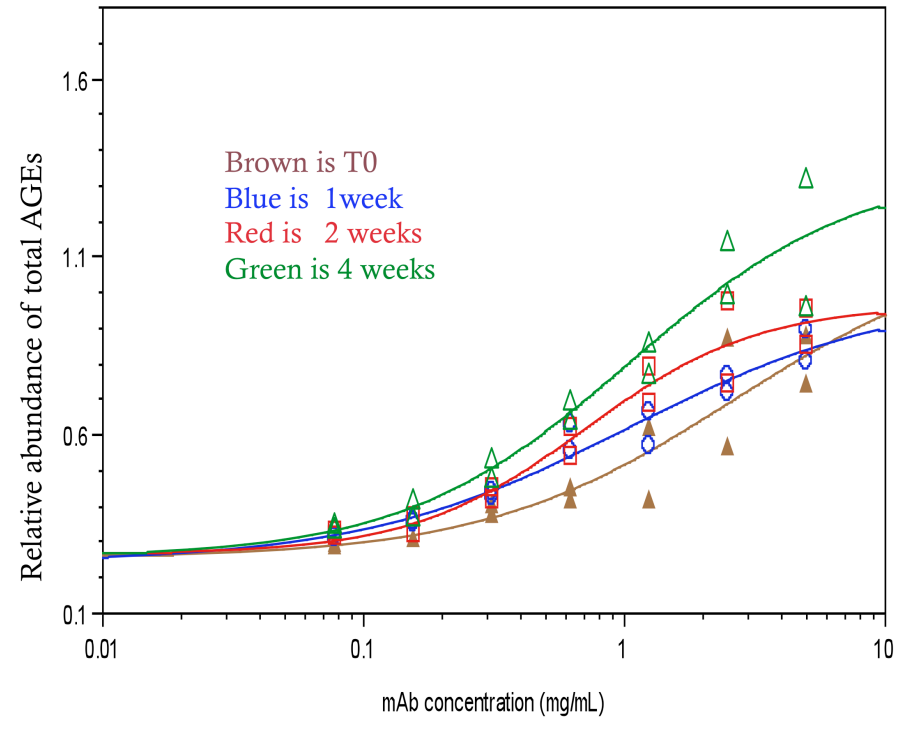

Figure 3-12: Graphic comparison of total AGEs increase upon thermal stress:
Brown color triangle trace is T0;
Blue color circle trace is one week;
Red color square trace is two weeks;
Green color circle trace is four weeks.

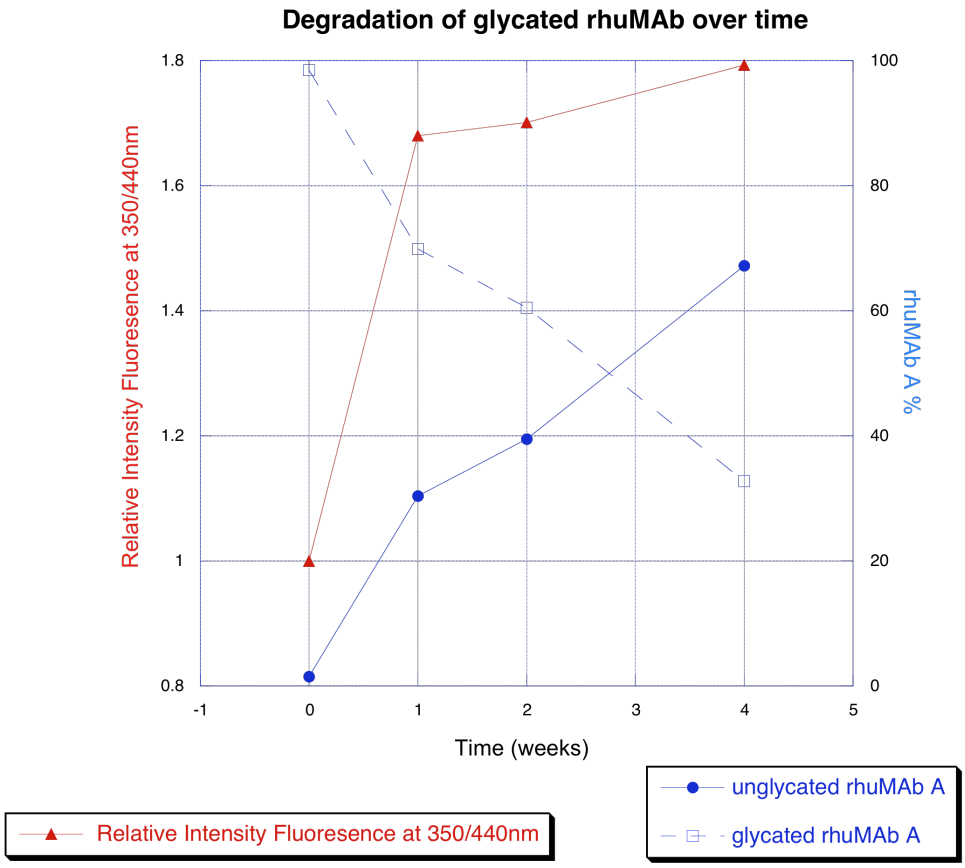

Figure 3-13: Comparison on degradation rates of glycated rhuMAb A.

1) AGEs formation represented by fluorescence relative intensity 350/440nm jumped in first week then plateaued out.
2) Loss of affinity to BAC continued over four weeks.

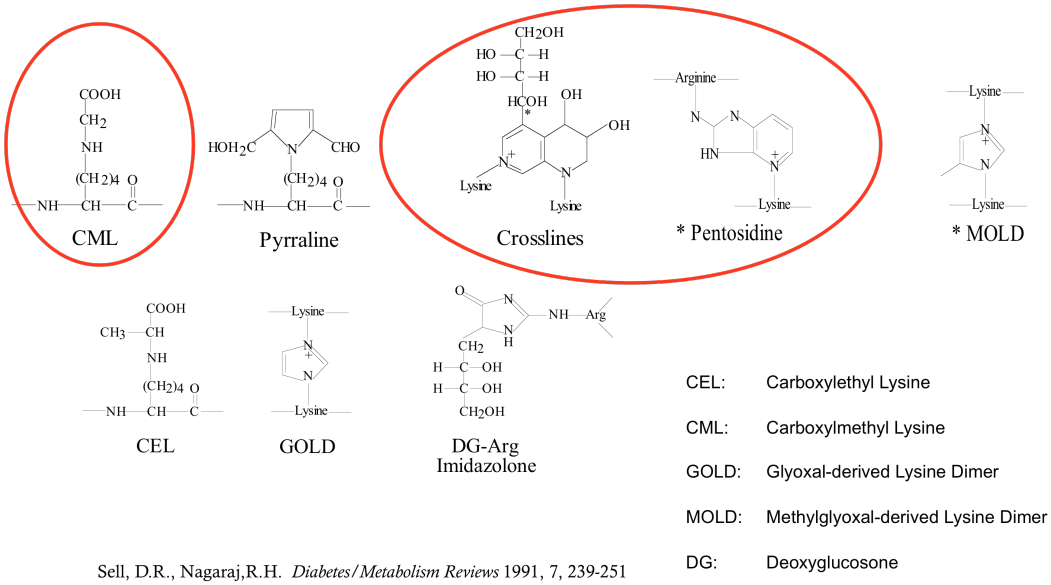

Figure 3-14: Potential detected AGEs structures.

Reference: Sell, D. R., Nagaraj, R. H., Grandhee, S. K., Odetti, P., Lapolla, A., Fogarty, J. and Monnier, V. M. (1991), Pentosidine: A molecular marker for the cumulative damage to proteins in diabetes, aging, and uremia. *Diabetes /Metabolism Reviews* **7**: 239–251.

Stress Cond. / Glycation sites	Buffer 1 Time 0			Buffer 1 Time 4 wks at 40 °C		
	WT (%)	Ketoamine (%)	CML (%)	WT (%)	Ketoamine (%)	CML (%)
LC-K49	8.1	90.5	1.5	86.3	9.7	4.0
LC-K149	99.1	0.9	0	99.2	0.8	0
HC-K64	99.5	0.5	0	99.6	0.4	0
HC-K75	97.8	2.2	0	98.5	1.5	0
HC-K133	99.5	0.5	0	99.6	0.4	0
HC-E1	95.0	4.9	0	99.9	0.1	0
LC-D1	99.8	0.3	0	100	0	0

Table 3-1: Summary of degradation products detected by peptide map.

Citations:

Quan, C.P., Alcala, E., Petkovska, I., Matthews, D., Canova-Davis, E. and Taticek, R. (2008). A study in glycation of a therapeutic recombinant humanized monoclonal antibody: where it is, how it got there, and how it affects change-based behavior. *Analytical Biochemistry*, **373**, 179–191.

Zhang, B., Yang, Y., Yuk, I., Pai, R., Mckay, P. and Eigenbrot, C. (2008). Unveiling a glycation hot spot in a recombinant humanized monoclonal antibody. *Analytical Chemistry,* **80**, 2379–2390.

Yuk, I.H., Zhang, B., Yang, Y., Dutina, G., Leach, K.D., Vijayasankaran, N., Shen, A.Y., Andersen, D.C., Snedecor, B.R., Joly, J.C., (2011) Controlling glycation of recombinant antibody in fed-batch cell cultures. *Biotechnology and Bioengineering***,** **108**, 2600-2610.

Munch, G., Thome, J., Foley, P., Schinezel, R., Riederer, P. (1997). *Advanced glycation end products in Aging and Alzheimer's disease* Brain Research Reviews **23,**134-143.

Li, A., Pfuller, U., Larsson, E.V., Jungvid, H., Galaev, I.Y., and Mattiagsson, B., (2001) Separation of misletoe lectins based on the degree of glycosylation using boronate affinity chromatography. *Journal of Chromatography,* **925** 115-121.

Dutta, U, Cohenford, M.A. and Dain, J.A. (2005). Nonenzymatic glycatoin of DNA nucleosides with reducing sugar. *Analytical Biochemistry*, **345** (2):170-180.

Chapter 4

Study of Glycation Adduct Degradation and the Influencing Parameters

Hong Liu[1,3], Yi Yang[2]. Heather Flores[1], Trevor Swartz[1],

Thomas Patapoff[1], and Joel A. Dain[3]

is in preparation for submission to Journal of Pharmaceutical Sciences

1 Early stage pharmaceutical development, Genentech, 1 DNA way, South San Francisco, CA 94404.

2 Protein analytical chemistry, Genentech, 1 DNA way, South San Francisco, CA 94404.

3 Department of Chemistry, University of Rhode Island, 51 Lower College Road, Kingston, RI 02881.

Abstract

A forced glycation model on rhuMAb A and boronate affinity chromatography technology were applied to evaluate the effect of drug product compositions on the degradation of glycation adduct. Three formulation composition factors were studied, such as pH, buffer, and oxidation control. The results demonstrate that the pH is the key parameter to control degradation pathways, as pH also determines the hydrolysis rate constant of glycated rhuMAb A. The unique structure of rhuMAb A forms a rich electron donating environment around K49. This unique environment determines the pH dependence of glycation adduct's hydrolysis rate. Buffer species and oxidation levels do not impact the glycation adduct stability under the studied pharmaceutical conditions. In addition, the effect of rhuMAb A's glycation level was also evaluated. The study demonstrated that higher protein glycation levels slow down the overall hydrolysis rate of the glycation adduct, presumably by providing a complex electron transferring system on protein.

I. Introduction

In previous studies, it was shown that rhuMAb A can be used as a model to study site-specific glycation and glycation adduct degradation pathways. In addition, the boronate affinity chromatography (BAC) coupled with UV and fluorescence detection is suitable to monitor both glycation level change and AGEs formation. Previous protein characterization work and stability study demonstrated that the glycation adducts of rhuMAb A degraded via two pathways, under thermal stress in a typical pharmaceutical formulation at pH 6.5. The main reaction was hydrolysis to reform unglycated rhuMAb A, while a minor reaction was the formation of AGEs.

To understand which parameters control the stability of glycation adducts (Schiff base or Amadori product) during the final drug product storage, we used glycated rhuMAb A as a MAb model and BAC as the analytical tool to investigate the effect of four key parameters on glycation adduct stability, in a set of thermal stress studies. These parameters included three important factors for formulation compositions: pH conditions, buffer species, oxidative conditions. The final factor, relevant to the protein, was the initial glycation level, which is based on rhuMAb A's (the active pharmaceutical ingredient) production process.

II. Experimental

II. 1. Materials and Reagents

rhuMAb A lot I (22 mg/mL, PBS buffer, pH 7.4) and lot II (27 mg/mL, PBS buffer, pH 7.4) bulk materials were produced using stable recombinant CHO cells cultured using in-house using proprietary, serum-free media with and without controlled glucose levels, respectively. D-Sorbitol (minimum 98%), R-D-glucose (ACS reagent), iodoacetic acid (IAA; _99%), and R-cyano-4-hydroxycinnamic acid (CHCA) were procured from Sigma-Aldrich (St. Louis MO). HPLC grade acetonitrile (ACN) and methanol were purchased from Fisher Scientific (Fair Lawn, NJ). Water used in all experiments was obtained from a Milli-Q Plus purification system (Millipore, Bedford, MA).

II.2. Stability Study Setup and Parameters

pH conditions

Since both formation of Schiff bases and rearrangement of Amadori products are pH depended, we investigated the overall effect of pH on the stability of glycated rhuMAb A. Six different pH conditions were tested between pH 4.5 and pH 7.0, which is a typical pH range for protein therapeutics formulations. One drug product lot, containing 36% glycated rhuMAb A, derived from common cell culture was used in the pH study. The rhuMAb A drug product was buffer exchanged into six different pH conditions, including 20mM sodium acetate buffer at pH 4.5 and 5.0, and 20mM histidine/histidine hydrochloride buffer at pH 5.5, 6.0, 6.5, and 7.0. In all samples, the final protein concentration was 0.5mg/ml with 8% trehalose, and 0.04% polysorbate 20.

Buffer species:

Watkins, *et al*. had reported that phosphate ions could bind to the active site of RNase and serve as a local catalyst for Amadori rearrangement of lysine residues near the RNase's active site. They established the buffer effect on the kinetics, and specificity of glycaiton of RNase. (Watkins, N.G. *et al*. 1985 and 1987). To explore the buffer effect on glycated rhuMAb A, we tested its stability in three buffers:

- phosphate, to test the effect of phosphate ions on stabilizing glycated rhuMAb A;
- arginine, to test its inhibition effect on AGEs formation;
- histidine as a typical formulation control.

In this study, 99% glycated rhuMAb A was buffer exchanged into three different buffers: 20mM histidine hydrochloride, 20mM arginine phosphate and 20mM sodium phosphate at pH 6.5. Final samples contained 20 mg/ml with 8% trehalose and 0.04% PS20.

Control on Oxidative Conditions

Oxidation involved pathways are the keys for initiating AGEs formation. In this study, one drug product lot with 15% glycated rhuMAb A was placed three different oxidation conditions:

- regular drug product vial with air in the head space;
- drug product vial with N_2 in the head space;
- drug product vials with phenol added as an oxidation scavenger.

The overall composition of this drug product lot is of 150mg/ml rhuMAb A in 200mM histidine buffer, pH5.8 with 0.02% polysorbate 20.

Glycation level:

As previously reported, cell culture conditions impacted the final glycation level of rhuMAb A (Yuk, I.H. *et al*. 2011). It is unknown if glycation adduct hydrolysis under in vitro storage would vary with initial glycation levels, so we compared hydrolysis of glycated rhuMAb A among three different initial glycation levels: 13%, 42% and 99%. Final samples contained 20mg/ml protein in 20mM histidine buffer at pH 6.5.

Stability set up:

After samples were prepared under each condition, samples were stressed thermally at 40°C for four weeks. After stresses, samples were analyzed to evaluate the stability of glycated rhuMAb A. All the collected time points were analyzed with boronate affinity chromatography with UV and fluorescence detection (BAC/UV/FLuo) assay. Total glycation level and AGEs formation were monitored by boronate affinity chromatography.

II.3. Boronate Affinity Chromatography (BAC)

High performance liquid chromatography (HPLC) with solvent delivery system were used, where the analyte separation were performed with an Agilent 1100 series HPLC equipped with a thermostatic auto-sampler.

Early stage glycation adducts often can be identified by a BAC method using A TSK gel boronate 5PW column 7.5x75mm. The mobile phase A was 50mM EPPS, 10mM Tris, 200mM NaCl, at pH 8.7, and mobile phase B was 500mM sorbitol in mobile phase A. The mobile phase flow rate 1 mL/min and the column temperature will be maintained at 40°C with UV detector at 280 nm and fluorescence detector at 350/440nm. The gradient for HPLC elution had been optimized for this rhuMAb A. Due to the difficulty for quantification of fluorescence signal, the exact amount of fluorescent AGEs cannot be determined, only relative fluorescence intensity is used to compare different stability conditions.

II. 4 Enzymatic Digestion of rhuMAb A

Several enzymatic treatments were performed on rhuMAb A samples before they were analyzed for reverse phase-HPLC, or mass spectrometric analyses, to determine the amino acid sequence and structural integrity of rhuMAb A.

PNGase F Treatment. PNGase F was used to remove the oligosaccharides in the Fc portion of a MAb. The rhuMAb A samples were buffer exchanged into 50 mM Tris buffer, pH 7.5, using a NAP-5 column. The protein concentration was adjusted to 2.5 mg/mL. PNGase F was added in an enzyme-to-substrate ratio of 1:600 (w/w). The digestion was performed at 37°C overnight (15 h).

Tryptic Digestion. Prior to tryptic digestion, rhuMAb was reduced with DTT and then alkylated with IAA. Typically, 250 μL of antibody sample (2 mg/mL) was mixed with 20 μL of 1 M DTT in 730 μL of 6 M guanidine, 50 mM Tris, pH 8.0. The mixture was incubated at 37 °C for 1 h. It was then cooled to room temperature, and 50 uL of 1 M (IAA) in 1 M NaOH was added for carboxymethylation. The alkylation reaction was incubated at room temperature in the dark for 15-20 min. The residual IAA was quenched by the addition of 10 μL of 1 M DTT. The reduced and carboxymethylated rhuMAb A was then buffer exchanged into the digestion buffer, which contained 25 mM Tris, 1 mM $CaCl_2$, pH 8.3, using a PD-10 column (Sephadex G-25 medium, GE Healthcare). Trypsin was added at an enzyme-to-substrate ratio of 1:50 (w/w). The solution was mixed briefly and incubated in a 37°C water bath for 5 h. The digestion was terminated by adding 0.3% (v/v) trifluoroacetic acid (TFA) to the solution. The digest was then stored at -70°C until analysis.

II.5. Tryptic Peptide Mapping

Peptides profiles of tryptic-digested rhuMAb A were analyzed subsequently by an RP-HPLC using a Jupitor C18 2.0x250 mm column at 45°C and UV detection at 214nm. The flow rate was at 0.25ml/min, in mobile phase A: 0.1% TFA in water and B: 0.09% TFA in acetonitrile. The gradient was optimized for this rhuMAb A. By comparing the peptide maps of time zero and stressed glycated rhuMAb A, the distinctive peptide factions on degraded glycated rhuMAb A were collected for further characterization by MALDI-TOF MS/MS sequencing.

II.6. Protein Chip Matrix Assisted Laser Desorption Ionization- Time-Of-Flight mass spectrometry (MALDI-TOF)

Isolated tryptic peptides were spotted individually on a SCOUT 384 multi-probe plate with a CHCA matrix and analyzed in the positive mode using a Bruker Ultraflex-I MALDI-TOF-TOF mass spectrometer (Bremen/Leipzig, Germany). Sele8cted precursor ions were subjected to collision-induced dissociation with argon as the collision gas. LIFT mode was used to analyze all fragment ions in single sweep, and data were processed with Flex Analysis software.

III. Results and Discussion

pH conditions:

BAC-UV 280nm to measure total glycation level change

The pH study revealed that glycation adduct stability is greatly dependent on pH conditions. By comparing affinity chromatograms of the final time point (40°C 4weeks) at different pH conditions, we found that as pH increased, the rhuMAb A samples lost the affinity to boronate ligand upon thermal stress (Figure 4-1), indicating loss of glycation adduct. The total remaining glycation level is summarized in Table 4-1. It shows that samples stored at pH 4.5 had the highest remaining glycation level, 32.0% compared to 36% at time zero. From pH 5.5 to 6.0, remaining glycation level dropped from 22.0% to 8.7%, while pH 7.0 had the lowest remaining glycation level, only 5.6%.

The graph of glycation level *vs.* pH, confirms that the remaining glycation level is inversely dependent on pH values (Figure 4-2). More importantly, the graph shows a non-linear relationship between pH and remaining glycation level. There were three pH responding sections, in which the glycation adduct's stability responded to pH change differently. From pH 4.5 to 5.5, the glycation adduct level change remained fairly mild. After thermal stress, the remaining glycation level differed about 5% per 0.5 pH unit, which is a modest response to pH change. From pH 5.5 to pH 6.0, this region showed the most drastic relation ship between on the remaining glycation level and pH. In this narrow pH range, with only 0.5 pH unit increases, the remaining glycation level dropped 13.3%. From pH 6.0 to 7.0, the final glycation level decreased rapidly. In this range, the remaining glycation level was less than 8.7 %.

However, the difference of remaining glycation level between pH 6.0 and pH 7.0 is small, only approximately 2% per 0.5 pH unit. Therefore pH 5.5 to pH 6.0 is the most sensitive pH range for glycated rhuMAb stability.

BAC-Fluorescence 350/440nm to measure AGEs formation

In contrast to loss of glycation adducts, fluorescence traces on BAC showed two peaks with fluorescence signals at 350/440nm, which represent formation of AGEs. Peak 1, at retention time 2.4 min, overlapped with unglycated adducts. Peak 2, at retention time 3.6 min, is a new peak formed upon thermal stress. (Figure 4-3)

Comparing the fluorescence signals of different pH conditions after thermal stress, we found that the intensity of fluorescence signal increased with increasing pH (Figure 4-4). It is notable that, at pH 4.5, 5.0, 5.5 and 6.0, only peak 1, the unglycated peak was observed. At pH 6.5 and pH 7.0, both peak 1 and peak 2 were observed. This characterization result indicates that a new pentosidine-like AGEs-protein species was formed upon thermal stress at higher pH conditions. However, even at pH 6.5 and 7.0, the majority of fluorescence signal intensity was attributed to peak 1, the unglycated rhuMAb A. AGEs formation demonstrated by peak 2, represented a relatively small portion of total fluorescence intensity.

Comparing the pH dependence of total glycation level (Figure 4-2) and pH dependence of AGE formations (Figure 4- 4), it is notable that below pH 6.5, the most pronounced fluorescent peak was the hydrolysis product, unglycated rhuMAb A. This indicates that at low pH range, pH 4.5 to pH 6.0, the hydrolysis of glycation adducts was the main degradation pathway. At higher pH range, pH 6.5 to 7.0, both peak 1 and

peak 2 were formed, but the intensity of peak 2 was small compared to peak 1. This observation reveals AGE formation plays a minor role in the degradation pathway for rhuMAb A. Overall, the preferred degradation pathways of glycation adducts were driven by the pH conditions.

Determination of the hydrolysis rate constant

We can calculate the rate constant of hydrolysis at different pH conditions based on the following two assumptions: the hydrolysis reaction rate was is much greater than AGEs formation rate at all pH conditions; and the hydrolysis reaction was a first order reaction, as we learned in Chapter 3.

The rate constant k can be derived from this function

$$k=ln([A_0]/[A_n])/t_n.$$

Where, *k* is the reaction's rate constant and *n* is the particular time point, e.g. four weeks etc. *[A]* is the concentration of reactant, $[A_0]$ is the initial concentration, $[A_n]$ is the final concentration. In our study, *[A]* represents the concentration of glycation adducts measured by BAC.

The half-life of glycation adducts at each condition can be calculated as:

$$t_{1/2} = ln2/ak$$

Where, $t_{1/2}$ is the half-life of glycated rhMAb A. It means at this time point, the concentration of glycation adducts equals to half of the initial concentration of glycation adduct. The parameter *a* is the molar ratio of reactant for glycation adduct. In our study, *a* =1. Table 4-1 summarizes the hydrolysis rate constant at different pH

values. It demonstrates that the lower the pH, the slower glycation adduct hydrolysis. Therefore, pH conditions determine the rate of hydrolysis of glycation adducts.

BAC can measure the amount of both Schiff base (aldimine) and Amadori product (ketoamine). The total glycation level is the sum of these two species in which cis-hydroxyal groups are still attached to rhuMAb A molecules.

Historically, Schiff base is known to be thermally unstable, and to undergo reverse reaction easily in aqueous solution. Several studies have reported the mechanism of Schiff bases hydrolysis (Figure 4-5). Jenck, *et al.* reported formation and hydrolysis of the Schiff base intermediates such as transitional oxime and semi-carbozone (Jenck, W.P., *et al. 1963)*. Their study demonstrated a transition of the rate limiting step. As pH conditions decreased, rate-determine step changed from Schiff base formation/ hydrolysis under neutral to alkaline pH (step 1), to rate-determine amine attack / decomposition of carbinol-amine under acidic pH (step 2). They also found that the rate of hydrolysis markedly decreased in strong acid, which agrees with the results in our study. Furthermore, Jencks's group showed that under more acidic conditions, a large fraction of Schiff base exists as the conjugate acid. The hydrolysis rates decrease with decreasing pH for Schiff bases indicating an electron-donating functional group on the molecule. The changes in rate with pH are correlated with the conversion of Schiff bases to their conjugate acids.

We can determine the pKa of glycation adduct of rhuMAb A by plotting % glycated rhuMAb A vs. pH, or k_{obs} hydrolysis vs. pH (Figure 4-6). The plateau area at pH 5.75 represents the maximum glycation level change upon pH changes. pH 5.75 is the pKa value of glycation adduct in Schiff base /conjugate acid form (Figure 4-6).

The other aspect of glycation adduct stability is the Amadori rearrangement. After dehydration, the Amadori rearrangement is favored at alkaline conditions (Figure 4-7) at pH >7.0. The Amadori product is considered more stable than the Schiff base. However, there are studies (Acharya, A.S. and*, et. al., 1984, 1991*) that have shown the ketoamine linkage between glucose and protein to be reversible. In our particular study subject of glycated rhMAb A, the major change in glycation was observed on K49, the preferred glycation site. The observed rate of hydrolysis decreased with decreasing pH. This pH-dependent hydrolysis indicates the electron donor-enriched environment around lysine K49. The catalyst effect of three aspartic acid residues surrounding K49 facilitates the formation of the Amadori product (ketoamine) on K49. They also promotes K49 Amadori product reverse to Schiff base (aldimine), then Schiff base reverse to unglycated rhuMAb A.

Therefore, between pH 4.5 and 5.5, the attack from nitrogen on the lysine amine group to the carbon on carbonyl group of glucose is the rate-limiting step, while adding a water to Schiff base to form conjugate acid is favored. The BAC was able to detect both Schiff base and its conjugate acid. Since the conjugate acid is stable in lower pH conditions (pH <5.5), overall glycation level of rhuMAb A is maintained. At slightly higher pH, pH 5.5 to 6.0, around the pKa of the conjugate acid of Schiff base (pH 5.75), the amounts of base and conjugate acid were equal. A big change of Schiff base is needed to shift the pH of Schiff base/ conjugated acid system. Thus, we observed at pH 5.5 to pH 6.0, there was a significant difference on the remaining glycation level. BAC detected glycation adducts were mainly in Schiff base form. In addition to rapid loss of glycation adducts, at pH 6.0 to 7.0, Amadori rearrangement

occurred leading to a minor advanced glycation reaction. The BAC detected glycation adducts are both Schiff base and Amadori products. Hence, the overall main reaction in the studied pH conditions, from pH 4.5 to pH 7.0, is the reverse of glycation adduct by Schiff base hydrolysis.

We can conclude that pH condition controls both the direction and rate of Schiff base hydrolysis. Below the pKa of the Schiff base, glycation adducts are relatively stable. However, at the pKa and above, Schiff base hydrolysis becomes the preferred reaction, with Amadori rearrangement as a secondary reaction, leading to loss of glycation adducts and an increase in prevalence of AGEs.

Buffer species

After 4 weeks of thermal stress at 40°C, no difference on BAC was found among three buffer systems: histidine, arginine and phosphate buffers. Using the same approach as described in the previous section, we calculated the degradation rate constant in three buffers. The result demonstrated similar rate constants among histidine, arginine, and phosphate buffer systems, with 0.10 $week^{-1}$, 0.11 $week^{-1}$, and 0.13 $week^{-1}$, respectively. This observation indicates that these buffers did not cause any difference on the reversibility of glycation adducts (Figure 4-8, Table 4-3). In addition, the trends of AGE formation in three buffers detected by BAC were parallel at fluorescence 350nm/440nm (Figure 4-9). Peptide mapping results confirmed that even at the amino acid level, the degradation products are similar in three buffers (Figure 4-10). Glycated rhuMAb A was shown to degrade to wild type rhuMAb A (>80%) while a small portion (<10%) degraded to carboxyl-methyl-lysine (CML)

(Figure 4-10), The relative proportion of these two degradation products were at similar levels in all three buffers after thermals stress at 40ºC for 4 weeks.

Watkins, *et al*. has reported the catalysis effect of phosphate buffer on the kinetics, and specificity of glycation on RNase (Watkins, N.G. *et al*. 1985/1987). By binding the RNase active site, phosphate ion was localized on RNase, creating a negatively charged environment. This increase of electron density helped nearby lysine residue to form Amadori product during glycation. However, based on the structure and function of the studied rhuMAb A, there is no phosphate ion binding site to keep phosphate ion localized on protein. From the characterization work from previous study and published work by Zhang (Zhang, B. *et al.* 2008), K49 was still the primary susceptible site in both phosphate and sodium bicarbonate buffers. Presence of phosphate ion did not catalyze the glycation on this rhuMAb A. From the presented stability result in this study, phosphate buffer did not show any effect on glycated adduct hydrolysis, either. Thus, we hypothesize that phosphate ions cannot serve as a catalyst in the glycation reaction of this rhuMAb A or be involved in the glycation adduct hydrolysis without the active site to ensure its localization on rhuMAb A. Therefore, phosphate ions did not affect hydrolysis rate of glycated rhuMAb A.

On the AGE formation, arginine was thought to be able to slow down the advanced glycation reaction, by competing with rhuMAb A's own amine groups, to react with any carbonyl group on glycated rhuMAb A. However, in the presented study, arginine did not affect AGEs formation on glycated rhuMAb A. One possible reason is that advanced glycation reactions were minor at the studied pH condition, pH 6.5.

Oxidation Control:

The oxidation controlled study showed very similar hydrolysis rate constants for all conditions. Nitrogen (N_2) purged vials resulted in the slowest rate constant, at 0.2%/week; then regular air purged vials at 0.22%/week; followed by phenol, an oxidation scavenger, contained vials at 0.23%/week (Figure 4-11 and Table 4-3). This indicated the degradation of the glycated rhuMAb A did not slow down at pH 6.5 in absence of oxidative reagent.

Initial Glycation Level

Table 4-4 summarizes the rate constants for all three initial glycation levels. The hydrolysis rate dropped from 0.46 to 0.39 $week^{-1}$ for the glycated rhuMAb A species at 13% to 42% respectively. When the protein was 99% glycated, the glycated adduct degradation rate decreased to only 0.10 $week^{-1}$, with a half life of ~ 7 weeks (Figure 4-12, Table 4-4). From BAC fluorescence signal, the AGEs formation was fastest at the high glycation level (Figure 4-13).

Furthermore, analysis of size heterogeneity at different glycation levels was done by size exclusion chromatography. The result demonstrated that at higher glycation level, more protein aggregates were formed. It is a evidence that protein to protein interaction was more pronounced at higher glycation levels (Figure 4-14).

As previous study showed (Chapter 2), the heavily glycated rhuMAb is a mixture with complex structural modifications. With higher total glycation level, not only K49 was glycated to a higher level, but other lysine residues were also modified.

Previous studies by Zhang, *et al.* had shown that rhuMAb A can be glycated to different levels. Table 4-4 summarizes the total glycated levels at each sites detected, 13% one (one site K49 only); 42% (6 sites, K49 level primary) ; 99% (7 sites, K49 primary about 90% as in chapter 2) (Zhang, B. *et al.* 2008).

In the forced glycation model, lysine residues buried inside the protein were modified without the strong catalysis effect provided by neighboring aspartic acids. Moreover, these glycated lysines were hard to be hydrolyzed (Table 3-1 in Chapter 3). These much stable glycation sites may lead to further AGEs formation, as well as protein-protein interaction to provide a complex protein network. Thus, we hypothesize that the complexity and heterogeneity of final glycation states contributes to a slower overall hydrolysis rate. The presence of more enduringly glycated sites may provide a complex electron –transfer network on rhuMAb A that allows electron transferring within the molecule, stabilizing the Schiff base.

IV. Conclusions

1) Among the studied formulation parameters, pH is a key parameter to control glycation adduct degradation pathways, it also determines the hydrolysis rate constant of glycated rhuMAb A.
2) The unique structure of rhuMAb A creates a rich electron donating environment around K49, which determines its site specific glycation and contributes to the pH dependence of hydrolysis rate.
3) Buffer species and oxidation levels do not affect the glycation adduct stability under the studied conditions.
4) Initial protein glycation level does affect the overall hydrolysis rate of glycation adduct on rhuMAb A. This may be related to protein-protein interaction involving electron transferring system among different glycated sites.

Peak 1 Peak2

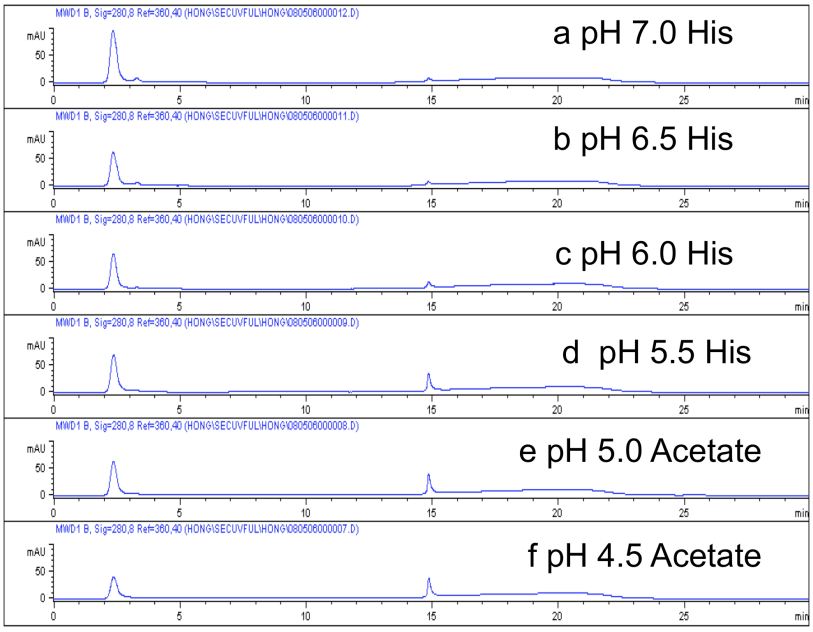

Absorbance unit at 280nm

Retention time (min)

Figure 4-1: Glycation level after 4 weeks at 40°C.

UV 280nm on boronate affinity chromatography for pH 4.5 to 7.0.
It showed glycation level was the lowest at pH 7.0

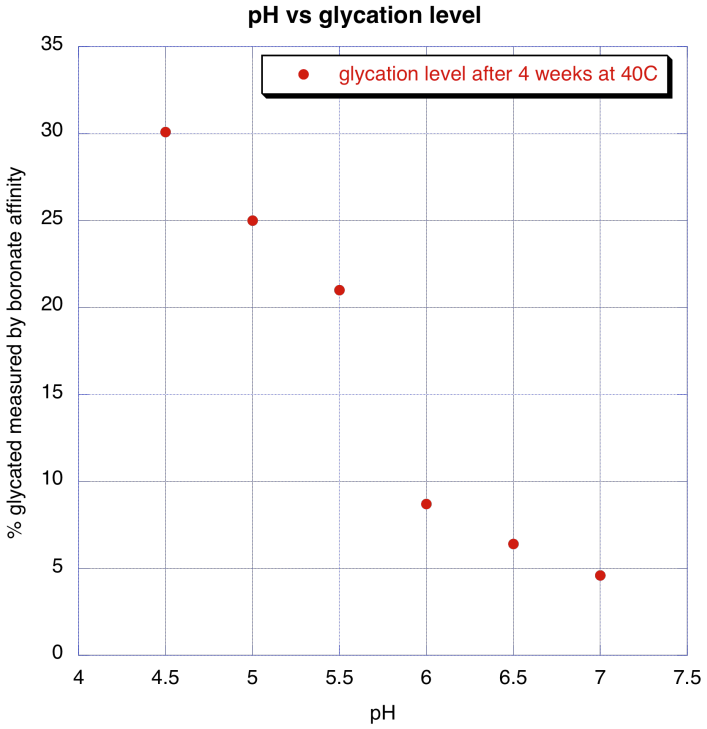

Figures 4-2: pH vs. remaining glycation level.

The pH dependence on glycated rhuMAb stability at 40°C pH 5.5 – 6.0 showed to be the most sensitive pH range for glycation change.

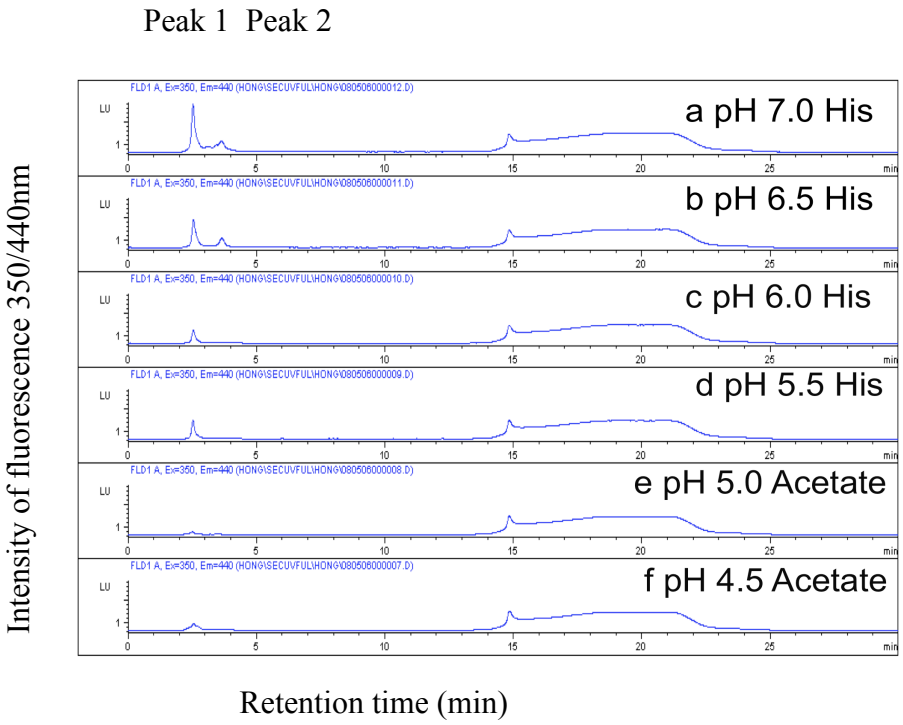

Figure 4-3: AGEs formation after 4 weeks at 40°C.

Fluorescence 350/440nm on boronate affinity chromatography for pH 4.5 to 7.0. AGEs fluorescence was the highest at pH 7.0.

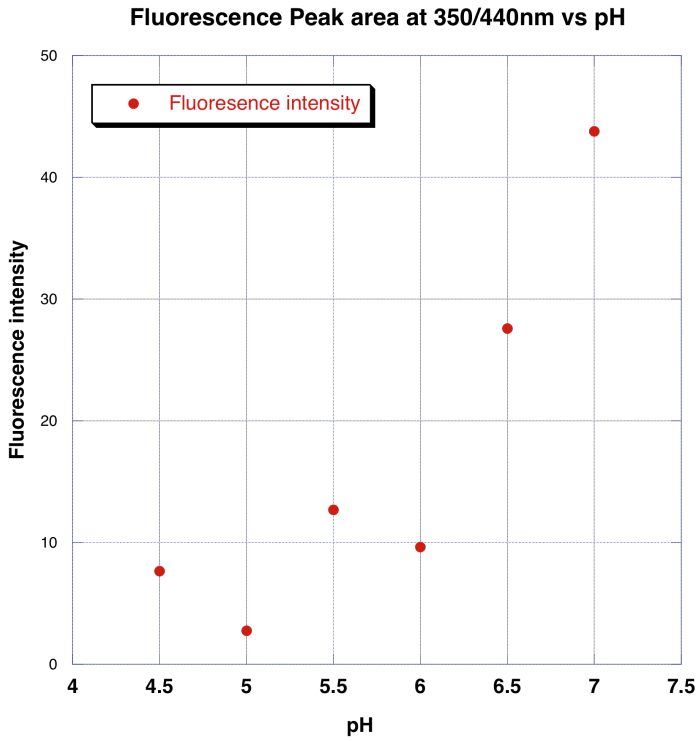

Figure 4-4: Fluorescence peak area at 350/440nm vs. pH.

It indicates the pH6.5 and pH 7.0 had significant AGEs formation after 4 weeks at 40°C.

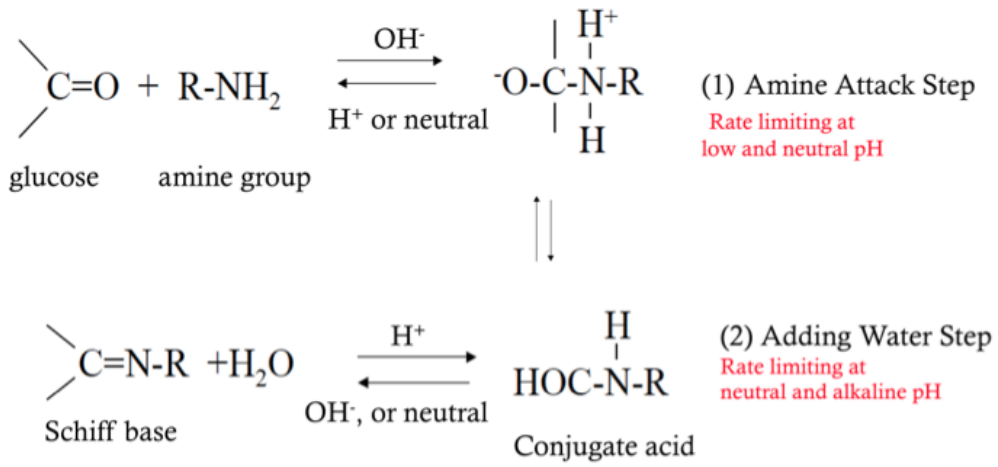

Figure 4-5: Illustration of Schiff base formation and hydrolysis.
At neutral to alkaline conditions, step 1 is the rate limiting step
At acidc pH, step 2 is the rate limiting step.

From reference: E.H.Cordes, and W. P. Jenck 1963. The Mechanism of Hydrolysis of Schiff Base Derived from Aliphatic Amines Journal of American chemistry Society. 85 (18) 2843-2848

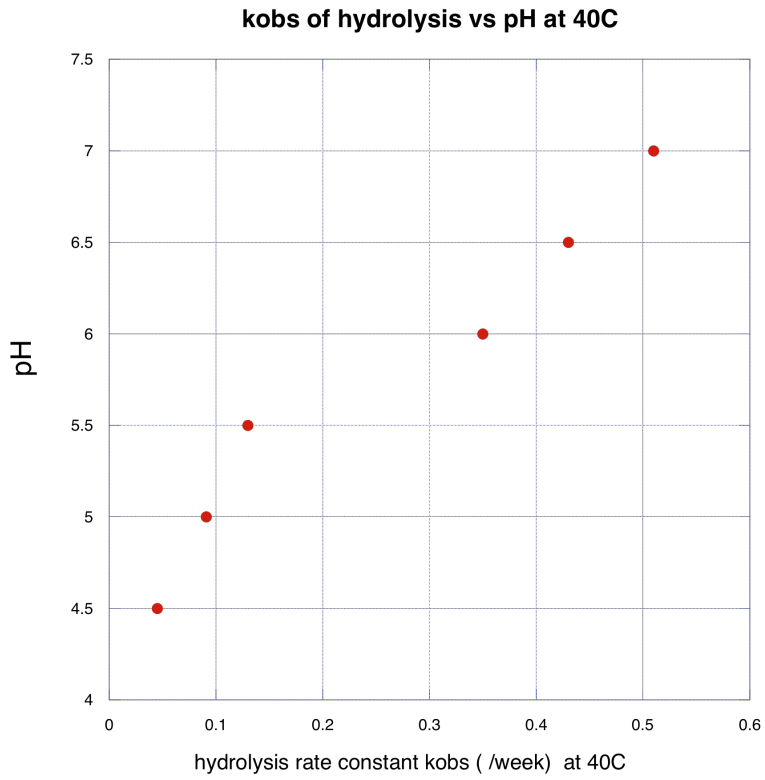

Figure 4-6: The pH dependence of glycation adduct hydrolysis.

Hydrolysis rate decreased with low pH. The pKa of Schiff base is around pH 5.75.

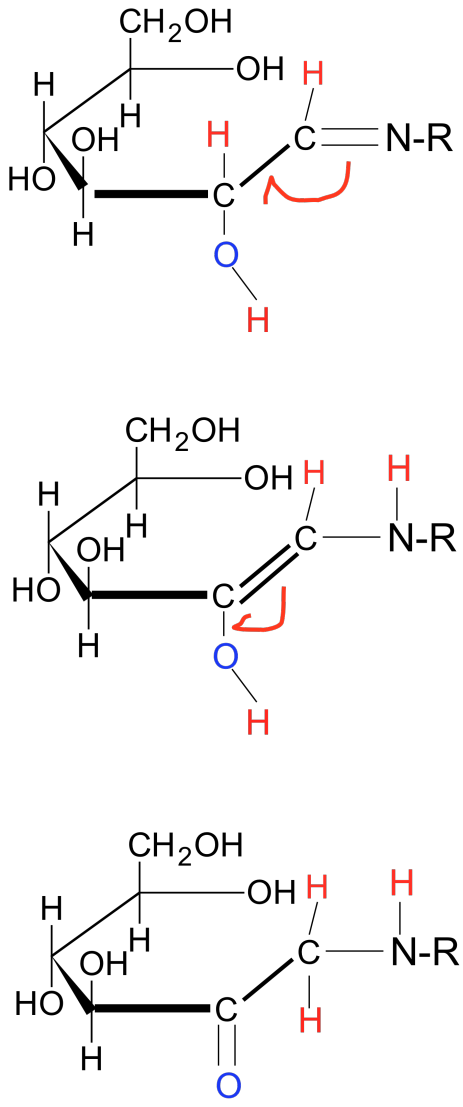

Figure 4-7: Amadori rearrangement: the C=N shifts to C=O, is favored at high pH.

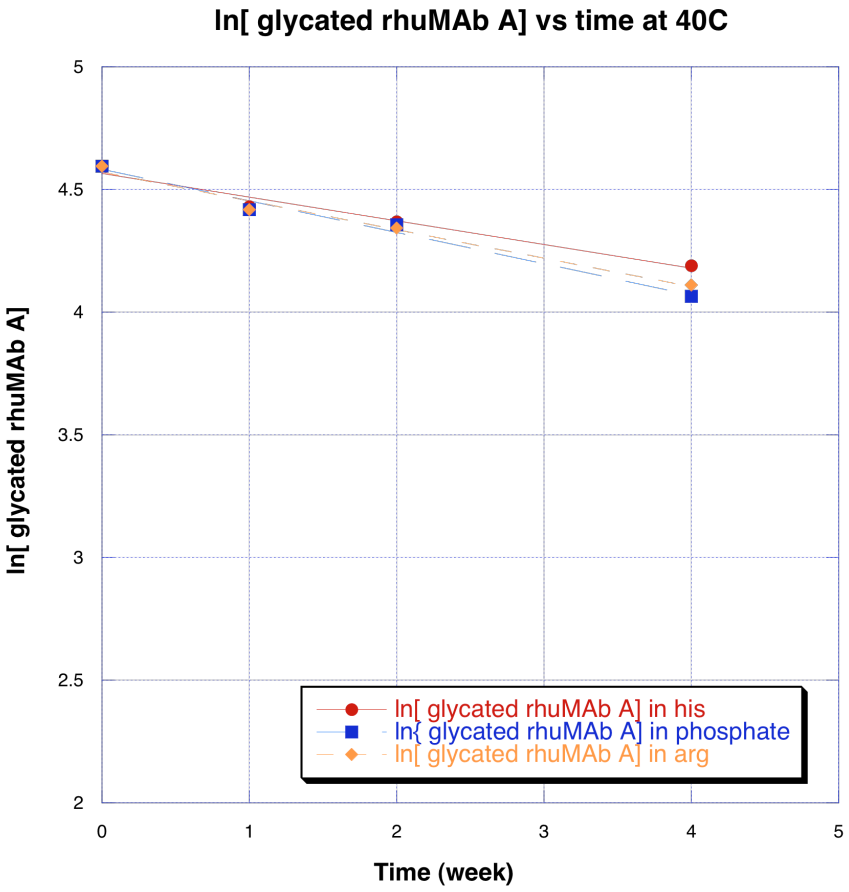

Figure 4-8: Glycation level drop in three buffers.
It fits into linear plot on ln[glycated rhuMAb A] vs time,
indicating, first order reaction rate of rhuMAb A hydrolysis.

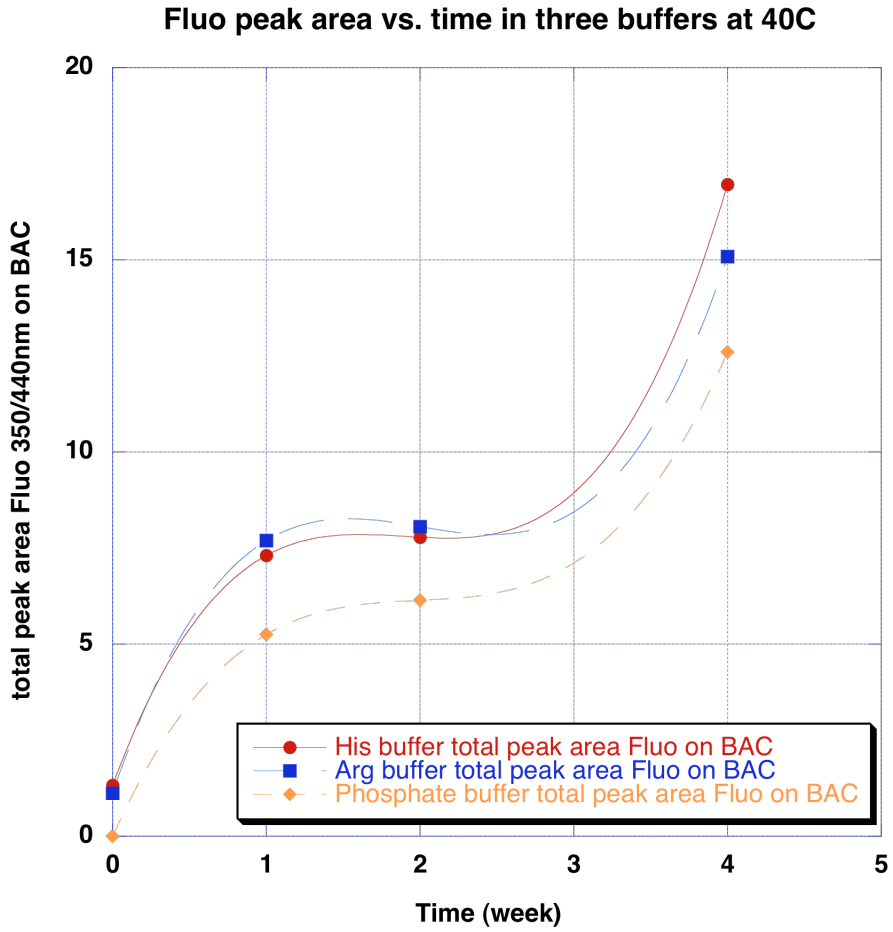

Figure 4-9: Fluorescence peak area vs. time in three buffers at 40°C. Total peak area of fluorescence signal 350/440 nm for pentosidine-like AGEs increased over time.

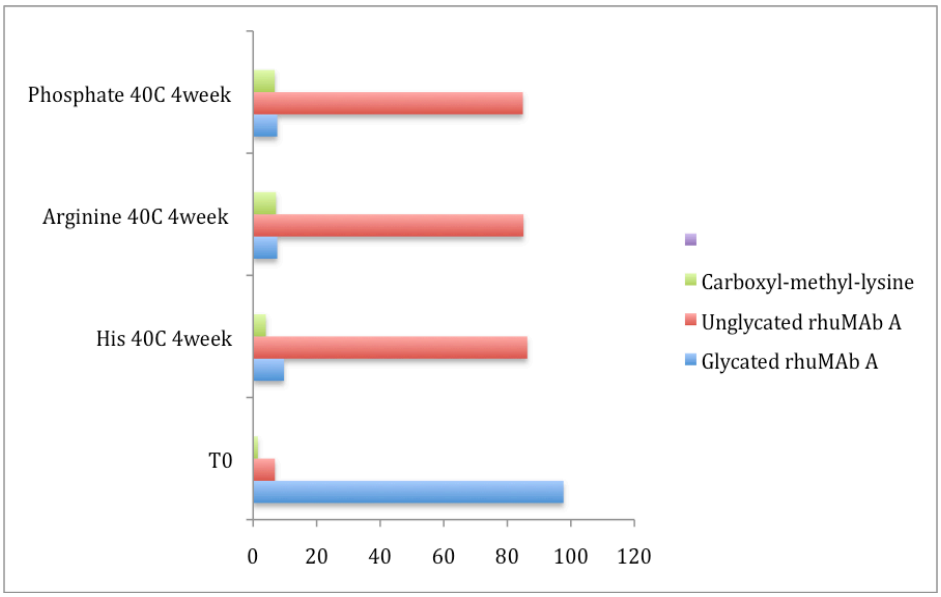

Figure 4-10: Comparison of degradation product of glycated rhuMAb A upon thermal stress in three buffers: 20mM histidine, 20mM arginine phosphate, 20mM sodium phosphate at pH 6.5. This bar graph showed there are no glycation adduct degradation difference in the three buffer systems.

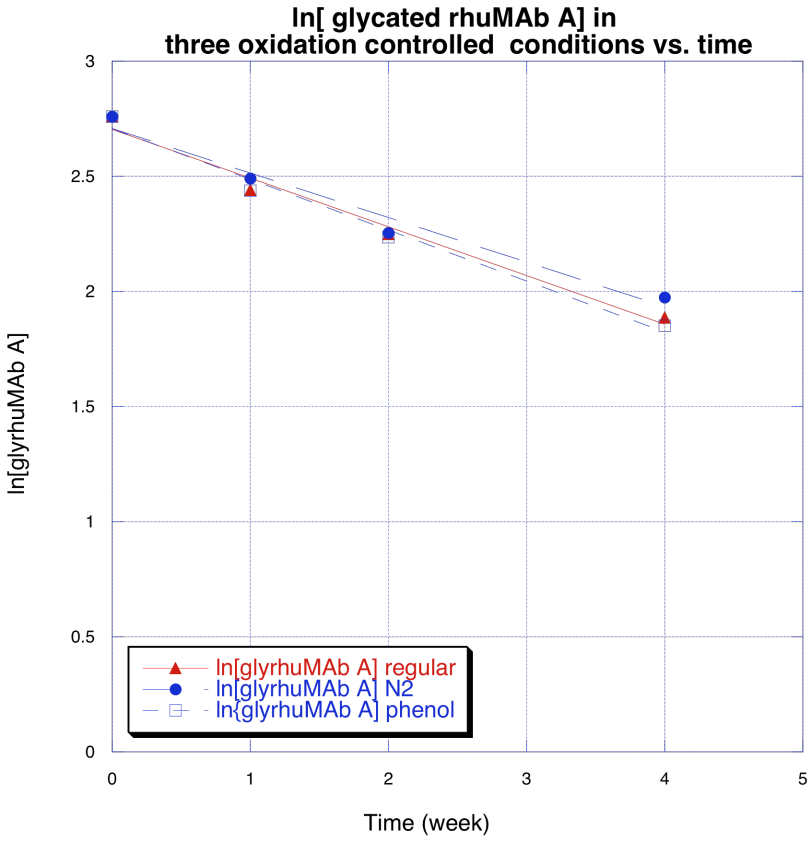

Figure 4-11: Comparison of glycated rhuMAb A hydrolysis in three oxidation controlled conditions. N2 purged vial showed a slightly slower hydrolysis rate.

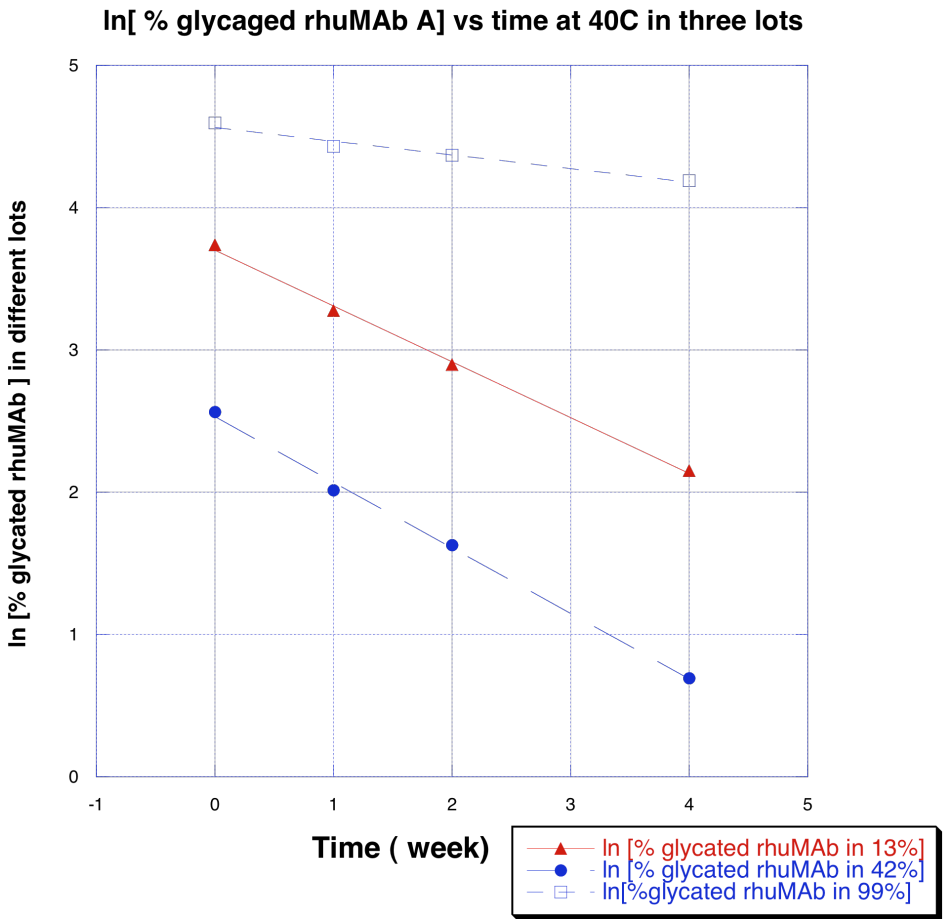

Figure 4-12: Decreased glycation level in three lots with different initial glycation levels at pH 6.5.

The rate of hydrolysis fits a linear regression, indicating a first order reaction. At higher glycation level, hydrolysis rate was slower.

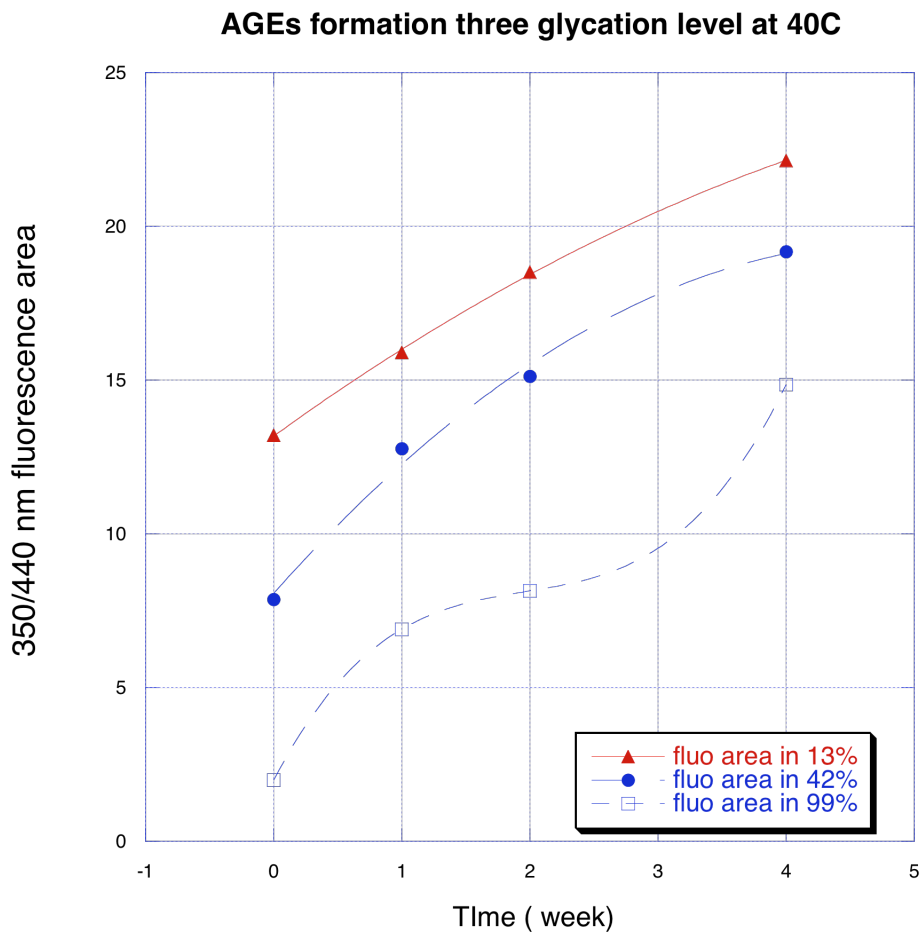

Figure 4- 13: AGEs formation of glycated rhuMAb A over 4 weeks at 40°C in three different initial glycation levels.

Higher glycation level showed faster AGEs formation.

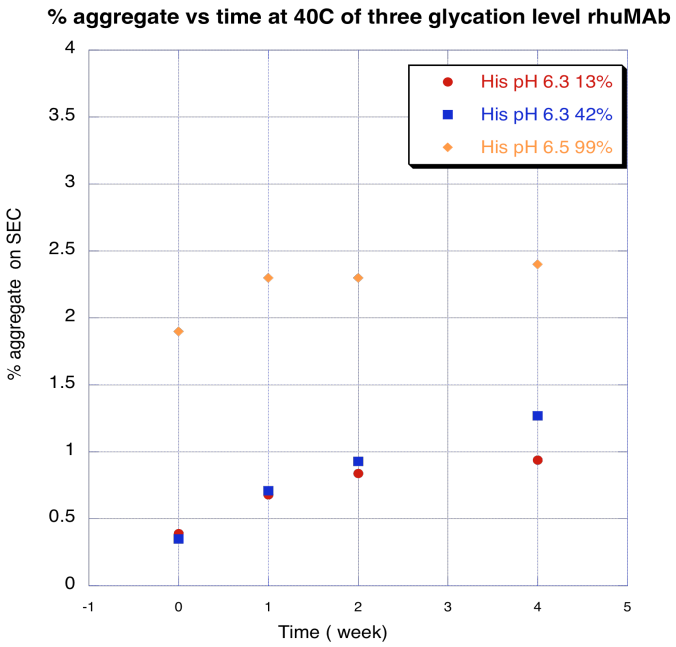

Figure 4-14: Comparison of aggregate levels at 40°C of glycated rhuMAb A in three different initial glycation levels. Higher glycation level had higher initial aggregation level.

pH condition	rate constant k (week^{-1}) at 40°C	remaining glycation %	$t_{1/2}$ (week)
4.5	0.045	32.0	15.4
5.0	0.091	25.0	7.6
5.5	0.13	22.0	5.3
6.0	0.35	8.7	2.0
6.5	0.43	6.4	1.6
7.0	0.51	5.6	1.4

Table 4-1: Summary of first order rate constant of glycated rhuMAb degradation at 40°C in different pH conditions (with initial glycation level 36%).

Buffer species	initial glycation level	rate constant k ($week^{-1}$) at 40°C	$t_{1/2}$ (week)
Histidine	99.3%	0.10	6.9
Arginine	99.3%	0.11	6.3
Phosphate	99.3%	0.13	5.3

Table 4-2: Summary of rate constant of glycated rhuMAb A degradation at 40°C in three different buffers (pH is constant at pH 6.5).

Drug product condition	rate constant k ($week^{-1}$) at 40°C	half life $t_{1/2}$ (week)
Fill with regular air in the head space	0.22	3.2
Fill with N_2 in the head space	0.20	3.5
Phenol added to DP	0.23	3.0

Table 4-3: Summary of rate constant of glycated rhuMAb A degradation at 40°C in three different oxidation conditions.

Material	initial glycation level	rate constant k (week^{-1}) at 40°C	$t_{1/2}$ (week)	number of detected glycation sites
Lot a	13%	0.46	1.5	1 site
Lot b	42%	0.39	1.8	6 sites
Force glycated	99%	0.10	6.9	7 sites

Table 4-4: Summary of rate constant of glycated rhuMAb A degradation at 40°C in three different initial glycation levels.All samples were in 20mM histidine buffer pH 6.5.

Citations:

Watkins, N.G., Thorpe, S.R., and Baynes, J.W. (1985) Glycation of amino group in protein. *Journal of Biological Chemistry*, **260**, 10629-10636.

Watkins, N.G., Neglia-Fisher, C.I., Dyer, D.G., Thorpe, S.R. and Baynes, J.W. (1987). Effect of phosphate on the kinetics and specificity of glycation of protein. *Journal of Biological Chemistry*, **262**, 7207–7212.

Yuk, I.H., Zhang, B., Yang, Y., Dutina, G., Leach, K.D., Vijayasankaran, N., Shen, A.Y., Andersen, D.C., Snedecor, B.R., Joly, J.C., (2011) Controlling glycation of recombinant antibody in fed-batch cell cultures. *Biotechnology and Bioengineering***,** **108**, 2600-2610.

Jencks, W.P., and Cordes, E.H. (1963) The mechanism of hydrolysis of Schiff base derived from aliphatic amines. *Journal of the American Chemistry Society*, **85** 2843-2848.

Acharya, A.S. and Sussman, L.G. (1984). The reversibility of the ketoamine linkages of aldoses with proteins. *Journal of Biological Chemistry***, 259,** 4372–4378.

Acharya, A.S., Roy, R.P., and Dorai, B., (1991) Aldimine to ketoamine isomerization (amadori rearrangement) potential at the individual nonenzymic glycation sites of hemoglobina: Preferential inhibition of glycation by nucleophiles at sites of low isomerization potential. *Journal of Protein Chemistry*, **10**, 345-358.

Zhang, B., Yang, Y., Yuk, I., Pai, R., Mckay, P. and Eigenbrot, C. (2008). Unveiling a glycation hot spot in a recombinant humanized monoclonal antibody. *Analytical Chemistry,* **80**, 2379–2390.

Bibliography:

Acharya, A.S. and Sussman, L.G. (1984). The reversibility of the ketoamine linkages of aldoses with proteins. *Journal of Biological Chemistry***, 259,** 4372–4378.

Acharya, A.S., Roy, R.P., and Dorai, B., (1991) Aldimine to ketoamine isomerization (amadori rearrangement) potential at the individual nonenzymic glycation sites of hemoglobina: Preferential inhibition of glycation by nucleophiles at sites of low isomerization potential. *Journal of Protein Chemistry*, **10**, 345-358

Banks, D.D., Hambly, D.M., Scavezze, J.L., Siska, C.C., Stackhouse, N.L., and Gadgil, H.S. (2009). The Effect of Sucrose Hydrolysis on the Stability of Protein Therapeutics during Accelerated Formulation Studies. *Journal of Pharmaceutical Sciences* **98** (12): 4501-4510.

Basta, G., Lazzerini, G., Massaro, M., Simoncini, T., Tanganelli, P., Fu, C., Kislinger, T., Ster, D.M., Schmidt, A.M, and De Caterina, R. (2002) Advanced glycation end products activate endothelium through signal-transduction receptor RAGE: A mechanism for amplification of inflammatory responses, *Circulation* **105** 816-822.

Baynes, J.W., Thorpe, S.R. and Murtiashaw, M.H. (1984). Nonenzymatic glucosylation of lysine residues in albumin. In: Wold, F. and Moldave, K., editors. *Posttranslational modifications; Part A, Methods in Enzymology*, **106**. 88–98 New York: Academic Press, Inc. .

Beisswenger, P.J., Szwergold, B.S. and Yeo, K.T. (2001). Glycated proteins in diabetes. *Clinical Lab Medicine* , **21**, 53-56.

Berendsen, H.J.C., Postma, J.P.M., Vangunsteren, W.F., Dinola, A., Haak, J.R. (1984). Molecular-Dynamics with couping to an external bath. *Journal of Chemical Physics*. **81**, 3684

Brady, L.J., Martinez, T. and Balland, A. (2007). Characterization of nonenzymatic glycation on a monoclonal antibody. *Analytical Chemistry*,**79**, 9403–9413.

Brownlee, M. (1992). Advanced protein glycosylation in diabetes and ageing. *Annual Review of Medicine,* **46**, 223–234.

Bucola, R. and Cerami, A. (1992). Advanced glycosylation: Chemistry, biology, and implications for diabetes and aging. *Advanced Pharmacology,* **23,** 1–33.

Bunn, H.F. and Higgins, P.J. (1981). Reaction of monosaccharides with proteins: Possible evolutionary significance. *Science,* **213**, 222–224.

Bussi, G., Donalio, D., Parrinello, M. (2007) Canonical sampling through velocity rescaling *Journal of Chemical Physics* 126

Cameron, N.E. and Cotter, M.A. (1993). Potential therapeutic approaches to the treatment or prevention of diabetic neuropathy: evidence from experimental studies. *Diabetes Medicine,* **10**, 593–605.

Case, D.A., Cheatham, T.E., Darden, T., Gohlke, H., Luo, R., Merz, K.M., Onufrlev, A., Simmerling, C., Wang, B., Woods, R.J., (2005) The Amber biomolecular simulation programs. *Journal of Computation Chemistry*. **26** (16) 1668-1688.

Chang, B.S. and Hershenson, S. (2002). Practical approaches to protein formulation development. In: Carpenter, J.F., Manning, M.C., editors. *Rational design*

of stable protein formulations theory and practice. 1st edition. New York: Kluwer Academic / Plenum Publishers. pp. 1–25.

Chirino, A.J. and Mire-Sluis, A. (2004). Characterizing biological products and assessing comparability following manufacturing changes. *Nature Biotechnology* **22**, 1383–1391.

Cho, S.J., Roman, G., Yeboah, F. and Konishi, Y. (2007). The road to advanced lycation end products: A mechanistic perspective. *Current Medical Chemistry* **14**, 1653–1671.

Clark, K.J., Griffiths, J., Bailey, K.M. and Harcum, K.M. (2005). Gene-expression profiles for five key glycosylation genes for galactose-fed CHO cells expressing recombinant IL-4/13 cytokine trap. *Biotechnology and Bioengineering,* **90**, 568–577.

Cox, T.M. (1994). Aldolase B and fructose intolerance. *FASEB Journal*, **8** 62-71.

DeGroot, J. (2004). The AGE of the matrix: chemistry, consequence and cure. *Current Opinion in Pharmacology,* **4**, 301-305.

Dolhofer-Bliesener, R. and Gerbitz, K.D. (1990). Effect of nonenzymatic glycation on the structure of immunoglobulin G. *Biological Chemistry Hoppe Seyler* , **371**(8):693-7.

Fischer, S., Hoernschemeyer, J. and Mahler, H-C. (2008). Glycation during storage and administration of monoclonal antibody formulations. *European Journal of Pharmaceuticals and Biopharmaceuticals,* **70**, 42–50.

Frokjaer, S. and Otzen, D. (2005). Protein drug stability: A formulation challenge. *National Review Drug Discovery,* **4**, 298–306.

Gadgil, H.S., Bondarenko, P.V., Pipes, G., Rehder, D., McAuley, A. and Perico, N. (2007). The LC/MS analysis of glycation of IgG molecules in sucrose containing formulations. *Journal of Pharmaceutical Science,* **96**, 2607–21.

Gadgil, H.S., Bondarenko, P.V., Pipes, G., Rehder, D., McAuley, A., Perico, N. (2007). The LC/MS analysis of glycation of IgG molecules in sucrose containing formulations. *Journal of Pharmaceutical Science* **96**, 2607–21.

Garrett, R.H., Crisham, C.M., (2010) *Biochemistry 4th Edition.* Brooks/Cole

Goetze, A.M., Schenauer, M.R. and Flynn, G.C. (2010). Assessing monoclonal antibody product quality attribute criticality through clinical studies. *mAbs* **2:5**, 500-507.

Goetze, A.M., Liu, Y.D., Arroll, T., Chu, L., Flynn, G.C. (2012). Rates and impact of human antibody glycation *in vivo*.. *Glycobiology* , **22**(2):221-34

Goldin, A., Beckman, J. A., Schmidt, A. M., Creager, M. D. (2006). Advanced glycation end products: sparking the development of diabetic vascular injury. *Circulation,* **114**, 597-605.

Harris, R.J., Shire, S.J. and Winter, C. (2004). Commercial manufacturing scale formulation and analytical characterization of therapeutic recombinant antibodies. *Drug Development and Research,* **61**, 137–154.

Harris,T.K., Cole, R.N., Mildvan, A.S. (1998) Proton transfer in the mechanism of triosephosphate isomerase. *Biochemistry* **37,** 16828-16838

Hawe, A. and Friess, W. (2008). Development of HSA-free formulations for a hydrophobic cytokine with improved stability. *European Journal of Pharmaceuticals and Biopharmaceutical,s* **68**, 169–82.

Holmquist, W.R. and Schroeder, W.A. (1964). Properties and partial characterization of adult human hemoglobin A1. *Biochim Biophys Acta,* **82**, 639–641.

John, W.G. and Lamb, E.J. (1993). The Maillard or browning reaction in diabetes. *Eye,* **7**, 230-237.

Jakus, V.,and Riebrock , N. (2004) *Phyislogiocal Research*, **53**: 131-142.

Jencks, W.P., and Cordes, E.H. (1963) The mechanism of hydrolysis of Schiff base derived from aliphatic amines. *Journal of the American Chemistry Society*, **85** 2843-2848

Kennedy, D.M., Skillen, A.W. and Self, C.H. (1994). Glycation of monoclonal antibodies impairs their ability to bind antigen. *Clinical Experimental Immunololgy,* **98**, 245–51.

Lai, M.C. and Topp, E.M. (1999). Solid-state chemical stability of proteins and peptides. *Journal of Pharmaceutical Science,* **88**, 489–500.

Lapolla, A., Fedele, D., Garbeglio, M. and Martano, L. (2000). Matrix-assisted laser desorption/ionization mass spectrometry, enzymatic digestion, and molecular modelling in the study of nonenzymatic glycation of IgG. *Journal of American Society of Mass Spectrometry,* **11**, 53– 9.

Ledford, H. (2008). Monoclonal antibodies come of age. *Nature,* **455**, 437.

Lee, B., and Richards, F.M., (1971). The interpretation of protein structures: estimation of static accessibility, *Journal of Molecular Biology*, **55**, 379-400.

Li, A., Pfuller, U., Larsson, E.V., Jungvid, H., Galaev, I.Y., and Mattiagsson, B., (2001) Separation of misletoe lectins based on the degree of glycosylation using boronate affinity chromatography. *Journal of Chromatography,* **925** 115-121

Li, S., Patapoff, T.W., Overcashier, D., Hsu, C., Nguyen, T-H. and Borchardt, R.T. (1996). Effects of reducing sugars on the chemical stability of human relaxin in the lyophilized state. *Journal of Pharmaceutical Science,* **85**, 873–7.

Maas, C., Hermeling, S., Bouma, B., Jiskoot, W. and Gebbink MFBG. (2007). A role for protein misfolding in immunogenicity of biopharmaceuticals. *Journal of Biological Chemistry,* **282**, 2229–2236.

Maggon, K. (2007). Monoclonal antibody ‘‘gold rush’’. *Current Medical Chemistry,* **14**, 1978–1987.

Maillard, L. C. (1912). Action of amino acids on sugars. Formation of melanoidins in a methodical way. *Compt. Rend.* **154**, 66-68.

Miller, A.K., Hambly, D.M., Kerwin, B.A., Treuheit, M.J. and Gadgil, H.S. (2011). Characterization of site-specific glycation during process development of a human therapeutic monoclonal antibody. *Journal of Pharmaceutical Science,* **100**, 2543–2550.

Monnier, V. and Cerami, A. (1981). Nonenzymatic browning *in vivo.*: possible process for aging of long-lived proteins. *Science,* **211**, 491-493.

Munch, G., Thome, J., Foley, P., Schinezel, R., Riederer, P. (1997). *Advanced glycation end products in Aging and Alzheimer’s disease* Brain Research Reviews **23,**134-143

Namiki, M. (1988) Chemistry of Maillard reactions: recent studies on the browning reaction mechanism and the development of antioxidants and mutagens. *Advanced Food Research* **32**, 115-184

O'Brien, J. (1996) Stability of trehalose, sucrose and glucose to nonenzymatic browning in model systems. *Journal of Food Science***, 61**, 679–82.

Projan, S.J., Gill, D., Lu, Z. and Herrmann, S.H. (2004). Small molecules for small minds? The case for biologic pharmaceuticals. *Expert Opinion on Biological Therapy* , **4,** 1345–1350.

Quan, C.P., Alcala, E., Petkovska, I., Matthews, D., Canova-Davis, E. and Taticek, R. (2008). A study in glycation of a therapeutic recombinant humanized monoclonal antibody: where it is, how it got there, and how it affects change-based behavior. *Analytical Biochemistry*, **373**, 179–191.

Quan, C.P., Wu, S., Dasovich, N., Hsu, C., Patapoff, T., Canova-Davis, E. (1999). Susceptibility of rhDNase to glycation in the dry powder state. *Analytical Chemistry* , **71**, 4445–4454.

Reichert, J. and Pavlou, A. (2004). Monoclonal antibodies market. *National Review Drug Discovery*, **3**, 383–384.

Sell, D. R. and Monnier, V. M. (1989). Structure elucidation of a senescence cross-link from human extracellular matrix. Implication of pentoses in the aging process. *Journal of Biological Chemistry*, **264**, 21597-21602.

Sell, D.R, Nagara, T.H., Grandhee, S.K., Odetti, P., Lapolla, A., Fogarty, J., and Monnier, V.M., (1991) Pentodisine: A molecular marker for the cumulative

damage to proteins in diabetes, aging, and uremia. *Diabetes/Metabolism Reviews.* **7** , 239-251

Shaw, S.M. and Crabbe, M.J. (1994). Characterisation of a putative scavenger receptor for advanced glycosylation end-products. *Biochemical Society Transactions,* **22**, 82S.

Smales, C.M., Pepper, D.S. and James, D.C. (2000). Mechanisms of protein modification during model anti-viral heat-treatment bioprocessing of beta-lactoglobulin variant A in the presence of sucrose. *Biotechnology Applied Biochemistry,* **32**, 109–119.

Smales, C.M., Pepper, D.S. and James, D.C. (2001). Protein modifications during antiviral heat bioprocessing and subsequent storage. *Biotechnology Progress* **17**, 974–978.

Thorpe, S. R. and Baynes, J. W. (2003). Maillard reaction products in tissue proteins: new products and new perspectives. *Amino Acids,* **25**, 275-281.

Valcourt, U., Merle, B., Gineyts, E., Viguet-Carrin, S., Delmas, P. D. and Garnero, P. (2007). Non-enzymatic glycation of bone collagen modifies osteoclastic activity and differentiation. *Journal of Biological Chemistry,* **282**, 5691-5703.

Van Schaftingen, E., Delpierre, G., Collard, F., Fortpied, J., Gemayel, R., Wiame, E., Veiga-da-Cunha, M. (2007). Fructosamine 3-kinase and other enzymes involved in protein deglycation. *Advanced Enzyme Regulation,* **47**, 261–269.

Venkatraman, J., Aggarwal, K. and Balaram, P. (2001). Helical peptide models for protein glycation: Proximity effects in catalysis of the amadori rearrangement. *Chemical Biology***, 8**, 611–625.

Vrdoljak, A., Trescec, A., Benko, B., Hecimovic and D., Simic, M. (2004). In vitro glycation of human immunoglobulin G. *Clinica Chimica Acta* , **345**, 105– 111.

Walsh, G. (2006). Biopharmaceutical benchmarks. *Nature Biotechnology* **24**, 769–776.

Watkins, N.G., Thorpe, S.R., and Baynes, J.W. (1985) Glycation of amino group in protein. *Journal of Biological Chemistry*, **260**, 10629-10636

Watkins, N.G., Neglia-Fisher, C.I., Dyer, D.G., Thorpe, S.R. and Baynes, J.W. (1987). Effect of phosphate on the kinetics and specificity of glycation of protein. *Journal of Biological Chemistry*, **262**, 7207–7212.

Weiner, L.M., Surana, R. and Wang, S. (2010). Monoclonal antibody: versatile platforms for cancer immunotherapy. *Nature*, **10**, 317-327

Xuan, Y., and Yuan, J., Schiff base as a stimuli-responsive linker in polymer chemistry (2012) *Polymer Chemistry*, **3**, 3045-3055

Yuk, I.H., Zhang, B., Yang, Y., Dutina, G., Leach, K.D., Vijayasankaran, N., Shen, A.Y., Andersen, D.C., Snedecor, B.R., Joly, J.C., (2011) Controlling glycation of recombinant antibody in fed-batch cell cultures. *Biotechnology and Bioengineering***, 108**, 2600-2610

Zhang, B., Yang, Y., Yuk, I., Pai, R., Mckay, P. and Eigenbrot, C. (2008). Unveiling a glycation hot spot in a recombinant humanized monoclonal antibody. *Analytical Chemistry,* **80**, 2379–2390.

Zhang, Q., Ames, J.M., Smith, R.D., Baynes, J.W. and Metz, T.O. (2009). A Perspective on the Maillard Reaction and the Analysis of Protein Glycation by Mass Spectrometry: Probing the Pathogenesis of Chronic Disease. *Journal of Proteome Research,* **8(2),** 754–769

Zider, A. and Drakeman, D.L. (2010). The future of monoclonal antibody technology. *mAbs* **2:4**, 361-364.